THE NICOTINIC ACID RECEPTOR IN HUMAN ADIPOSE TISSUE

Liliane Chamas

St John's College

Oxford Centre for Diabetes Endocrinology and Metabolism

Radcliffe Department of Medicine

University of Oxford

DPhil Thesis

Trinity 2013

MEMORANDUM

The work in this thesis is the original work of the author. Experiments were carried out at the Oxford Centre for Diabetes Endocrinology and Metabolism, University of Oxford, under the supervision of Dr Fredrik Karpe and Dr Matthew Neville. Funding was provided by the Rhodes Trust, the Radcliffe Department of Medicine and the European Foundation for the Study of Diabetes.

A short Investigation of the transcript levels and polymorphisms in *HCAR2* and *HCAR3* (Chapters 4 and 5) will be written up as a manuscript soon later.

I hereby state that no part of this thesis has been submitted for any other degree at this or any other university.

This document is approximately 36,500 words

THE NICOTINIC ACID RECEPTOR IN HUMAN ADIPOSE TISSUE

Liliane Chamas, St John's College
Submitted in Candidature for the degree of Doctor of Philosophy, Trinity 2013

Abstract

Nicotinic acid (NA) has been clinically used for over 50 years to regulate lipid plasma levels. It is the only drug in current clinical use that significantly raises HDL cholesterol and reduces inflammatory markers. However, mechanistic understanding into its wide range of actions remains unclear. The recent identification of the G_i-coupled protein receptor HCAR2, for which NA is a potent agonist, provides intriguing insight due to its anti-lipolytic action and restricted, yet specific, expression in adipose tissue and immune cells.

The *HCAR2* gene is 96% homologous to *HCAR3*, but the HCAR3 receptor shares neither the specificity for NA, nor the range of functional effects. Moreover, the close homology makes it difficult to separate the genetic variability and regulation of the two genes. To this end, I resequenced *HCAR2* and *HCAR3* in a selected population to characterize the variability of the two genes and to inform the subsequent design of specific genotyping assays. The Oxford Biobank, which is a random population-based collection of 30-50 year old men and women in Oxfordshire with a wide range of collected phenotypes, was used to explore genetic associations. A preliminary trend with HDL and rs7314976 in *HCAR2* motivated the further search associations. However after increasing the sample size, the HDL association did not reach significance. When looking at inflammatory phenotypes, a 20% lower level of systemic hsCRP was found in males with a promoter region variant in *HCAR3* (N=1808, p=0.007 for rs55718746). Replication of this finding in two relevant cohorts (NPHS-II, N=2185 and Whitehall, N=4228) resulted in conflicting findings.

After optimising the specific detection of both *HCAR2* and *HCAR3* transcripts, I characterized gene expression in human AT biopsies. This revealed an 18% increase in *HCAR2* expression in the female abdominal depot (N=106, $p<0.0001$) and a reduction in abdominal *HCAR2* in both males ($\beta=-0.37$, $p<0.001$, N=107) and females ($\beta=-0.251$, $p=0.005$, N=106) with increasing adiposity. The rs55718746 variant in *HCAR3* was also seen to influence expression of both *HCAR2* (N=182, $p=0.018$ in the abdominal depot) and *HCAR3* (N=198, $p=0.005$) but surprisingly in opposite directions, establishing it as the first cis-eQTL for this genomic region.

Finally, I used human adipocyte *in vitro* culture systems to setup a pilot to study the anti-inflammatory effects of NA. The gene expression of *HCAR2* and *HCAR3* increased significantly with adipocyte differentiation *in vitro*. NA led to a drop in IL-6 transcript abundance in two out of three of the *in vitro* differentiated human adipocytes.

In conclusion, genetic variability in *HCAR2* and *HCAR3* shows weak associations with cardiovascular disease risk phenotypes relating to their respective pathways. The relevance of *HCAR2* and *HCAR3* gene expression and the role of the receptor in the control of inflammation will require further studies.

ACKNOWLEDGEMENTS

Over the last four years at Oxford and in OCDEM, I have been intellectually challenged and rewarded, and I have developed a wonderful network of mentors and friends.

I would like to extend my deepest gratitude to Dr. Fredrik Karpe who has patiently mentored me throughout. I was always nervous before our meetings, but then I always came out feeling reassured and confident. Thank you for believing in me and supporting me throughout my research as well as my extracurricular interests.

Dr. Matt Neville, I would have never imagined making it to this point without your technical expertise, wicked sense of humour and gorgeous baking. I am happy to say that I did not put on the dreaded 'OCDEM stone' and much of that is thanks to our lunchtime runs and Shotover sprints.

The Oxlip group, you have been an incredible family who always found humour in my silliness. Thank you Sandy for keeping me out of trouble, and Marje for all of our fun chats. Katherine, I have never met anyone as helpful and patient as you. Thank you for putting up with my never-ending stream of questions. Catriona, I consider myself lucky to have been your co-worker and friend and to have watched your lovely new family grow.

Mandy, Amy and Chris from the 'lab next door', you have provided me with the most precious technical advice and I am very thankful for that. Nicola and Mary, your own recent experience and down-to-earth advice got me through the last couple of months. I hope to continue this tradition.

The Rhodes Trust has provided me with not only this incredible opportunity through its financial support, but also with friendships that will last a lifetime. Don, Mary, Bob, John and Colin, you are the family away from home.

I could have not hoped for a better college than St John's. The opportunities to partake in international conferences and intern at the World health Organization would have never been possible without the College's generous support.

I must thank my mother and father who sacrificed so much to move us to Canada. This is as much your effort as it is mine, and it is through the hardworking principles that you taught me that I landed here. I have missed you and Rayan every day for the last four years.

Finally, Ryan you have been with me since day one and supported me in my best and my not-so-best. It was your balance and calm, along with your inspiring interests, that widened my horizons and allowed me to get through the tougher times. My style might be different, but I will try to reciprocate when it is your turn to write up next year. We have been so privileged to experience Oxford together and I cannot wait to embark on our future adventures.

TABLE OF CONTENTS

LIST OF TABLES

LIST OF FIGURES

ABBREVIATIONS

ABCA1 ATP-binding cassette transporter
ApoE Apolipoprotein E
AT Adipose tissue
BMI Body mass index
bp Base pairs
cAMP Cyclic adenosine monophosphate
cDNA Complementary deoxyribonucleic acid
cDNA Complementary DNA (reverse-transcribed)
CETP Cholesteryl ester transfer protein
Chr Chromosome
CRP C-Reactive Protein
CVD Cardiovascular disease
ddNTPs Dideoxyribonucleotide
DMEM+F-12 Dulbecco's Modified Eagle Medium for mammalian cell culture maintenance
DNA Deoxyribonucleic acid
dNTPs Deoxyribonucleotide
EC50 Concentration of substrate required to induce half maximal response in a receptor or enzyme
eQTL Expression quantitative trait loci
FFA Free fatty acids
gDNA Genomic DNA
GWAS Genome-wide association study
HDL High density lipoprotein
HKG Housekeeping gene
HPV Human papillomavirus
hTERT Human Telomerase Reverse Transcriptase
LD Linkage disequilibrium
LDL Low density lipoprotein
LP(a) Lipoprotein A
MAF Minor allele frequency
miRNA Micro ribonucleic acid
mRNA Messenger ribonucleic acid
NA Nicotinic Acid
NAD Nicotinamide adenine dinucleotide
NEFA Non-esterified fatty acids
NGS Next generation sequencing
NTC Non-template control
Nuclease-free water water treated to inactivate RNAses
OBB Oxford Biobank
PBS Phosphate buffered saline

PCR Polymerase chain reaction
PGK1 Phosphoglycerate kinase-1
PPIA Peptidylprolyl isomerase A
qPCR Quantitative polymerase chain reaction
RCT Randomized controlled trial
RFLP Restriction fragment length polymorphism
RNA Ribonucleic acid
RT Reverse transcriptase
SC Subcutaneous
SD Standard deviation
SNP Single nucleotide polymorphism
TG/TAG Triacylglycerol
UCSC University of California Santa Cruz
UTR Untranslated region
VLDL Very low density lipoprotein
WHO World health organisation
WT Wildtype
ΔΔCt Change in threshold value normalised to a housekeeping gene

Chapter 1 Introduction

1.1. Cardiovascular disease prevention

According to the World Health Organization, an estimated 17.8 million people died from cardiovascular disease (CVD)–related causes in 2008 (WHO, 2013). This figure is estimated to surpass 23 million deaths annually by 2030, putting an enormous amount of strain on already heavily burdened healthcare systems (Daar et al., 2007; Heneghan et al., 2013). A current re-evaluation of cost-effective evidence-based interventions for prevention and treatment is needed to inform and improve future guidelines worldwide.

European clinical guidelines for prevention of CVD are stratified in the population. In low-risk populations, the guidelines focus on environmental and lifestyle changes. In high-risk populations, the focus is on pharmaceutical management of major risk factors such as hypertension and dyslipidaemia (Perk et al., 2012). Dyslipidaemia – as established by genetic, pathological, as well as observational and interventional studies – is considered to be crucial in the development of CVD. Managing dyslipidaemia has therefore been on the forefront of CVD prevention strategies (Perk et al., 2012). Effective lipid-lowering therapies using statins have consistently been shown to result in a dose-dependent reduction of relative CVD risk in treated populations (Cholesterol Treatment Trialists, 2010). However, additional improvement of residual CVD risk is still required. Nicotinic acid (NA) is one therapeutic agent that has re-emerged in light of its potential CVD-preventive properties. It is this therapeutic agent and its receptor that form the focus of this thesis.

1.2. The nicotinic acid receptor

1.2.1. Nicotinic acid discovery

Chemically known as pyridine-3-carboxylic acid or niacin, NA is a water-soluble vitamin B. It was first characterized in the 1930s, when it was shown to cure pellagra, a disease caused by niacin, tryptophan and leucine deficiencies (Elvehjem, Madden, Strong, & Woolley, 1938). It was not until a couple of decades later that its lipid-modifying properties were discovered and its use in lipid management therapy began (Altschul, Hoffer, & Stephen, 1955). The administration of gram quantities of NA was not only shown to reduce total plasma cholesterol by 10% in healthy subjects and 20% in hypercholesterolaemic patients, it was also shown to exert beneficial effects in long-term prevention of atherosclerosis and coronary heart disease in some early studies (Bodor & Offermanns, 2008; Chai, Digby, & Choudhury, 2013a; Mahboubi et al., 2006). These effects will be described in 1.3.

1.2.2. Receptor Identification

Early studies of the targeted action of NA assessed tissue distribution of labelled [^{3}H]NA and identified adipose tissue as an almost exclusive sink along with some immune cells (macrophages and monocytes) and the spleen (Carlson & Hanngren, 1964). This finding gave mechanistic support to the observed drop in circulating free fatty acid levels after NA administration being attributed to the anti-lipolytic effect of NA on adipocytes (Carlson & Hanngren, 1964). NA was later shown to reduce cAMP levels in adipose tissue following a G_i-mediated inhibition of adenylyl cyclase – a now characterized signalling cascade common to this class of hydroxyl-carboxylic receptors. At the time, this fuelled the subsequent hunt for the NA

receptor amidst orphan G-coupled protein receptors (Aktories, Jakobs, & Schultz, 1980; Butcher, Baird, & Sutherland, 1968).

Initially, the murine orthologue of the NA receptor, PUMA-G (protein up-regulated in macrophages by INF-γ), was identified through investigations into differentially expressed genes upon stimulation with INF-γ and TNF-α in murine macrophages (Schaub, Fütterer, & Pfeffer, 2001). Although no connection to NA was made at that point, this investigation offered the first insight into NA's now known involvement with an inflammatory process, which will be discussed in 1.3.2. For its role as the NA receptor, HCAR2 (Hydroxycarboxylic acid receptor 2) was only identified after its homolog HCAR3 was found to be NA's low affinity receptor.

HCAR3 – first referred to as *HM74* – was first cloned in 1993 by genomic DNA library screening and PCR amplification of degenerate sequences that are conserved in signalling proteins. The intention at that point was to identify putative leukocyte chemotactic peptide receptors involved in inflammation processes (Nomura, Nielsen, & Matsushima, 1993). Follow-up bioinformatic searches of orphan receptors with sequence similarity finally identified HCAR2 (HM74A) as the high affinity receptor for NA (Soga et al., 2003; Tunaru et al., 2003; Wise et al., 2003).

1.2.3. Endogenous ligands

Following kinetic and binding studies, it was clear that NA was an unlikely physiological ligand to HCAR2 due to its low concentration in bodily fluids. Taggart *et al* (2005) subsequently identified the ketone body ß-hydroxybutyrate as an endogenous ligand for HCAR2 (EC_{50}=1.6mM) (Taggart et al., 2005). Normal

physiological concentrations of ß-hydroxybutyrate are between 20 and 200μM (Owen, Felig, Morgan, Wahren, & Cahill, 1969). Interestingly, the concentrations of ß-hydroxybutyrate required to activate HCAR2 correspond to those seen during extended fasting periods, diabetic ketoacidosis, a ketogenic diet or in the case of a mitochondrial fatty acid ß-oxidation disorder (in the range of 2mM to 6mM)(Ahmed, Tunaru, & Offermanns, 2009a). While intuitively, one would consider that this might serve as negative-feedback to maintain fatty acid stores in starvation periods, it presents a potential intriguing lipid signalling loop between the liver and the adipocyte. Indeed, G-coupled protein receptors are known to play an integral role in hormonal signalling however there are few examples of metabolites operating as receptor ligands to bridge metabolic substrate utilization and its tissue-specific regulation.

Despite the high homology between HCAR2 and HCAR3, which will be introduced in 1.2.4, HCAR3 shows different binding properties and does not respond to ß-hydroxybutyrate (Taggart et al., 2005). HCAR3 has an altogether different range of endogenous hydroxylated medium-chain fatty acid metabolite ligands, in particular 3-hydroxy-octanoate, an intermediate of fatty acid ß-oxidation (EC_{50} of 4 to 8μM) (Ahmed et al., 2009b). Similarly, the concentrations required to activate HCAR3 are under conditions of increased ß-oxidation flux, starvation, a ketogenic diet or diabetic ketoacidosis (Ahmed et al., 2009b; Costa et al., 1998; Jones, Tjoa, Fennessey, Goodman, & Bennett, 2002). At the required concentrations, both endogenous ligands initiate an anti-lipolytic cascade in the adipocyte through their corresponding receptors, as described in Figure 1.

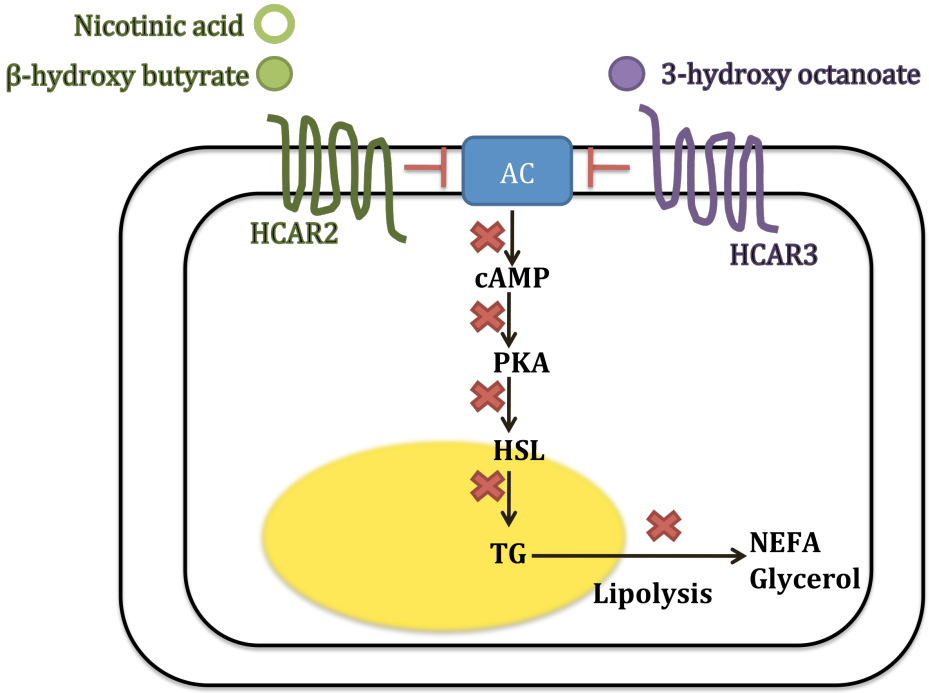

Figure 1: Anti-lipolytic signalling cascade in the human adipocyte that both receptors initiate.
It begins with the ligands' signal to the transmembrane G_i-coupled protein. This signal inhibits Adenylate Cyclase (AC) reducing the availability of cAMP and thus the phosphorylation of Protein Kinase A (PKA). The unphosphorylated PKA no longer activates Hormone Sensitive Lipase (HSL) thus blocking lipolysis of the stored triglycerides the release of non-esterified fatty acids and glycerol from the adipocyte (Karpe & Frayn, 2004).

1.2.4. Gene Homology

The NA receptor HCAR2 and its homolog HCAR3 belongs to a family of G-coupled protein receptors, all of which have seven trans-membrane helix domains and hydroxyl-carboxylic acids as endogenous ligands (D. K. Lee et al., 2001; Offermanns et al., 2011). Both receptors are also encoded by single-exon genes co-located on the long arm of chromosome 12 (details in Table 1).

	HCAR2	HCAR3
Other names	HCA2, GPR109A, HM74A, NIACR1	HCA3, GPR109B, HM74, NIACR2
Genomic location	One exon genes on 12q24.31	
Amino acid length	363	387
Expression in human tissue	Adipocytes, macrophages, neutrophils, epidermal langerhans cells, keratinocytes, intestinal epithelial cells	Adipocytes, neutrophils, macrophages, intestinal epithelial cells

Table 1: Current nomenclature and properties of the nicotinic acid receptor and its homologs in humans. Adapted from IJzerman et al. (2010).

HCAR2 and *HCAR3* share 96% DNA sequence homology that spans both promoter and coding regions (Offermanns, 2006). In the coding region, a 15 bp substitution and 5bp omission in *HCAR2* results in a 72bp earlier stop codon compared to *HCAR3* and a 24 amino acid truncation at the protein level (Wise et al., 2003). In addition, an important Arginine residue in the third trans-membrane helix domain in HCAR2 serves as an anchor site for the acidic group of its ligand. This residue, along with the 24 amino acid difference between HCAR2 and HCAR3, confers the binding specificity of NA to HCAR2 and the corresponding range of physiological effects (EC_{50}=0.1μM for HCAR2 and 100μM for HCAR3) (Taggart et al., 2005). An alignment of both *HCAR2* and *HCAR3* with 2kb of their promoter regions and their coding regions can be found in the Appendix.

Although *HCAR3* was the first *HCAR* identified in humans due to its sequence homology to murine *PUMA-G*, it is not present in rodents and orthology analysis shows that *HCAR3* is only present in higher mammals such as chimpanzees, indicating a recent event of gene duplication (Irukayama-Tomobe et al., 2009). As a result of the high degree of homology between *HCAR2* and *HCAR3* and possible ensuing non-homologous recombination events between the two regions during

cell division, many of the polymorphisms in either or both genes are not properly assigned to the appropriate gene (Zellner et al., 2005). Furthermore, this homology has hampered detailed genetic exploration in the region since it is unavoidable to co-amplify or detect both transcripts unless proper measures are taken (as will be discussed in detail in Chapters 3-5).

1.3. Nicotinic acid as a pharmacological tool

1.3.1. Effects on lipid metabolism

Pharmacological administration of NA (1-3g compared with the 10-20mg dietary requirement) reduces proatherogenic lipid and lipoprotein particles including total cholesterol, VLDL, LDL, Lipoprotein (a) and small dense LDL particles. Furthermore, it potently increases levels of larger HDL sub-fractions and apolipoprotein A-1 contained in HDL, presumed to be cardioprotective by mediating the reverse cholesterol transport pathway (recently reviewed in (Kamanna, Ganji, & Kashyap, 2013).

1.3.1.1. Mechanistic explanations

Debate still surrounds exactly how the lipid effect is mediated but two main trails of evidence have been put forward. Initial investigations into the mode of action of NA in cultured adipocytes showed there was a decrease in the release of free fatty acids (FFAs) due to an inhibition of triglyceride lipolysis, leading to a lowered plasma concentration of FFAs in humans (Carlson & Orö, 1962). For a long time, this was thought to mediate the lowering of plasma triglyceride concentrations by limiting the availability of FFAs as precursors for hepatic very low-density lipoprotein and trygliceride synthesis. However, this explanation did not offer a full picture since levels of FFA rebounded profoundly within hours of NA administration, casting doubt on the theory that the availability of serum FFAs is the limiting factor for triglyceride synthesis (Carlson, 2005).

In fact, after the discovery of the NA receptor, several studies challenged this theory. These studies used genetic and pharmacological approaches in mice and

clinical trials in humans to prove that the TG lowering effects of NA were not due to a reduction in adipose tissue-released FFAs. Mice lacking the NA receptor and thereby failing to exhibit the acute drop in FFAs still retained the triglyceride and LDL-lowering effects of NA. Similarly in humans, two distinct full agonists of the NA receptor were found to cause a profound drop in circulating FFAs but did not affect circulating serum lipids the way that NA does (Lauring et al., 2012). As a result of these studies, most of the NA-mediated lipid effects that will be described are not thought to be directly receptor-mediated.

The current suggested model of NA's TG lowering effects focuses on the liver as a site of control of synthesis of VLDL triglyceride particles. This is following evidence from a human hepatocyte cell line (Hep G2 cells) where NA was found to inhibit hepatocyte triglyceride synthesis by increasing intracellular post-translational degradation of apoB transcript. The resulting decrease in secretion of ApoB-containing VLDL and LDL particles corresponds to the observed lipid-modifying effects of NA (Jin, Kamanna, & Kashyap, 1999).

NA seems to affect a step in the control of the hepatocyte triglyceride synthesis by inhibiting diacylglycerol O-acyltransferase 2 (DGAT2), a microsomal enzyme that catalyses the final step in triglyceride synthesis (Ganji, 2004). This non-competitive inhibition of DGAT2 leads to a decrease in triglyceride synthesis in the liver and reduces the assembly of VLDL particles (Hu et al., 2012). A small, uncontrolled human study further supported this evidence where treatment of 39 dyslipidaemic patients with NA for 23 weeks significantly decreased their MRI-measured liver fat. Patients in this study with polymorphisms affecting DGAT2 function were found to have a smaller reduction in liver fat (Hu et al., 2012).

Similarly, the profound increase in serum HDL due to NA administration is not fully understood and is still being investigated. *In vitro* experiments indicate that NA affects the expression of β-chain ATP synthase on the hepatocyte, a HDL holo-particle receptor thereby decreasing the hepatic uptake of HDL-Apo-AI and resulting in increased HDL particles in circulation (Jin et al., 1999; L. Zhang, Kamanna, Zhang, & Kashyap, 2008). Studies in humans do not fully support this mechanistic model (Kamanna et al., 2013).

An additional proposed mechanism of NA's action relates to HDL biogenesis with the membrane protein ATP-binding cassette transporter A1 (ABCA1) at the hepatocyte cell surface. ABCA1 is critical during for the formation of HDL particles and recent *in vitro* evidence suggests that NA enhances HDL formation by increasing *ABCA1* transcription in hepatocytes (L. H. Zhang, Kamanna, Ganji, Xiong, & Kashyap, 2012).

1.3.1.2. NA and HDL in CVD prevention

Epidemiological studies and meta-analyses have consistently shown an inverse relationship between levels of HDL cholesterol and the risk of CVD, making the modulation of HDL target levels the cornerstone to reducing cardiovascular mortality (Emerging Risk Factors Collaboration et al., 2009; Prospective Studies Collaboration et al., 2007). However, it has been questioned whether the characteristics of the HDL particle rather than the overall HDL levels are more critical for improving cardiovascular risk (Wild & Byrne, 2008).

From a mechanistic perspective, HDL particles accept cholesterol from peripheral tissues and transport it back to the liver for excretion – a process known as reverse cholesterol transport. This process, along with further anti-inflammatory and

antioxidant mechanisms of HDL, have earned it the name “good cholesterol” (reviewed in (Fisher, Feig, Hewing, Hazen, & Smith, 2012)). Consequently, and in light of its profound effects on HDL levels, NA has been used as a treatment for atherosclerotic cardiovascular events for over 50 years.

Results from two main clinical trials provided support for NA’s historical role in CVD prevention. The first, the Coronary Drug project, was a five-year study in which NA treatment was shown to reduce non-fatal myocardial infarction with no change in total mortality in 1119 individuals (Canner et al., 1986). In the second clinical trial, the five-year Stockholm secondary prevention study, NA administration with clofibrate (another lipid-lowering drug) was shown to reduce ischemic heart disease incidence by 36% (Carlson & Rosenhamer, 1988). Although both these studies fell short of meeting the modern rigorous requirements of clinical trials, they were influential in causing NA to be considered a relevant add-on therapy beyond statins (Barter et al., 2007; Pedersen et al., 2005). Reduced patient compliance as a result of uncomfortable prostaglandin-induced cutaneous flushing and evidence of impaired glucose tolerance and myopathy has been a major limitation to NA’s widespread use (reviewed in (Karpe & Frayn, 2004), (Poynten et al., 2003)).

Nonetheless, the persistence of a residual CVD risk with statins and the possible benefits associated with increasing HDL levels and improving HDL functionality (Sorrentino et al., 2010), prompted the need to re-investigate the benefits of adding NA to the conventional first line treatment, i.e. a statin regime. The AIM-HIGH trial (Atherothrombosis Intervention in Metabolic syndrome with Low HDL/High triglycerides: Impact on Global Health Outcomes) studied the impact of

increasing HDL levels with NA therapy in subjects with statin-controlled LDL levels (AIM-HIGH Investigators et al., 2011). This trial was stopped early because of a higher number of ischemic strokes reported among patients in the treatment arm, causing the study's futility boundary to be crossed. The study's design and methodology have since been criticized because of its uncontrolled statin drop-in in the placebo group, which could have masked any beneficial effects of NA in the treatment arm (Nicholls, 2012; Rosenson, 2012).

The AIM-HIGH trial was shortly followed by HPS2-THRIVE (Heart Protection Study 2 Treatment on HDL to Reduce the Incidence of Vascular Events). This was a larger and appropriately powered study (N=25,673 patients at high risk for cardiovascular events) that investigated the potential cardiovascular benefit of NA in combination with statin therapy, versus statin therapy alone (HPS2-THRIVE Collaborative Group, 2013). Similarly, this study did not reach its primary endpoint and no added benefit of NA was found in this population. Moreover, a clear adverse signal for side effects was seen in the treatment arm. These results led the European Medicines Agency to recommend the suspension of all NA-based formulation for the treatment of patients with dyslipidaemia (European Medicines Agency press release, 18th January 2013).

1.3.1.3. NA and HDL: A story ending too abruptly?

The interpretation of the results of these recent clinical studies begs a degree of caution for many reasons. Firstly, there is fierce debate whether the inverse relationship between HDL and CVD is causal (and therefore allowing for therapeutic manipulation) or whether HDL levels are rather an overall risk marker of CVD (van Capelleveen, Bochem, Motazacker, Hovingh, & Kastelein, 2013). The

clinical trials assessing the effects of NA-based HDL-raising strategies assumed a degree of causality, with endpoints relating to HDL levels-based CVD targets (AIM-HIGH Investigators et al., 2011; HPS2-THRIVE Collaborative Group, 2013). Were the relationship not causal, then the benefits of modulating HDL by using NA for CVD prevention are arguably not relevant and this might explain the failure of the clinical trials in meeting their endpoints. Indeed, Mendelian randomization has recently provided evidence that genetically elevated HDL did not protect against myocardial infarction, thereby rejecting the observational causality between CVD and HDL (Voight et al., 2012). In light of this finding, it could be argued that the patient populations used in these trials were not relevant in relation to the possible mechanism of action of NA.

Secondly, although there is no evidence to support it, it is possible that Laropiprant, the additional molecule used in the HSP2-THRIVE to reduce the flushing side-effect, has negative effects that could have counter-balanced NA's benefit.

Thirdly, and as described in 1.3.1, NA manipulates a number of lipid parameters and the clinical trials assessing CVD endpoints have not accounted for all of them, rather focusing on the traditional HDL raising-effect. NA is also described to improve the 'quality' along with the 'quantity' of HDL but measures and mentions of these distinctions are not present in these trials (Sorrentino et al., 2010). Similarly, the triglyceride lowering effect of NA has not been the focus of these trials and neither were NA's anti-inflammatory effects. The latter is of particular interest in light of the reported 1.28 fold excess of gastrointestinal side effects in the treatment arm of HPS2-THRIVE and a 1.22 fold excess of lower respiratory

tract infections, the inflammatory significance of both not being particularly well understood (Rosenson & Gotto, 2013). This is intriguing as there is growing evidence supporting NA's role in vascular inflammation and atherosclerosis progression (reviewed in (Chai, Digby, & Choudhury, 2013a; Digby, Ruparelia, & Choudhury, 2012b; Karpe & Chamas, 2010) and discussed in 1.3.2). There remains much to be learnt about these non-lipid targets of NA and it could be argued that the deficient methods by which the assessment of NA treatment was carried out makes it premature to discount NA as a possible CVD line of treatment.

1.3.2. Effects on inflammation

The current sweeping clinical focus on the anti-inflammatory effects of NA (reviewed in (Chai, Digby, & Choudhury, 2013a)) is a result of the recently highlighted pleiotropic effects of NA (Creider, Hegele, & Joy, 2012; Karpe & Chamas, 2010). Along with the lipid and lipoprotein- modifying cardioprotective effects previously described, NA reduces systemic markers of inflammation such as high-sensitivity C-reactive protein (CRP), monocyte chemoattractant protein-1 (MCP-1), and tumour necrosis factor (TNF-α), and increases adiponectin (J. M. S. Lee et al., 2009; Plaisance, Grandjean, Brunson, & Judd, 2008). The mechanisms by which NA achieves these effects are not understood. However, the co-localisation of the NA receptor HCAR2 (and its homolog HCAR3) in cells that are accessible to *in vitro* experimentation such as adipocytes, keratinocytes, macrophages, neutrophils and Langerhans cells, has led to a surge of research into NA's anti-inflammatory targets (Hanson et al., 2010; Offermanns, 2006).

1.3.2.1. Inflammation and flushing

Earlier studies looking into the receptor's role in inflammation aimed at developing better formulations of NA and reducing cutaneous flushing, which had been a limiting factor for the drug's tolerability (Brinton et al., 2011). The current understanding of the flushing side-effect describes NA-activated cascades in keratinocytes and epidermal Langerhans cells (Dunbar & Gelfand, 2010). In Langerhans cells, NA promotes the release of arachidonic acid and the production of prostaglandin D_2 via cyclooxygenase (COX) enzymes. This leads to the activation of the corresponding prostaglandin receptor (DP_1 and $EP_{2/4}$ receptors) causing vascular smooth muscle relaxation and vasodilatation (Benyo, Gille, Bennett, Clausen, & Offermanns, 2006). Laropiprant, a prostaglandin D receptor antagonist that was developed to mitigate this reaction, fell short of completely eliminating flushing in clinical trials. This indicated the involvement of another unexplored pathway (Lai et al., 2007). Indeed, a similar set of cascades was activated by NA in keratinocytes, which involves cyclooxygenase 2 enzymes (COX-2), prostaglandin E_2 and its corresponding receptor $EP_{2/4}$. Suppressing this cascade in keratinocytes might offer added relief to the existing mode of suppression in the Langerhans cells (Hanson et al., 2010). Mechanistically, current investigations point to the involvement of HCAR2, albeit divergently from its G*i*-coupled anti-lipolytic cascade (introduced in Figure 1)(Walters et al., 2009). HCAR2 is thought to recruit β-arrestin mediators that feed into to some of NA's known downstream effects such as HDL biosynthesis and downregulating the NF-κB inflammation pathway (reviewed in Chai et al., 2013).

1.3.2.2. Anti-inflammatory effects in immune and endothelial cells

Immune cells, such as monocytes, macrophages, neutrophils and dendritic cells all express HCAR2 allowing manipulation of their *in vitro* models to pinpoint the cellular mechanisms responsible for the systemic anti-inflammatory effects seen with NA (mentioned in 1.3.2) (Knowles, Poele, Poole, Workman, & Harris, 2006; Kostylina, Simon, Fey, Yousefi, & Simon, 2008). Considering that monocytes and macrophages and their associated chemokines play a central role in the progression of atherosclerosis (Choudhury, Lee, & Greaves, 2005) the investigations into the role and potential therapeutic applications of NA in these cells have taken centre stage (Digby, Martinez, Jefferson, Ruparelia, et al., 2012a).

In a human monocyte cell line, NA exposure led to a rapid decrease in expression and secretion of pro-inflammatory cytokines of TNF-α, IL-6 and MCP-1 in response to an inhibition of expression of toll-like receptors TLR-4 and TLR-2. Monocytes treated with NA also reduced their pro-atherosclerotic behaviour with a suppression of NF-κB pathway and a reduction of chemotaxis to the vascular endothelium, which are all key events in vascular inflammation. SiRNA targeting *HCAR2* proved that these effects were all receptor-dependent (Digby, Martinez, Jefferson, Ruparelia, et al., 2012a).

Further along the atherogenic progression, and in macrophages, NA has been shown to promote cellular cholesterol efflux to HDL particles by upregulating the expression of ABCA1 transporters (as introduced in 1.3.1.1) (L. H. Zhang et al., 2012). These proteins are also gaining importance in the pathology of vascular inflammation (Lukasova, Malaval, Gille, Kero, & Offermanns, 2011).

Furthermore, in LPS-induced murine macrophages that secrete pro-inflammotary chemokines, NA exposure was shown to reduce the levels of IL-6, TNFα, IL-1β and

IL-12p40. This effect was shown to be HCAR2-mediated and was only seen in activated macrophages – in this case LPS-stimulated – where *HCAR2* mRNA expression had been upregulated in a dose-dependant manner. NA exposure also reduced chemotaxis and LDL uptake into the activated-macrophages, another HCAR2-receptor dependant function (Zandi-Nejad et al., 2013). These anti-atherogenic NA effects observed in cell culture were independent of the previously described lipid-modifying effects and their impact on vascular health. Their exact mechanisms however are still being uncovered, with the NF-κB macrophage activation pathway being central to the investigations(Zandi-Nejad et al., 2013).

1.3.2.3. Anti-inflammatory effects in adipose tissue

Beyond adipose tissue's role in fatty acid storage and release, it is now also recognised as an endocrine organ involved in the secretion of a range of pro-inflammatory adipokines, such as leptin, tumour necrosis factor TNF-α, interleukin IL-6, IL-10, monocyte chemoattractant protein-1 (MCP-1), and the anti-inflammatory adipokine adiponectin. These secretions can influence both local and systemic inflammatory processes that are implicated in the progression of vascular inflammatory disease and atherosclerosis (Spiroglou, Kostopoulos, Varakis, & Papadaki, 2010).

Recently, it has become evident that NA can also influence human adipokine secretion. Adiponectin, a molecule with possible anti-inflammatory and insulin-sensitizing adipokine properties, shows a significant increase in expression after NA administration and this appears to be mediated by HCAR2 (Plaisance et al., 2008). Similarly, RANTES, fractalkine and MCP-1 – all being pro-inflammatory chemokines – are seen to be downregulated with NA (Digby et al., 2010). Increased

secretion of pro-inflammatory cytokines and chemokines contributes significantly to the recruitment of inflammatory T-cells and macrophages into atherosclerotic lesions and progression of vascular inflammation. NA, through its effect on adipose tissue, has the potential to affect both local and systemic inflammation in the context of atherosclerosis progression (Digby, Ruparelia, & Choudhury, 2012b).

Both of the described anti-inflammatory effects in immune cells and in adipose tissue highlight the value of investigating the effects of NA through HCAR2 as a second line of defence in the pathophysiology of atherosclerosis and the prevention of CVD. Indeed, recent clinical studies have demonstrated that adding NA to statin treatment leads to an expected beneficial lipid profile – 19% LDL reduction and 23% HDL increase – along with a significant reduction in carotid atherosclerosis, as measured by imaging studies within 12 months (J. M. S. Lee et al., 2009). While the focus on clinical studies in lipid management might have been exhausted, work on inflammation offers an easier cellular experimentation avenue, and there remains much to be understood about NA's role and the involvement of HCAR2.

1.4. Project aims

Nicotinic acid appears to have disease-preventive hypolipidaemic and anti-inflammatory effects that require further clinical and basic science substantiation. Current knowledge about NA's targets along with HCAR2 cell distribution (summarized in Figure 2) still falls short of predicting its full mechanism of action.

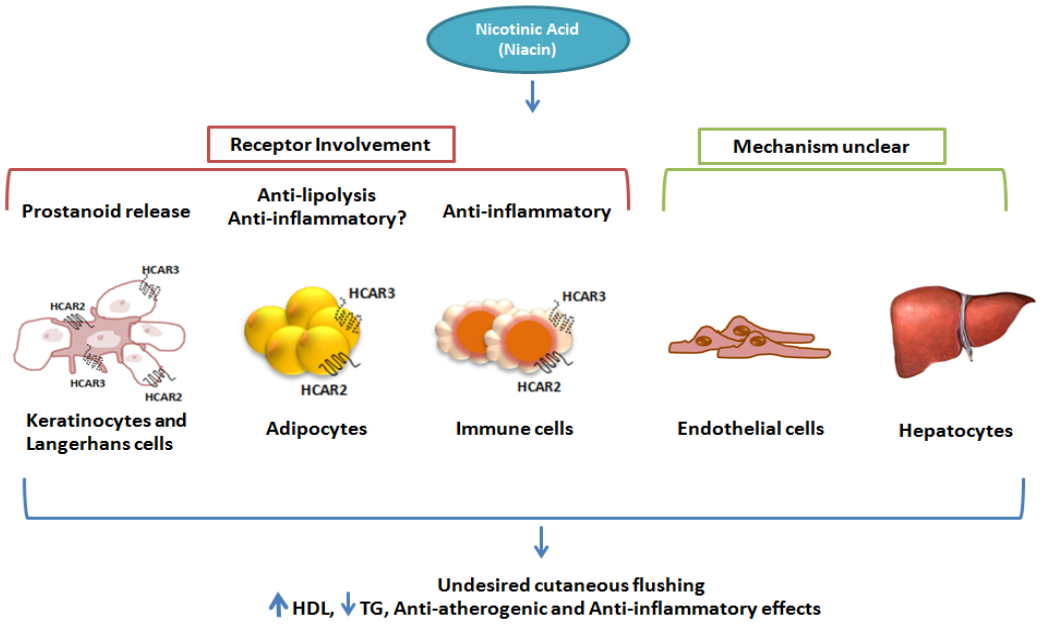

Figure 2:Current understanding of the pleiotropic range of NA's action along with receptors' localization.

The aim of this project was to investigate the functional significance of HCAR2 in adipose tissue. First, and as discussed in Chapter 3, genetic variability in and around the genomic region of *HCAR2* and its 96% homologue *HCAR3* has not been properly described. Existing sequence analysis performed on *HCAR2* to identify putative single nucleotide polymorphisms (SNPs) for genotypic and phenotypic analysis appeared to be flawed by the high degree of homology with *HCAR3*. SNPs that were identified from the National Centre for Biotechnology Information SNP

database seemed to consider the base differences between the two genes as polymorphisms. This reinforces the need for deep resequencing in order to properly identify SNPs that will discriminate between the two genes and offer haplotype information that could show relevant association with lipid metabolic phenotypes (Zellner, Pullinger et al. 2005). I hypothesize that adequately assessed interindividual genetic variability would uncover relationships with the receptor's ligands and known systemic targets. In particular, deep resequencing of the receptor and its homolog as presented in Chapter 3 would also further the exploration of specific genetic variants of interest and the resulting phenotypes as shown in Chapter 4.

Secondly, as described in Chapter 5, I aimed to characterize at the transcript level both *HCAR2* and its homologue *HCAR3* in adipose tissue and relate them to metabolic parameters. Transcriptional characterization is important since the receptors are mainly expressed in adipose tissue, and key adipose tissue genes have displayed transcript differences based on depots, gender and BMI that translate into general metabolic health (Tchkonia et al., 2006). Furthermore, and as described in Chapter 5, earlier attempts to measure *HCAR2* and *HCAR3* transcripts did not differentiate between the two genes, prompting the need for method development to ensure that the specific transcripts of choice was targeted.

Finally, *in vitro* exploration of the role of the NA receptor in modulating inflammation have either focused on immune cells or on adipocyte models that do not express its homolog *HCAR3*. A further aim was therefore to explore the role of HCAR2 and the potential involvement of HCAR3 by choosing human primary pre-adipocytes isolated and differentiated from biopsies that express both receptors.

In Chapter 6, I present and discuss the results and challenges of these investigations.

Chapter 2 General Methods

2.1. The Oxford Biobank (OBB)

The Oxford Biobank is a register of more than 6000 healthy people aged 30-50 year old and resident of Oxfordshire and is part of the National NIHR BioResource (http://bioresource.nihr.ac.uk/). Anthropometric, metabolic and biochemical data has been recorded for all subjects. This includes serum samples for various biochemical and metabolic measurements as well as whole blood for the extraction of genomic DNA. A subset of the individuals in the OBB have also given adipose tissue biopsies from abdominal and gluteal subcutaneous depots. Unless stated otherwise, the OBB was used as the main resource for tissue and DNA work in this thesis. DNA and tissue samples from the OBB have been pre-processed by the technicians in the group and stored at -80°C until needed unless indicated differently.

2.2. DNA samples

2.2.1. DNA extraction

OBB genomic DNA was extracted by LGC Genomics (Hoddeston, UK) from whole blood samples. This was stored at -80 °C and later arrayed for genotyping (Chapter 4) or amplified with polymerase chain reactions (PCR) to create positive controls to test the specificity of PCR products and the long range and nested PCR amplification for re-sequencing (Chapter 3), as well as controls for gene expression and genotyping assays (Chapter 3,Chapter 4). Specifics of PCR parameters used will be described in the related chapters.

2.2.1. Genotyping on genomic DNA

Genotyping was performed using Taqman® technology (Life Technologies, Paisley, UK) and KASP™ genotyping technology (LGC Genomics, Hoddesdon, UK) on genomic DNA extracted from the OBB unless otherwise stated. Based on both companies' technical bulletins, the Taqman® technology employs two unlabelled primers (one forward, one reverse) and two labelled probes to detect the allele differences in a sample. KASP™ genotyping technology on the other hand, uses two unlabelled competing forward primers and one reverse along with unlabelled probes for accurate allele detection. The absence of a fluorescent label on the primers and probes is cost effective and allows for greater flexibility in assay design and targeting complicated regions. Rather, the fluorescent label that is detected upon amplification is in the master mix and binds to a universal sequence on the forward primer complimentary to the allele in question.

The samples to be genotyped were diluted in nuclease-free water to a concentration of 5ng/µl and 10ng of each was plated on 386 well plates (4titude, Wotten, UK) along with appropriate non-template controls and dried by incubating at 80°C for 10 minutes. The genotyping assays amplified the selected genomic region in the presence of differentially labelled fluorescent probes (VIC/FAM) specific to the two possible alleles as described in the previous paragraph.

2.2.1.1. Assay Design

When there was no doubt about the effects of homology on the functioning of the genotyping assays (will be further explained in Chapter 3), inventoried Taqman® genotyping assays were obtained from Life Technologies (Paisley, UK). Assay details are provided in the relevant chapters. When sequence homology between

genes was thought to affect specificity of primers and probes in detecting the required transcripts, assays were designed using genomic sequence obtained from the National Centre for Biotechnology Information (NCBI) and double-checked with results from in-house deep resequencing (Chapter 3). Designed primer/probe mixes were synthesised and validated by LGC Genomics (Hoddeston, UK).

2.2.1.1. Assay Design- MfeI assay

There was a need early on in the project to distinguish with certainty that specific amplification of the genes in question was achieved. Zellner et al. had previously developed a restriction fragment length analysis method with discriminating restriction digests that confirmed selective amplification of each of *HCAR2* and *HCAR3* (Zellner et al., 2005). The use of the described primers in our hands lead to unspecific amplification of both genes rather than the one sought after (seen as the products with unspecific old primers in Figure 4). We therefore needed to develop a quick and reliable method of verifying our own selective amplifications. Since restriction isotyping can detect allele differences down to a base pair, the method was selected to detect differences between PCR products for *HCAR2* and *HCAR3*.

The developed assay detects the Thymine base (T) in the previously described MfeI restriction palindrome site unique to HCAR3. Using the KASP™ genotyping technology detection system, it allows clear distinction between the two different products amplified from the two gene regions since HCAR2 lacks the base pair in question. Figure 3 shows a graphic depiction of the region the genotyping assay was based on.

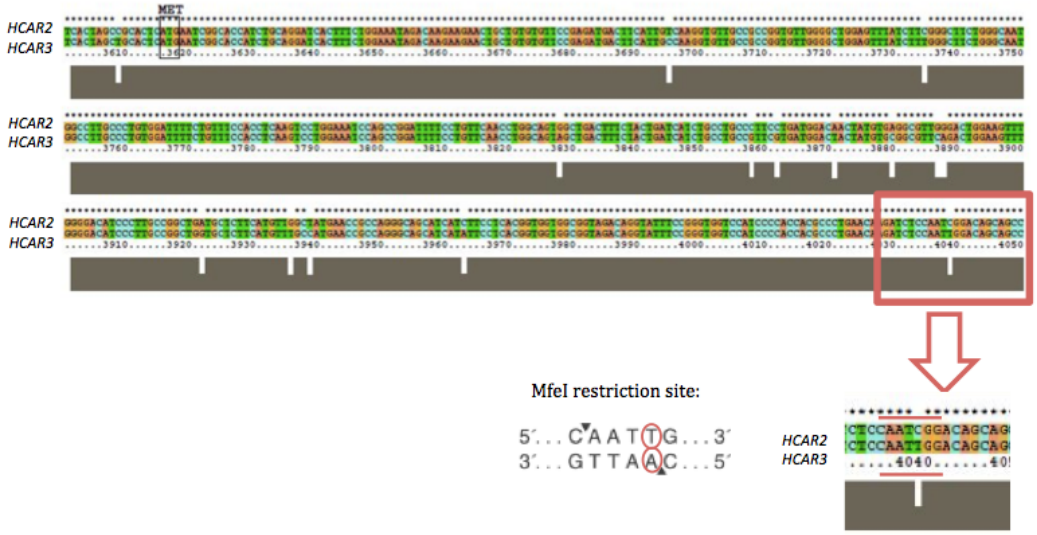

Figure 3: Clustalx alignment showing a close-up of a known MfeI RFLP on the basis of which the specificity genotyping was designed.

The assay serves as a checkpoint to verify that the specificity of PCR products for either gene for sequencing (Chapter 3) and the gene expression assays (Chapter 5), and was run after the samples in question were amplified using PCR and diluted 1/1000 in 0.01M Tris buffer. The samples were run with some of the unspecific products created with previous primers. These were visualized as a heterozygous reading on the allelic discrimination plots since they contained both HCAR2 and HCAR3 products (therefore both the T and C alleles). Negative controls (Tris samples) and unspecific PCR products created with primers specific for GAPDH that do not encompass the MfeI genotyping site were also included.

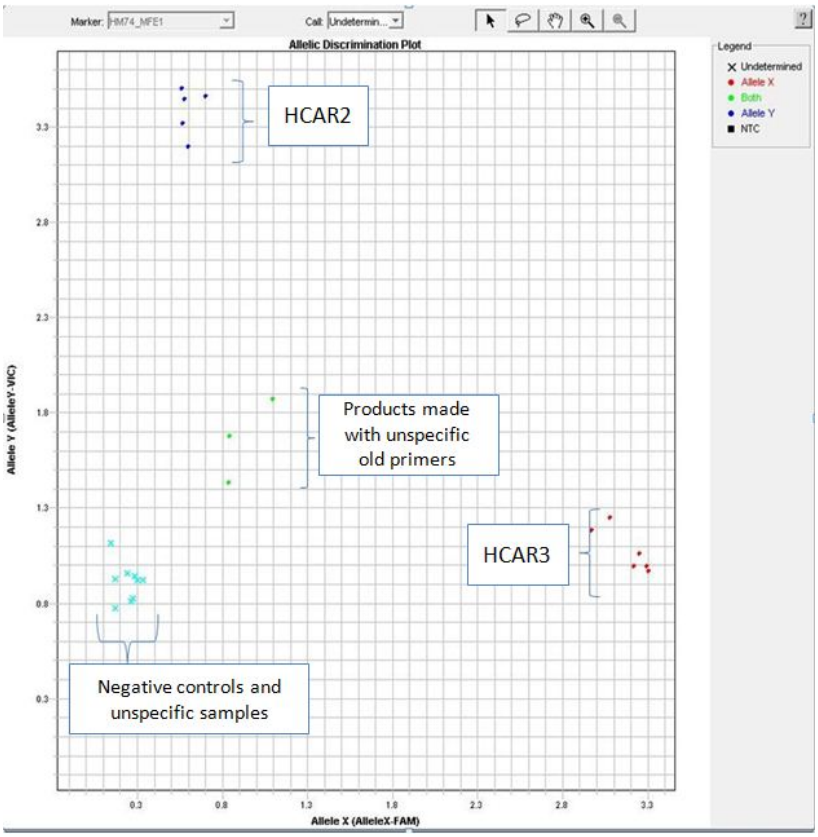

Figure 4: Example of MfeI-based genotyping cluster plot as produced by SDSv2.3 software.
FAM (G allele) fluorescence (x-axis) is plotted against VIC (A allele) fluorescence (y-axis). Red points represent TT homozygous samples or presence of HCAR3 product; blue points represent CC or presence of specific HCAR2 product while mixed products made with unspecific primers are green points heterozygotes.

2.2.1.1. Genotyping Reaction

Reactions were conducted in a 4µl volume, comprising 2µl genotyping mastermix (containing polymerase and dNTPs, LGC Genomics, Hoddesdon, UK), 1.95µl nuclease-free water and 0.05µl assay. After brief centrifugation, samples were heated to 95°C for 10 minutes (polymerase activation) and underwent 40 or 50 cycles (detailed in relevant chapters) comprising: 92°C for 15 seconds (DNA melting) and 60°C for one minute (combined annealing and extension step).

2.2.1.2. Genotyping determination

When the genotyping reactions were done, the plates were centrifuged and genotype of samples was determined through post-read allelic discrimination on a Life Technologies, Paisley, UK 7900HT machine, using SDSv2.3 software and standard analysis settings. Genotypes were assigned according to proprietary algorithms, but visually checked. When necessary, some genotypes were reassigned if the clustering was visually easy to dissect and when needed a second opinion from a postdoctoral colleague was sought. Each genotyping plate included at least three sample duplicates and three non-template control (NTC) wells (containing nuclease-free water or Tris). Results were discarded if NTCs showed a signal or if the duplicates were discordant.

2.2.2. Primer design

Forward and reverse primers for PCR reactions were designed using the National Centre for Biotechnology Information (NCBI) web-based software Primer-BLAST (http://www.ncbi.nlm.nih.gov/tools/primer-blast/). Corresponding gene sequences were obtained from NCBI and the University of Santa Cruz Genome Bioinformatics website (http://www.ncbi.nlm.nih.gov/gene/ and http://genome.ucsc.edu/). Primer pairs were initially selected based on length (18-27bp), desired amplicon length, melting temperature (55°C-65°C) and guanine and cytosine (GC) content (40-60%). When the design encompassed a polymorphic site, it was noted and replaced with the corresponding IUPAC code to amplify all existing variants of the sequence in question. For sequencing, Universal M13 tags (F- TGTAAAACGACGGCCAGT, R-CAGGAAACAGCTATGACC) were added to the primers in question as required by the protocol. Primers were synthesized by Sigma-Aldrich Co (Gillingham, UK).

2.2.3. PCR validation with Gel electrophoresis

Agarose gel electrophoresis confirmed the synthesis of the expected PCR products. The concentration of agarose in the gel was determined by the size of the expected products determined. Larger products were run in a 0.8% gel by dissolving agarose (Sigma-Aldrich, Gillingham, UK) in a 1X Tris/Borate/EDTA (TBE) (NBS Biologicals, Huntingdon, UK) in a 800 W microwave for 3 minutes. After cooling for about 10 minutes, the intercalating agent Ethidium Bromide (Sigma-Aldrich, Gillingham, UK) was added to a final 0.002% concentration. The volume of the gel depended on the number of samples to be run. A standard small gel contained 1.2g agarose, 150ml of TBE and 2µl ethidium bromide. Reagents were scaled according to the size of the gel. Gels were set in moulds containing combs of an appropriate well size and spacing (Appleton Woods, Birmingham, UK) and then covered with 1X TBE (NBS Biologicals, Huntingdon, UK).

5µl PCR product was added to 5µl Orange G loading buffer (4g sucrose in 10ml nuclease-free water and 20mg Orange G [Sigma-Aldrich, Gillingham, UK]) and then loaded to a sample well in the gel. Similarly, 4µl (0.2µg) of 1kb DNA ladder (New England BioLabs, Hitchin, UK) was loaded as a reference. For the smaller gels and PCR products around 4Kb, an electrical current of 80V was passed through the gel for 40 minutes to allow fragment visualization. Gels were visualized using Ultra Violet technology (UV) on a Gel Doc 2000 illuminator system and Quantity One v4.3.1 software (both BioRad, Hemel Hempstead, UK).

2.2.4. DNA Sequencing

The Life Technologies, Paisley, UK BigDye v3.1 Cycle Sequencing Kit was used. This kit adopts a modified version of the chain termination Sanger sequencing method.

It includes fluorescently-labelled dideoxynucleotide triphosphates (ddNTPs), which lack a 3'-hydroxyl group and are therefore unable to form a phosphodiester bond with subsequent nucleotides in an extending DNA sequence. The resulting PCR products incorporate universal M-13 tails from the specific M-13 sequencing primers (F- TGTAAAACGACGGCCAGT, R-CAGGAAACAGCTATGACC). Each ddNTP has a different fluorescence emission spectrum, allowing premature chain termination at each nucleotide to be determined via capillary electrophoresis. (Rosenblum et al., 1997; Sanger, Nicklen, & Coulson, 1977; L. M. Smith et al., 1986).

2.2.4.1. Initial clean-up of PCR products

Clean up was performed to remove residual PCR contaminants of the products to be sequenced. Exonuclease I (EXO, New England Biolabs UK Ltd) and shrimp alkaline phosphatase (SAP, Promega UK Ltd) were combined in a 10:0.5 unit ratio of each enzyme respectively per µl. One microlitre of this mix was added to 1µl of PCR product, mixed gently and centrifuged briefly. This mixture was then incubated at 37°C for 30 minutes and then heated at 80°C for 15 minutes to denature the enzymes.

2.2.4.1. Sequencing reactions

The sequencing reactions each contained 2µl of the clean-up reaction (1µl of PCR product + 1µl of EXO:SAP) and 8µl of master mix following the manufacturer's instructions (Table 2). Sequencing primers that were added were complementary to the M13-tailed PCR products. The sequencing reaction was run for 25 cycles of 96°C for 10 seconds, 50°C for 5 seconds and 60°C for 4 minutes. Sequencing products were then centrifuged briefly and 5 µl of nuclease-free water added to each sample.

Reagent	Volume in reaction (µl)
Big Dye Terminator Sequencing Mix v3.1	0.25
Big Dye Dilution Buffer	1.88
M13 sequencing primer (2.5 µM)	2.00
Nuclease-free water	3.88

Table 2: Big Dye Sequencing Reagents

2.2.4.2. Sequencing product clean-up

To remove residual sequencing contaminants, samples were passed through a 96-well Performa DTR V3 short clean up plate according to manufacturer's protocol (VH Bio, Gateshead, UK) by centrifugation (850xg for 5 minutes). Eluent was collected and heated at 70°C for 90 minutes to dry down.

2.2.4.3. Capillary electrophoresis and analysis

Samples were sent to the university's core sequencing facility at the Department of Zoology where they were sequenced using capillary electrophoresis (ABI3730xl DNA Analyzer, standard run module, 15 seconds injection, v3.1 dye set and analysis module). Fluorescence from the ddNTPs was converted into .ab1 output files and visualized using Mutation Surveyor v3.4 (Soft Genetics, Cambridge, UK).

2.3. RNA samples

RNA samples were obtained from both human biopsies to study adipose tissue gene expression (Chapter 3) and from differentiating pre-adipocytes obtained from biopsies (Chapter 6).

2.3.1. Adipose tissue biopsies

The taking of human adipose tissue samples was approved by the Oxfordshire Clinical Research Ethics Committee and all subjects gave written, informed consent. The biopsies were taken by a nurse or clinician following an established protocol that ensured consistency between operators. Using a 12 gauge needle and syringe

under local anaesthetic, paired subcutaneous adipose tissue biopsies of healthy volunteers were obtained from abdominal subcutaneous AT (taken from the abdominal wall about 2 inches away from and at the level of the umbilicus) and gluteal AT (taken from the upper outer quadrant of the buttock). For the isolation of preadipocytes, the biopsy was immediately transported on ice to the laboratory otherwise it was processed for RNA extraction.

2.3.1. Adipose tissue processing before RNA extraction

Adipose tissue samples were either snap-frozen in liquid nitrogen immediately after the biopsy was taken and stored at -80ºC or extracted straight away. At extraction, samples were rapidly weighed and transferred to 2ml tubes (Eppendorf, UK) containing a "coneball" ball bearing (Retsch, Leeds, UK) and 1ml Trizol (Life Technologies, UK). Tissues were homogenized for 1.5 minutes at a frequency of 25 Hz on a Mixer Mill MM 400 free standing homogenizer (Retsch, Castleford, UK). Lysate was transferred to a clean 1.5ml RNase-free tube (Life Technologies, UK) and centrifuged at 12,000xg for 20 minutes (4˚C) to pellet any insoluble fragments and separate a lipid layer. The homogenate fraction was removed by pipette through the upper lipid layer and transferred to a clean 1.5ml RNase-free tube with 200µl chloroform (FisherScientific, Loughborough, UK).

2.3.2. RNA extraction

When RNA needed to be extracted from cell culture, the cells in question were initially washed with PBS (Sigma Aldrich, Gillingham, UK) and then scraped in 500µL of Trizol (Life Technologies, Paisley, UK) and stored at -80°C until extraction. Otherwise, both the tissue samples and cell culture samples were extracted the same way. After adding 100µl chloroform, tubes were shaken

vigorously by hand for 15 seconds to begin organic and aqueous phase separation, before incubation at room temperature for 5 minutes. Phase separation was completed by centrifugation at 12,000xg for 15 minutes (4˚C), producing a pink organic phenol phase at the base of the tube, a white interphase containing DNA and a clear top aqueous phase containing RNA. The aqueous phase was transferred by pipette to a clean 1.5ml RNase-free tube, and an equal volume of isopropanol (Fisher Scientific, Loughborough, UK) was added to precipitate the RNA. After incubation for 5 minutes at room temperature with repeated inversion, the solution was stored overnight at -20˚C. The following day, samples were centrifuged at 12,000xg for 15 minutes (4˚C) to pellet RNA. The liquid phase was removed carefully, ensuring the pellet was not dislodged, and 1ml 75% ethanol (Sigma Aldrich, Gillingham, UK) was added to wash the pellet. After centrifugation at 12,000xg for 15 minutes, the same procedure was repeated with 1ml fresh 75% ethanol. The final ethanol wash was removed and the RNA pellet allowed to air dry for 10 minutes, before re-suspension in at least 12µl RNase-free water.

2.3.1. RNA quantification

Resuspended RNA was left to equilibrate in RNase-free water overnight and quantified the next day by spectrophotometry using the Nanodrop ND-1000 Spectrophotometer (ThermoScientific, UK) and following the manufacturer's manual. This allows quick assessment of absorbance at wavelengths of 230, 260 and 280nm. RNA with a 260/280 ratio in the range 1.7-2.1 and a 230/260 ratio in the range 1.5-2.2 is thought to be of acceptable purity for further analysis and quantification.

Briefly, RNase-free water was used to initially blank the instrument. The function for measuring nucleic acids and RNA was selected and1µl of each sample was loaded onto the pedestal. Following the absorbance recorded, the instrument gives the calculated value of nucleic acids in the sample along with the purity ratios. The concentration of RNA in the sample is then noted for each sample and they are stored at -80˚C until cDNA synthesis.

2.3.2. cDNA synthesis

cDNA was synthesized from extracted RNA to quantify mRNA transcripts of desired genes (Chapters 5 and 6). Single stranded cDNA was generated following manufacturers protocol using the High Capacity cDNA Reverse Transcription Kit containing the MultiScribe™ Reverse Transcriptase (Life Technologies, UK). Briefly, 500ng of RNA diluted in 10µl of nuclease-free water was mixed with 10µl of the master mix containing the reverse transcriptase, random primers, buffer and dNTPs in volumes outlined in the table below. This was done on ice until the samples were moved to the PTC-225 Peltier Thermal-Cycler (MJ Research, Waltham, Massachusetts, USA) and the cycling program was started. The first step consisted of a 10 minutes incubation at 25 °C to anneal the primers and then 37 °C for 120 minutes to generate the cDNA.

Component	**Volume/Reaction (µl)**	
	Kit with RNase Inhibitor	**Kit without RNase Inhibitor**
10x RT Buffer	2.0	2.0
25x dNTP Mix (100 mM)	0.8	0.8
10x RT Random Primers	2.0	2.0
MultiScribe™ Reverse Transcriptase	1.0	1.0
RNase Inhibitor	1.0	-
Nuclease-free H2O	3.2	4.2
Total per Reaction	10.0	10.0

Table 3: Reaction components for Reverse transcription

2.3.3. Taqman gene amplification

Gene expression was quantified using quantitative (real-time) PCR (qPCR) and Taqman chemistry (Life Technologies, Paisley, UK). Taqman probes have a fluophore and quencher attached to their 5' and 3'ends in close enough proximity to prevent fluorescence emission. During PCR, the exonuclease activity of Taq polymerase releases the fluophore from its quenched state when the specific cDNA template is present. This makes the fluorescent levels directly proportional to the quantity of the specific template cDNA amplified. When fluorescence reaches a critical threshold during the exponential phase of the PCR, specific template cDNA and the initial mRNA concentration can therefore be inferred (Holland, Abramson, Watson, & Gelfand, 1991).

When issues of gene homology were not of concern, inventoried assays were obtained. These were all FAM-labelled. When possible, they were selected to encompass an exon-exon boundary in order not to result in unspecific amplification of contaminating genomic DNA. Negative controls were included in all the reactions and the results were discarded if they resulted in amplification.

2.3.3.1. Housekeeping gene selection

Gene expression was quantified using the 'relative gene quantitation' method whereby the gene of interest is expressed relative to an invariant endogenous control transcript or transcripts (Pfaffl, 2001). For all of the adipose tissue work, peptidylprolyl isomerase A (*PPIA*) and phosphoglycerate kinase 1 (*PGK1*) were used as endogenous controls as they have been proven the most consistent (Table

4) (Neville, Collins, Gloyn, McCarthy, & Karpe, 2010). The average of the two housekeeping genes was used as a 'normalization factor' for the results.

Gene	Housekeeping gene assay ID
PPIA (peptidylprolyl isomerase A)	Hs99999904_s1
PGK1(phosphoglycerate kinase 1)	Hs99999906_g1

Table 4: Housekeeping genes Assay ID

2.3.3.2. Standard curve generation

In order to calculate amplification efficiency, a standard curve was generated from serial dilutions of pooled samples. Pools were created by taking an equal volume from each cDNA sample (usually 1-3µl) and diluted in 0.01M Tris buffer (pH=8). Around five concentrations were generated to fit around the dilution of the sample cDNA in the experiment. For example, if the sample cDNA was diluted at 1:50, dilutions were generated at 1:10 to 1:250. Fresh standards were generated for each experiment.

2.3.3.3. Reaction Components

Reactions were performed in a final volume of 6µl comprising 2.7µl of diluted cDNA, 0.3µl of assay and 3µl of mastermix (Life Technologies). Samples and standards were always run at the same time and in triplicate.

Thermal cycling and fluorescence detection was performed on an ABI7900 HT using the following amplification programme: 95°C for 10 minutes followed by 40 cycles of 95°C for 15 seconds and 60 °C for 1 minute.

Every amplification cycle ended with a fluorescence reading on the Life Technologies, Paisley, UK 7900HT machine. These were analyzed using SDSv2.3 software (Life Technologies, Paisley, UK) by selecting the comparative threshold

point (C_T) at which fluorescence levels were increasing exponentially for all samples and the efficiency of the reaction was optimal.

2.3.3.4. Analysis

When assays were not previously tested on the specific samples in hand, a trial run was performed with a range of concentrations from a pool of the samples to minimize wasting and to assess the performance of the cDNA dilution. An assay was deemed not working if there was no amplification detected after 35 cycles at 1:10 dilution.

mRNA was quantified using the $\Delta\Delta C_T$ method (Pfaffl, 2001). Briefly, C_T values for target genes were calibrated to a calibrator value ($CalC_T$), determined as the lowest C_T value from all of the samples, using the formula:

$$\Delta C_T = E^{(CalC_T - C_T)}$$

where assay efficiency E is

$$(10^{\frac{-1}{slope}}) - 1$$

and the slope refers to the gradient where C_T (x axis) was plotted against log(dilution)of the standards. The resulting ΔC_T was normalized by dividing by the corresponding ΔC_T of the endogenous housekeeping gene. The normalized value $\Delta\Delta C_T$ was used for all of the analysis.

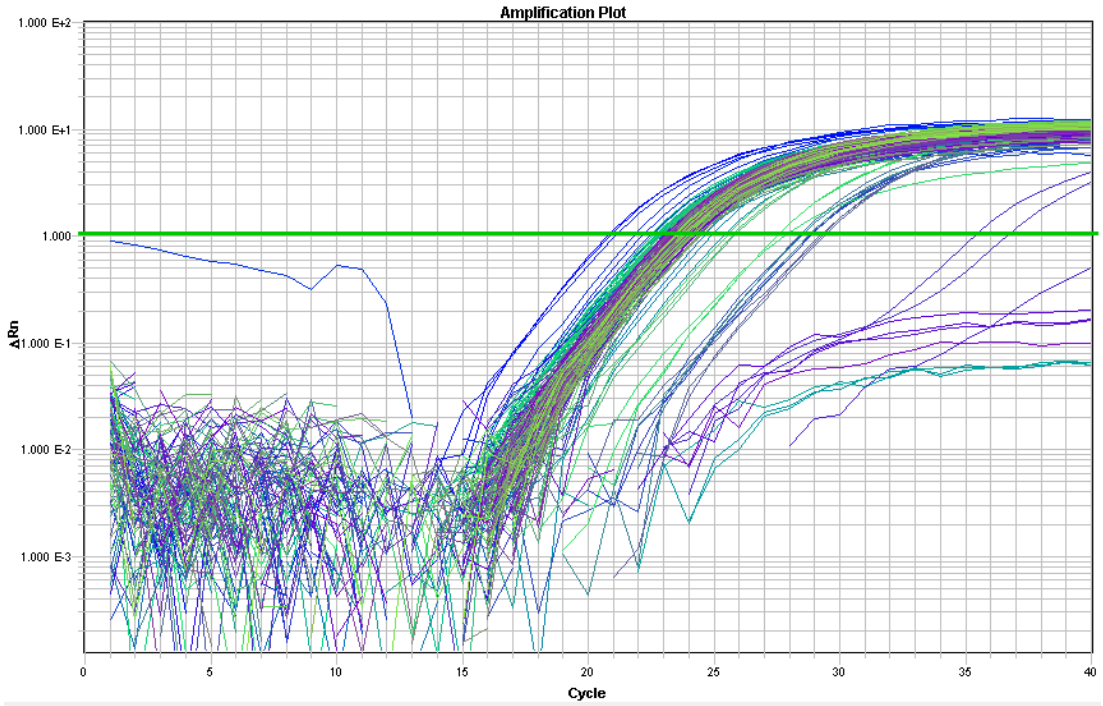

Figure 5: Example amplification plot for mRNA quantification (*PPIA*).
PCR cycle number (x-axis) is plotted against normalised fluorescence intensity (y-axis). As amplification of specific transcripts occurs, fluorescence intensity increases proportional to the starting quantity of transcript. The green horizontal line represents the critical threshold, as set by SDSv2.3 software during the exponential phase of the reaction. C_T score is the x-axis value where the amplification curve for each sample crosses the critical threshold – in this case, between 18 and 25 cycles.

2.4. *In Vitro* experiments

2.4.1. Preadipocytes isolation for cell culture

Adipose tissue from biopsies was mechanically minced using scissors, washed twice with Hank's buffered salt solution (HBSS) to remove contaminating blood, then enzymatically digested in 1mg/ml collagenase (Roche, Burgess Hill, UK) in HBSS in a shaking water bath (60 rpm) at 37 °C for 45 minutes. The digested tissue was centrifuged at 1000 rpm for 5 minutes at 4 °C. The buoyant mature adipocytes and supernatant were removed, and the pellet containing the stromal-vascular cells resuspended in growth medium (Dulbecco's Eagle's Medium Nutrient Mixture (DMEM)/F12 HAM (v/v, 1:1), 10% foetal calf serum (FCS)

(Invitrogen, Paisley, UK), 1 µl/100 ml fibroblast growth factor (FGF), 100 U/ml penicillin and 0.1 mg/ml streptomycin). The resuspended cells were filtered twice through nylon mesh (SEFAR, Bury, UK), firstly with pore size 250 µm, then through 100 µm to remove any large cells. The filtered cells were centrifuged again at 1000 rpm for 5 minutes at 4 °C, the supernatant removed and resuspended in growth medium. Cells were plated in tissue culture flasks. After one day, contaminating red blood cells were washed off with phosphate buffered saline (PBS, Sigma Aldrich, Gillingham, UK) and medium replaced. Preadipocytes were passaged up to three times before being used for experiments.

2.4.2. Preadipocyte differentiation

When the preadipocytes reached about 80% confluence, a differentiation regime for 14 days was started. This consisted of a standard differentiation medium adapted from the method of Hauner *et al.* (Hauner et al., 1989), consisting of Dulbecco's Modified Eagle's Medium/Nutrient Mixture F-12 Ham (DMEM/F12 HAM) (1:1) containing 2 mM glutamine, 17 µM pantothenate, 100 nM human insulin, 1 nM triiodo-$_L$-thyronine (T_3), 33 µM biotin, 10 µg/ml transferrin and 1 µM dexamethasone. 3-Isobutyl-1-methylxanthine (IBMX) (250 µM) and Troglitazone (2 µM) were added for the first 3 days and culture medium was changed every other day. The differentiating cells were examined under a light microscope for presence of lipid droplets and differentiation capacity was further established by measuring gene expression of key adipogenic transcription factors (PPARγ and C/EBPα) and adipocyte markers (Leptin)(Rosen & Spiegelman, 2000). When looking at differentiation in primary adipocytes, some differences between depots were seen, however those were not consistent. Bigger

differences in differentiation potential were seen between individuals and will be further discussed in Chapter 5.

2.4.3. ELISA

A Sandwich Enzyme-Linked Immunosorbent Assay (ELISA) kit was used to measure concentrations of low levels of secreted protein in the cell supernatants (Chapter 6)(R&D Systems, Abingdon, UK). The Sandwich employs a sensitive alkaline phosphatase amplification system that leads to the formation of a coloured product suitable for colorimetric detection. Interleukin 6 (IL-6) presence was assayed from the cell culture supernatants using the Human IL-6 Quantikine HS Enzyme-Linked Immunosorbent Assay kit (R&D Systems, Abingdon, UK). It is a 5.5 hour solid-phase assay that contains an *E. coli*-expressed recombinant human IL-6 with a detection limit of 0.156 - 10 pg/mL.

Supernatants from cell culture wells (200µL) were collected after appropriate incubations and snap-frozen at -80°C until ready to run the assay. Sample supernatants are deposited in wells coated with an antibody for the protein to be measured. After an adequate time incubation, an amplifier solution containing a secondary antibody also complementary to the protein sought binds to the previous antibody-protein complex. The final addition of substrate solution to initiate the colourometric detection followed by a stop solution to halt the reaction before recording the absorbance of the formed coloured product at the suitable wavelength. All the samples are run with an appropriate standard dilution that comes with the kit and allows calibration of the result with a standard curve. These curves are generated for each set of samples assayed, and when possible, samples of one experiment were assayed together on the same plate and in duplicate.

2.4.4. Protein concentration determination

After removal of supernatant, cells were washed with PBS (Sigma Aldrich, Gillingham, UK) followed by 0.5ml of Radio-Immunoprecipitation Assay Buffer RIPA before scraping the cells (Sigma-Aldrich Co, Gillingham, UK). The buffer solubilised the proteins and samples were stored at -80°C while waiting to be measured.

Total cellular protein was determined using the QuantiPro™ Bicinchoninic assay (BCA) assay kit (Sigma-Aldrich Co, Gillingham, UK). The kit is based on an assay similar to the Lowry procedure where a reduction of Cu^{2+} to Cu^{1+} under alkaline conditions is detected proportionally to the absorbance readings with a spectrophotometer. The BCA/copper complex is water-soluble, shows a strong linear absorbance at λ = 562 nm proportional to protein concentrations and is highly sensitive. A Bovine Serum Albumin (BSA) standard was used with a working range of 25–2000 µg/ml. The other reactants were part of the kit and were 1% SDS as the diluent and the BCA working reagent in a final volume of 2.1 ml. The tubes were incubated at room temperature for 30 minutes and read at λ = 562 nm. A standard curve was constructed for each set of samples to calibrate and allow the determination of protein concentration.

2.5. Statistical analysis

All statistical analysis was performed in SPSSv18.0 (PASW statistics 18). In Chapter 4, group differences were analyzed using linear regression, Kolmogorov-Smirnov and Kruskal-Wallis tests. Differences between paired adipose tissue samples in Chapter 5 were analyzed using the related samples Wilcoxon signed rank test. Metabolic associations in Chapter 5 were correlated using Spearman rho

correlation test for non-parametric variables and the Pearson correlation coefficient when data were normally distributed. Regression analysis was used to predict outcomes with statistical significance was defined as $p<0.05$ for all tests.

Chapter 3 Deep Resequencing of *HCAR2* and *HCAR3*

3.1. Difficulties in duplicons

Five percent of the human genome comprises DNA stretches longer than 1kb in sequence with over 90% similarity to other regions of the genome, referred to as segmental duplications or duplicons (Venter et al., 2001). Genes located in these duplicons are challenging to study not only because of concerns regarding unspecific off-target amplification and detection of homologous transcripts (Ghani, Sato, & Rogaeva, 2013), but also because much of the sequence variation in these duplicons is poorly understood (Estivill, Cheung, Pujana, Nakabayashi, Scherer, & Tsui, 2002a).

A recently described artefact of overlooked off-target amplification explains the first instance well: 65-70% of the sequences of the popular housekeeping genes *GAPDH* and *β-actin* can be found elsewhere in the genome due to segmental duplication events. These two genes can therefore be amplified at different genomic loci in qPCR in case of gDNA contamination, leading to the documented unreliable levels of transcripts detected (Ghani et al., 2013).

Similarly, previous investigations into sequence variations or polymorphisms in duplicons found that these variations are over-reported by a factor of 2 and are better explained as single nucleotide differences (SNDs) between the homologous sequences (Bailey et al., 2002; Estivill, Cheung, Pujana, Nakabayashi, Scherer, & Tsui, 2002b; Fredman et al., 2004). Sequencing small fragments when using next generation sequencing does not easily discriminate between homologous sequences since fragments do not always 'bridge' into unique sequence features.

This has resulted in erroneous labelling and overestimation of either variants or nucleotide differences as will be illustrated in section 3.6 (Musumeci et al., 2010).

With the known increased gene density in duplicons (Gut & Lathrop, 2004), the mismatch between nucleotide difference annotations and SNPs, and the implications for genotyping and association studies, there is a need to better explore sequence variation in duplicons.

3.2. Not all validated sequence variation is verified

The current NCBI dbSNP (build 137, Jun 26, 2012) reports 53,558,214 reference SNPs (rs) in *Homo Sapiens* of which 38,077,993 (or 71%) are validated. At the start of this project in October 2009, the NCBI dbSNP (build 130, April 30, 2009) reported a much lower number of 17,804,034 reference SNPs in *Homo Sapiens*, of which 6,573,584 were validated (or 36%). Efforts using bioinformatics and experimental methods have identified that as many as 8% of the previously validated SNPs in dbSNP are rather sequence variations between two highly homologous duplicated sequences (Musumeci et al., 2010). With the number of submission and validations having almost doubled, the chances of erroneous validated labelling in duplicons have doubled as well. The duplicated gene nucleotide database (dbDNV) recently tried to address this issue by meticulously aligning homologous sequences covering over 10% of known genes and cataloguing duplicated region variants in the database (Ho, Tsai, Chen, & Lin, 2011). When the work on our project commenced in 2009, there was no such known effort and since most of the validated SNPs at the time escaped the duplicated areas of the genome (Fredman et al., 2004), there was added value of

resequencing duplicated genes of interest to differentiate SNPs from SNDs in my gene of interest.

3.3. Examining variation in *HCAR2* and *HCAR3*

Shortly after the identification of the nicotinic acid receptor in 2003, Zellner *et al.* published a paper exploring coding region variation in *HCAR2* and *HCAR3.* It similarly argued that in light of the high homology in the coding region of both genes, and their genomic location in a duplicated area (as discussed in 1.1.4), it was unlikely that existing characterization of the polymorphisms was accurate. The study re-evaluated these polymorphisms by developing a method to selectively amplify and resequence each specific gene product independently in 77 unselected individuals. The results showed that 12 out of 17 SNPs in the coding region of *HCAR2 i*n the corresponding dbSNP build (NCBI dbSNP, Build 121, June 1, 2004; www.ncbi.nih.gov/SNP) were spurious. Furthermore, haplotype assembly of the verified SNPs, showed that *HCAR2* and *HCAR3* belong to a single haplotype block. This meant that most of the variation in the two genes and 90% of the established haplotypes in the coding region could be tagged by choosing to genotype on variants from 5 major haplotypes (Zellner et al., 2005).

In this chapter I focus on expanding Zellner's work and extending the exploration of the variants in the nicotinic acid receptor and its homolog beyond the coding region. Specifically, I was looking to test whether any variants had effects on anthropometric variables in the OBB related to lipid metabolism and inflammation.

Early work to replicate Zellner's method showed that the primers used to create specific *HCAR2* and *HCAR3* PCR products were unspecific in my hands. My project therefore began by redesigning and testing new specific primers as well as

developing a more effective method of validating the specificity of different PCR products (as explained in 2.2.1.1) to perform my own resequencing.

3.4. Early leads with coding variants

Genotyping *HCAR2* was undertaken to assess whether any coding variants that could modify HCAR2 function, had measurable effects on lipid paramaters known to be afftected by NA administration, particularly HDL. During the early stages of genotyping of coding region SNPs in *HCAR2* and to avoid possible off-target genotyping that would confound results, it was decided rather, to work on validated specific PCR products. Examining part of an alignment of the coding region of both genes, the difficulties of targeting certain variants from genomic DNA become clear (Figure 6).

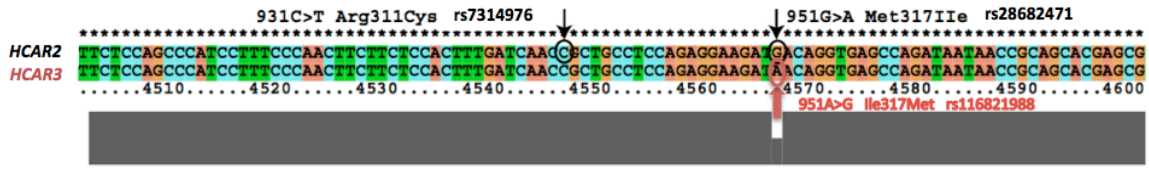

Figure 6: ClustalX alignment of a part of *HCAR2* and *HCAR3* coding regions.
This alignment shows the nucleotide sequence of *HCAR2* and that of *HCAR3* below it. The white gap in the grey block beneath indicates a base difference between the two sequences. The alignment also features three amino acid modifying variants, and their positions in both genes.

As seen from the alignment, the two main amino changing variants in *HCAR2* are not easy targets for genotyping assays on genomic DNA: the rs7314976 polymorphism in *HCAR2* is a C to T variation, while at the corresponding position in *HCAR3,* the nucleotide expected is always a C. A genotyping assay that will have its primers and probe designed to match that nucleotide sequence will detect both genes on gDNA, thus distorting the signal and showing a call ratio of '4,3,2' alleles rather than the usual '2,1,0'. Similarly, but with an added level of complexity, the

rs28682471 polymorphism in *HCAR2* is also polymorphic in *HCAR3* with a different minor allele frequency. Again, the need for initial isolation of both gene products becomes evident when attempting to study the effect of the polymorphisms on *HCAR2* alone.

To this effect, PCR products were created for 1200 individuals from the OBB, validated for gene identity with the MfeI genotyping assay (as explained in 2.2.1.1) and then they were diluted for another round of genotyping on the variant of interest. This laborious effort was undertaken by a senior scientist in my group and uncovered two interesting lipid associations within the above coding region SNPs. The first amino acid-modifying variant, rs7314976 (931C>T, Arg311Cys, MAF= 0.05), showed a dose dependant reduction in HDL levels in all subjects (p=0.028, N=1200, Kruskal-Walis) (Figure 7).

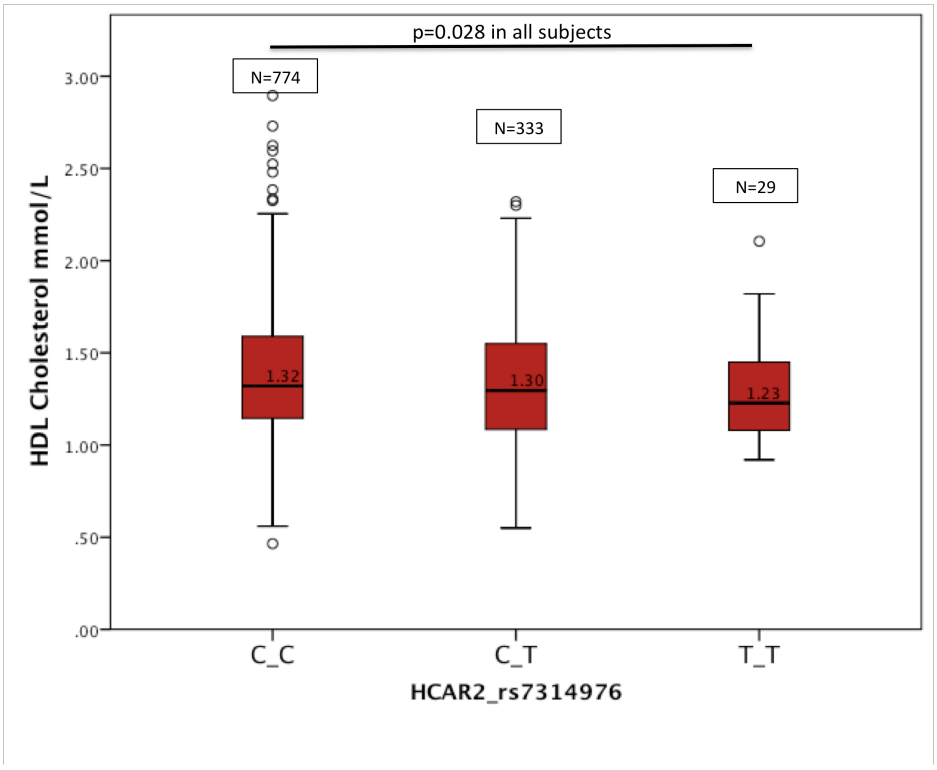

Figure 7: Variation in HDL levels with rs7314976 genotypes.

When accounting for exsisting differences in HDL levels between genders, a non-signifcant trend is seen with the rare variant, one that needs replication on a larger cohort considering the polymorphism's possible functional implications.

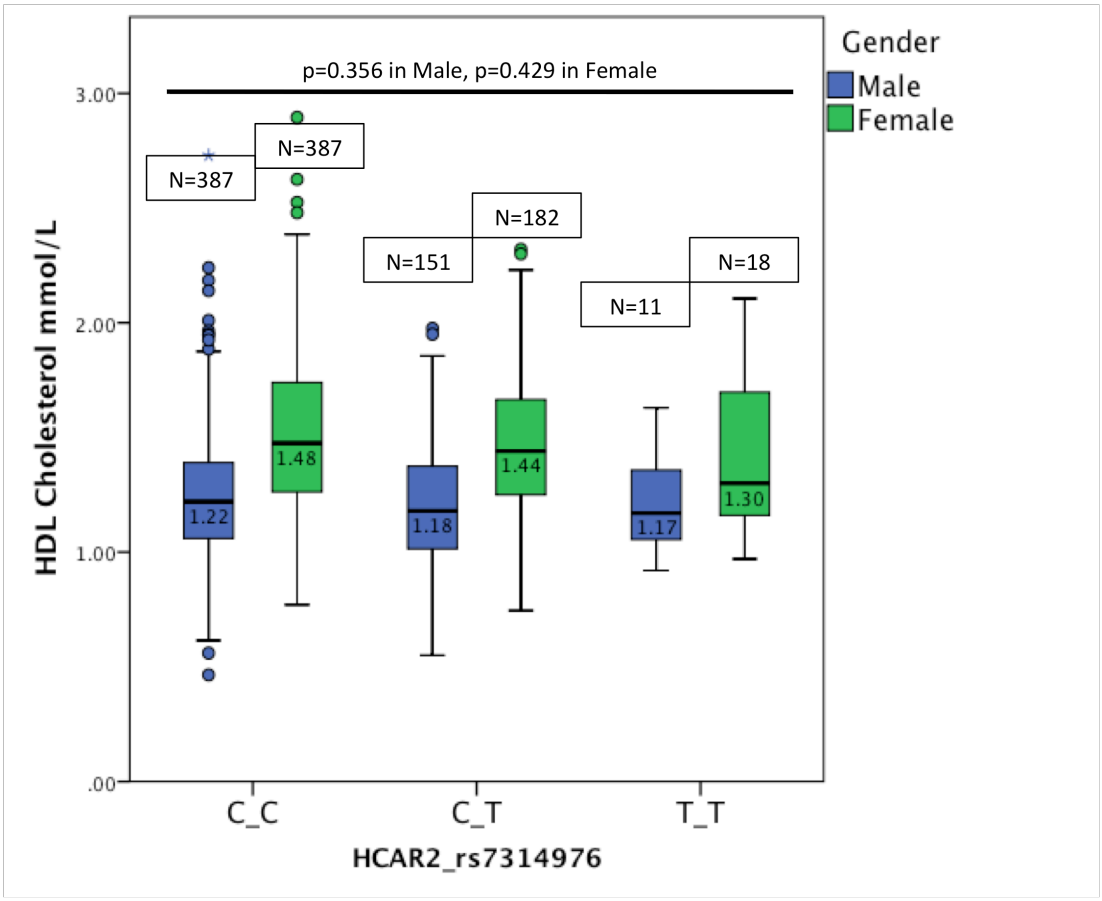

Figure 8: Trend in dose-dependant HDL variation seen with rs7314976 and divided by gender

The second variant of interest in *HCAR2*, rs28682471 (951G>A, Met317Ile, MAF=0.29) was similarly genotyped on validated HCAR2 PCR products, and a similar trend was seen with HDL cholesterol (p=0.072, N=1200, Kruskal-Wallis) (Figure 8).

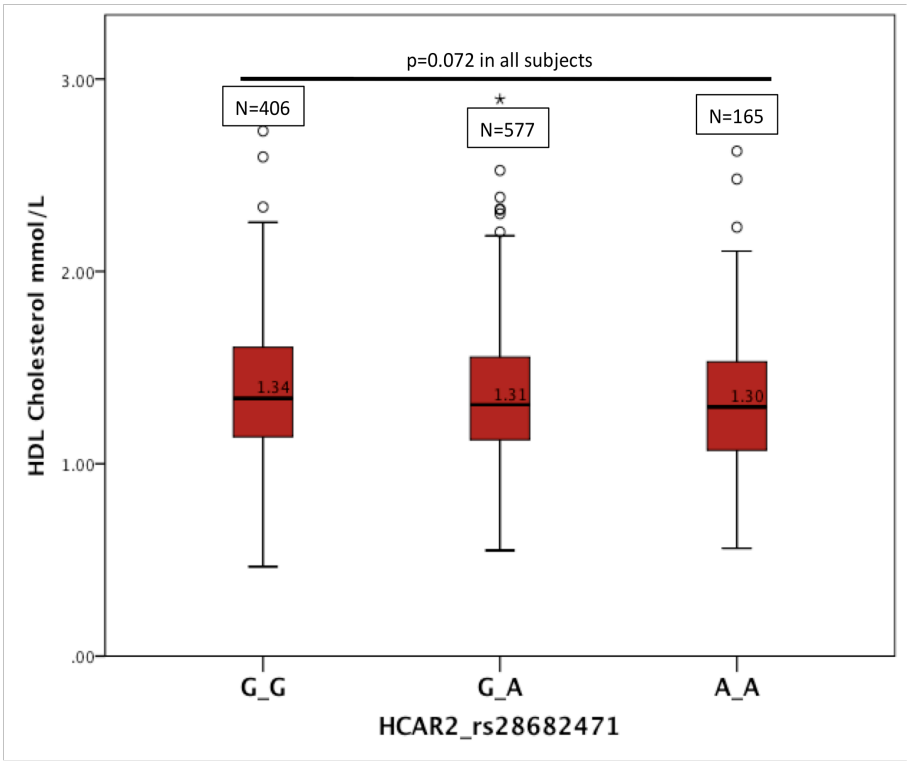

Figure 9: Dose dependant HDL variation with rs28682471 genotypes.

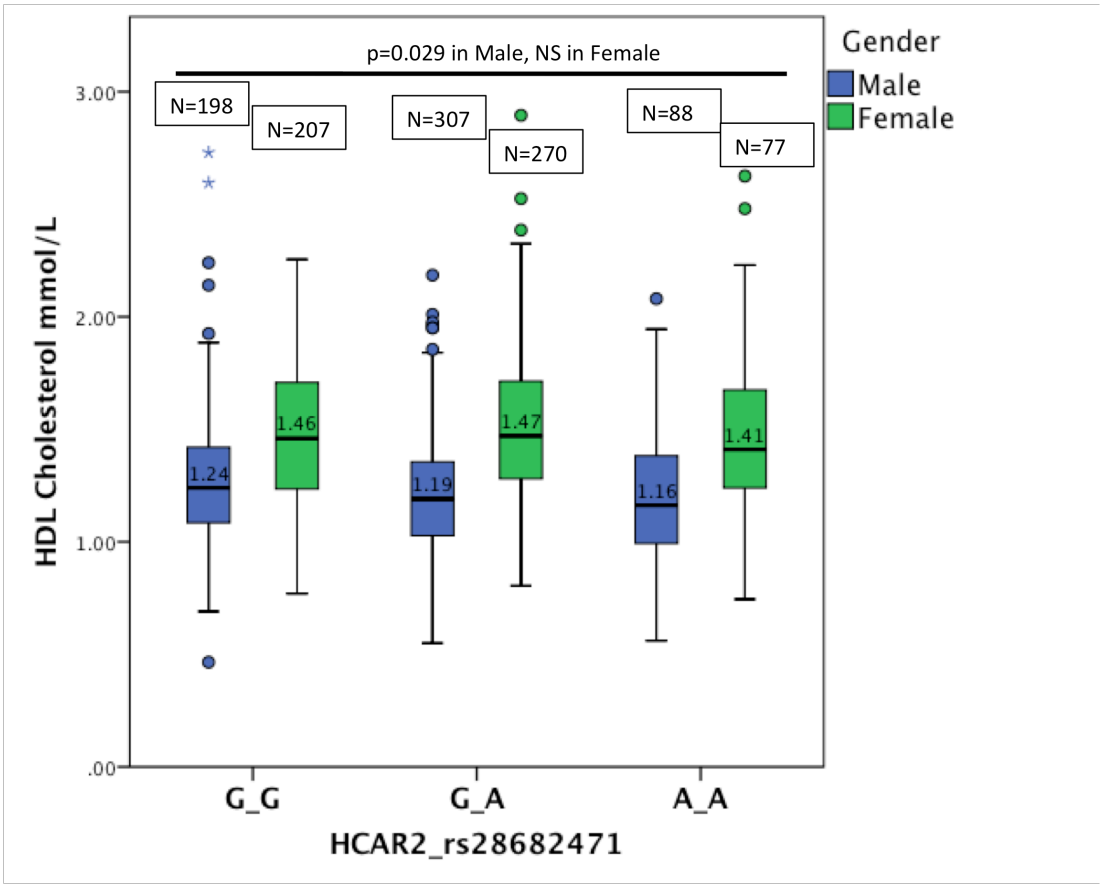

Figure 10: Dose dependant HDL variation with rs28682471 divided by gender

Similarly, when accounting for existing gender differences in HDL levels, a significant difference in HDL levels is seen in males ($p=0.029$, $N=593$, Kruskal-Wallis). Post-hoc analysis using the Bonferoni adjustement confirmed that there was a significant difference in normalized HDL levels and rs28682471 alleles at the $p<0.05$ level between the three genotypes in male subjects [$F(2,590)=3.987$, $p=0.019$].

Both the trend in rs7314976 and the significant result with males in rs28682471 required replication with a larger cohort, especially considering the limited number of individuals with the rare allele of the rs7314976 variant.

However when replicating these findings in a larger cohort and considering the expansion to genotype on other SNPs, several problems arose: to begin with, creating PCR product from genomic DNA and validating them for a large number of individuals is a laborious and impractical process and DNA quality differences between cohorts affect the success of this sensitive PCR synthesis. Secondly, most cohort genotyping facilities are setup with gDNA samples that are dried down at low concentrations making them not amenable to my PCR amplicon method. This highlighted the need for a proxy SNP that could tag the SNPs and haplotypes of choice and be unique so it can be targeted directly on gDNA. Finally, initial doubts about the validity of some of the listed polymorphisms and about the extent of 'missed' or 'mislabelled' variability especially beyond the coding region reinforced the need to undertake an initial deep resequencing effort.

3.5. Population-based resequencing

Targeted population-based resequencing uncovers low and rare frequency variants to understand how genetic variation contributes to complex human traits. Over half of the variation in serum HDL is known to be under genetic control, much of which is not completely understood (Qasim & Rader, 2006),(Razzaghi, Santorico, & Kamboh, 2012). Considering NA's pronounced effect on blood lipids (as described in 1.2.1), and the associations that were found with HDL with the two SNPs described in section 3.4, I selected a population with extremes in HDL levels for resequencing and to gain additional insights to potential variants in *HCAR2* that affect serum HDL.

I therefore hypothesized that along with the contributions of resequencing in delineating variants associated with HDL between the two genes and uncovering potential rare variants, there was also the added value of finding a proxy SNP that could be genotyped on gDNA and could tag the haplotype that contained the two complex SNPs as introduced in 3.4.

3.6. Method development

Current automated sequencing methods generate random short products that make classification of homologous genes complex at the stage of sequence alignment as these small fragments cannot, in many cases, bridge the regions of high homology to unique selected regions as illustrated in Figure 9 (Musumeci et al., 2010).

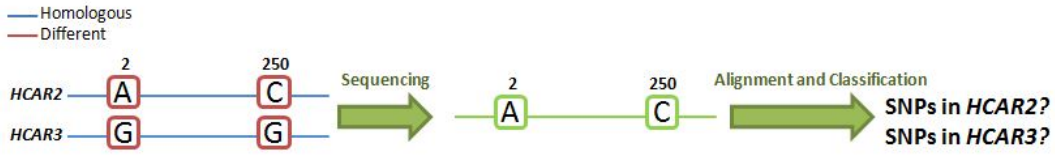

Figure 11: Non-specific sequencing goes wrong
In this simplified example *HCAR2* and *HCAR3* only differ at position 2 and 250 in their sequences. When short fragments of these two genes are co-amplified in sequencing due to poor primer design, the mismatch in the sequences of the products could be misinterpreted for a SNP in the sequence in question rather than the existing single nucleotide difference between the two genes.

Alignment and classification of variation in these sequences complicates matters more when the two homologous genes differ at a nucleotide that is polymorphic in one of the genes and not the other (Figure 10).

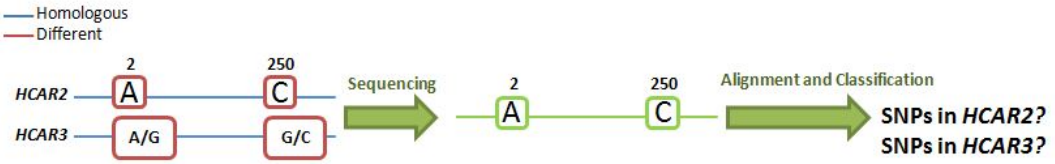

Figure 12: Non-specific sequencing gets more complicated
When the single nucleotide differences in the gene are genuine polymorphisms in the other, untargeted sequencing will add even more uncertainty to classifying them between SNPs and SNDs.

Furthermore, as is the particular case with the variant at position 951 in *HCAR2* and *HCAR3* (rs28682471 in *HCAR2* and rs116821988 in *HCAR3*, introduced in 3.4), there is even more room for error when a nucleotide is polymorphic at both genes in different frequencies and exists on different haplotypes. Indiscriminate sequencing will invariably capture a mixture representation of these variants that will not represent their actual allele frequencies in the population (Figure 11).

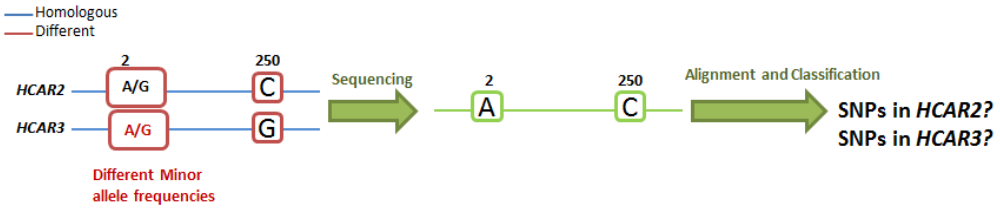

Figure 13: Non-specific sequencing in homologous genes and complicated polymorphisms
When the fragments to be sequenced encompass a region of high homology as well as nucleotides that are polymorphic in both genes as the particular case with rs28682471 in *HCAR2* and rs116821988 in *HCAR3*, a targeted method of resequencing needs to be established to ensure proper detection of both genes

The in-house developed resequencing method took all of these concerns into consideration. This method consisted of separately amplifying each of the two homologous genes, verifying that the product needed was the one amplified and then creating smaller nested products separately for each gene for forward and reverse Sanger sequencing (Illustrated summary in Figure 12).

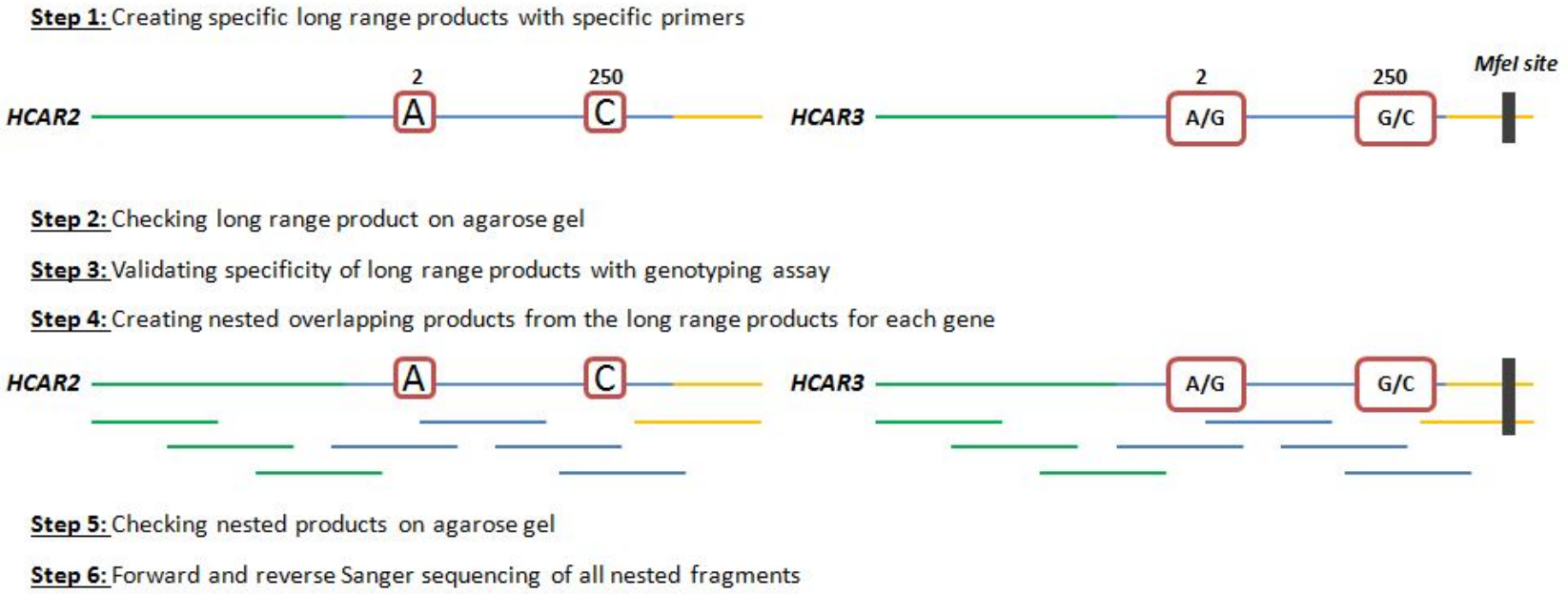

Figure 14: Outline of the experimental design for resequencing in our cohort.
Each gene is amplified with specific primers expanding to the promoter region (region in green). The extent amplified includes the region that allows for discrimination between the two (region in yellow) with the designed genotyped assay around the *MfeI* site (as described in 2.2.1.1). Products are first checked for amplification success on an agarose gel. They are later diluted and genotyped to make sure specific amplification occurred. Nested products with M13 tails for sequencing are then created for each gene. These products are checked again on a gel and then cleaned up for Sanger sequencing. The figures are illustrative and do not reflect actual sequence features.

3.7. Sample Selection

DNA samples from 64 subjects were obtained from the OBB (stored at -80°C) in accordance with ethics guidelines from the Wellcome Trust Centre for Human Genetics (research ethics committee no. 05/Q1605/130). These samples equally represented male and female individuals matched for BMI with varying HDL phenotypes in order to increase the power of detecting the uncommon and extreme HDL genotypes. Specifically, upon examination of candidate biochemical data, individuals from the OBB database at the time (N=1218) were classified into quartiles and only 64 individuals displaying HDL levels below the bottom quartile and above the upper quartile were selected. The chosen individuals were not taking any blood pressure or lipid medications (full details in Table).

	Mean (± s.d.)			
	Low HDL group		**High HDL group**	
	Female (N=21)	Male (N=21)	Female (N=12)	Male (N=12)
BMI (kg/m^2)	24.96 (±3.6)	26.09 (±3.5)	23.96 (±3.7)	28.18 (±2.8)
WHR	0.79 (±0.06)	0.93(±0.06)	0.78 (±0.05)	0.95 (±0.05)
SBP (mm/Hg)	108.96 (±6.9)	113.95 (±11.3)	119.86 (±16.3)	134.18 (±12.7)
DBP (mm/Hg)	72.8 (±6.4)	75.1 (±8.9)	78.33 (±10.0)	88.54 (±11.1)
Glucose (mmol/L)	4.84 (±0.4)	5.3 (±0.5)	4.86 (±0.4)	5.73 (±0.6)
Insulin (mU/L)	8.13 (±2.4)	8.4 (±3.0)	7.92 (±4.5)	12.96 (±6.4)
Total Cholesterol (mmol/L)	4.36(±0.6)	4.9(±0.9)	5.73(±0.8)	6.38 (±1.0)
TG (mmol/L)	0.58 (±0.08)	0.86 (±0.5)	1.65 (±0.3)	2.76 (±0.7)
LDL (mmol/L)	2.91 (±0.6)	3.58 (±0.8)	3.05(±0.8)	3.62 (±1.0)
HDL (mmol/L)	1.17 (±0.09)	0.96 (±0.12)	1.92 (±0.1)	1.51 (±0.1)

Table 6: Full details of cohort selected for resequencing.

3.8. Specific resequencing

3.8.1. Long range PCR products synthesis

I initially aimed to isolate 10kb of the coding and flanking promoter region for each gene to increase detecting polymorphisms that affect function and regulation of expression. Nine primer pairs were created and tested for the long range product of *HCAR2* and over twenty primer pairs for the long range product of *HCAR3*. After trialling them with different enzymes, cycling conditions and salt concentrations, it was not possible to achieve the target 10kb products. As a result, the successful long range fragment lengths were 4930bp for *HCAR2* and 2164bp length for *HCAR3*. The corresponding primers are listed in Table 5.

Gene	Primer Sequence (5'-3')	Tm°	Product size bp
HCAR2	F- CCTGATCCACAAGGAGCAGTACC	67.9	4930
	R- AGCGTCAGAGATGAAGCAAAAG	66.2	
HCAR3	F- TTAAATCACTTGAGCACAGAAGCA	65.4	2164
	R- AGCGTCAGAGATGAAGCAAGTT	64.2	

Table 5: Long range primer sequences for *HCAR2* and *HCAR3*

Long range polymerase chain reaction (LR-PCR) was used to exponentially amplify the specific area of genomic DNA for further processing for nested PCR reactions and sequencing. LR-PCR was setup following manufacturer's instructions from the SequalPrep™ Long PCR Kit with dNTPs by Life Technologies. Briefly, 50ng of genomic DNA in DNase-free water was added to the reaction mix detailed in Table 6.

Reagent	Volume in reaction (µl)
SequalPrep™ 10X Reaction Buffer	2
DMSO	0.4
SequalPrep™ 10X Enhancer A	1
SequalPrep™ Long Polymerase, 5U/µl	0.36
DNase-free water	14.24

Table 6: Long range PCR reaction Mix

The tubes were briefly mixed and centrifuged and run with thermocycling parameters recommended by the manufacturers with an initial 2 minute enzyme activation step at 94°C followed by 10 cycles of 94°C for 10 seconds, 60°C for 30 seconds for primer annealing, and 68°C for 9 minutes. The second round of extensions for 25 cycles starts with another enzyme activation at 94°C for 10 seconds, primer annealing at 60 °C for 30 seconds and fragment extension at 68°C for 18 minutes. The final extension step was for 5 minutes at 72°C.

3.8.2. Long range PCR products validation

All long range PCR products were run and visualized on a 0.8% agarose gel for predicted band visualization (as described in 2.2.3). Once the bands were confirmed, specificity of the fragments was tested with the MfeI genotyping assay as previously discussed in Chapter 2 (2.2.1.1) as the regions amplified for both genes encompassed the genomic region of the MfeI restriction site (present in *HCAR3*).

LR-PCR products were serially diluted with nuclease-free water to 1:10,000, gently mixed and briefly centrifuged. Two microlitres of each sample was mixed with the reaction mix containing the MfeI specific genotyping assay (2.2.1.1) as detailed in Table 7. Samples were setup in triplicate with the suitable amount of non-template controls (NTCs). Thermocycling conditions were adapted from the manufacturer and consisted of an initial 15 minutes at 94°C (polymerase activation) and then 35

cycles of 94°C for 10 seconds (DNA melting) and 57°C for 60 seconds (combined annealing and extension steps).

Reagent	Volume in reaction (µl)
DNA	2
2X KASpar reaction mix	2
Mfe I assay mix	0.055
$MgCl_2$ (50Mm)	0.032

Table 7: Genotyping reaction mix

When the thermocycling program ended, plates were briefly centrifuged and transferred to the post-read allelic determination phase on a Life Technologies, Paisley, UK 7900HT machine, using SDSv2.3 software and standard analysis settings.

3.8.3. Nested PCR products synthesis

For each long range PCR product, short (400-500 bp) overlapping nested products were designed with each pair of "nested primers" (Table 8) containing forward and reverse M13 tags to allow for resequencing (as described in 2.2.2).

***HCAR2* Nested Primers**			
Fragment name	**Primer Sequence (5'-3') Forward then Reverse**	**Tm°**	**Product size bp**
11	ACACCTTGCAACCAGTCTCC CCATCGTCTTTGTCATCTGC	60.1 59.2	560
12	GATAAAGAACGCCAGGTCCA CTATGTGAGGCGTTGGGACT	60.1 60.1	577
13	TACCTGTCTACCGCCACCAC AAACAGCAGGTTGCATAAGAGC	61 60.8	591
14	TCCACGCCTGCCTTTATG TGGAGATGAATGGCAGAGTTC	60.8 60.2	596
15	GTTGCCTGTTTGATGAGGAC TAAGGTCCCAAGGACATAAAAC	58.1 57.2	555
16	TTAGTACCCCATAAGCTGTCTGTTC AGGTTTTGCGTGTGTGGAG	60 59.7	591
17	CCCAAAGTGCTGGGATTAC GGTGGCTTGCACCTGTAG	58 57.8	556
18	TGAGATGGAGTTTCGCTCTG	59.1	603

	AAACAAGCAACTATAAAAGCACTGA	58.7	
19	CCGAGTAGCTGGGACTACAG	57.6	593
	CACCTCAGCCTCCAAAAGT	57.9	

***HCAR3* Nested Primers**			
Fragment name	**Primer Sequence (5'-3') Forward then Reverse**	**Tm°**	**Product size bp**
9	ATTCCTGCGGTCACACC	61	441
	ACTCTAGCTTCACCTACATGAACAG	62	
10	GAGCGCCTCTGGTTTTGTT	60	542
	CCTCCTGAAGAAGAAGTTGCTG	60.5	
11	CTGGCTGAGCAGAACAGGA	60	577
	GCTGTGTGTTCCGAGATGACT	60.3	
12	CCAGGACTTGAGGTGGAAAC	60	516
	TTCCAAAGGGATGTCCTTCA	60.4	
13	CCCTGGGCATACAGGAAC	59	593
	AATCACTTGAGCACAGAAGCA	58.7	

Table 8: Nested primer sequences for *HCAR2* and *HCAR3*

Several enzymes and kits were trialled for the nested products and the IMMOLASE™ DNA Polymerase from Bioline (Bioline Reagents Ltd, London, UK) was found to perform the best. Validated long range samples were diluted to 1:10,000 in nuclease-free water and reactions were setup according to the manufacturer's protocol. Each reaction contained 1µl of diluted long range PCR product and the reaction mix as detailed in the table below for a total volume of 25µl.

Reagent	**Volume in reaction (µl)**
10X ImmoBuffer	2.5
50mM $MgCl_2$	1
IMMOLASE™	0.5
Primers 0.1µM	0.25
dNTP	0.5
nuclease-free water	19.25

Table 9: Nested PCR Reaction mix

Similarly to long range product validation, nested PCR products' synthesis was checked by visualizing the corresponding size band on a 2% agarose gel and 100bp ladder, with the protocol to account for the difference in fragment sizes (as described in 2.2.3).

3.8.4. Sequencing of nested products

Targeted re-sequencing was performed on the validated specific nested PCR products to reveal novel variation in the region and any mislabelled SNPs as described in 2.2.4.

3.8.5. Reference comparison and sequence analysis

To detect new and mislabelled variants, the best quality forward and reverse sequences were compared to each other rather than the Genome Reference Consortium GRCh37 files available from UCSC (hg19). By comparing sequences to each other I eliminated the risk of potential erroneous variability from the database transferring through to my analysis. Variations from the reference sequence were visualized, checked in forward and reverse fragments when possible and compiled with Mutation surveyor v3.4 (Soft Genetics, Cambridge, UK)(Figure 13).

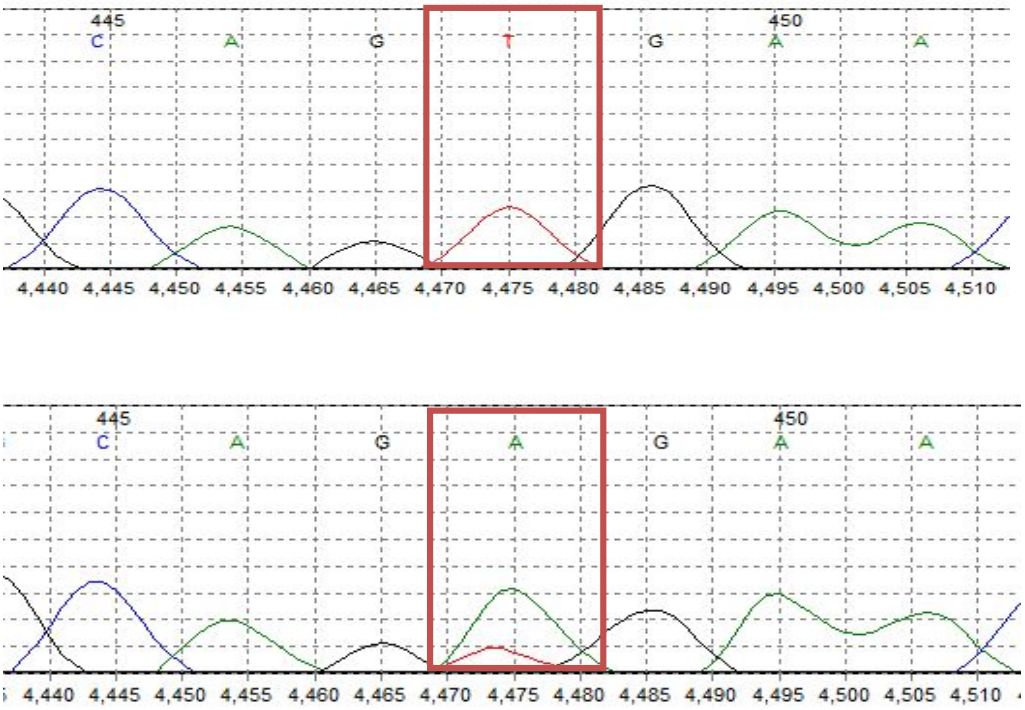

Figure 15: Example Electropherograms.
The bottom electropherogram traces from capillary sequencing of the nested PCR product shows a heterozygous at position 448 compared to the top reference sequence.

3.9. Resequencing problems due to genomic complexity

Genomic sequence complexity (as introduced in 1.2.4) in the region hampered multiple attempts of synthesizing the long range products (over 29 primer pair trials), synthesizing the nested products (over 5 primer trials for each nested fragment) and getting good quality readouts in fragments from Sanger sequencing. As a result, the initially optimistic target of synthesizing a 10kb long range product encompassing promoter and coding regions of each *HCAR2* and *HCAR3* could not be attained. Instead, the long range products were 4252bp long for *HCAR2* and 2100bp long for *HCAR3.* The corresponding lengths of the nested products for each gene are shown in Table 10.

When analysing sequence features of the genomic region of *HCAR2* in detail with RepeatMasker (v3.2.9) (http://www.repeatmasker.org), it is not surprising that the initial 10kb target fragment could not be synthesised and problems were encountered. Almost 50% of the sequence is interspersed with Short Interspersed Nuclear Elements (29% SINEs), Long Interspersed Nuclear Elements (7% LINEs) and Long terminal repeat retrotransposons (12% LTRs, with full details in Figure 14). Because of the homology between the two genes, the sequence analysis for *HCAR3* with RepeatMasker is almost identical and is not shown. The combination of these repeats and the high GC content (46.36%) required many optimization steps following established complex amplification and sequencing protocols (Kieleczawa, 2006), not all of which were successful. As a result, the length of both *HCAR2* and *HCAR3* initial long range fragments needed to be reconsidered and reduced and some failed nested fragments needed to be abandoned.

RepeatMasker(v3.2.9) Analysis Summary:

```
==================================================
file name: RM2HCAR2_1282574518
sequences:             1
total length:       9880 bp  (9880 bp excl N/X-runs)
GC level:         46.36 %
bases masked:       5073 bp ( 51.35 %)
==================================================
               number of      length   percentage
               elements*    occupied  of sequence
--------------------------------------------------
SINEs:                11         2860 bp   28.95 %
      ALUs            10         2718 bp   27.51 %
      MIRs             1          142 bp    1.44 %

LINEs:                 3          685 bp    6.93 %
      LINE1            1          113 bp    1.14 %
      LINE2            1          362 bp    3.66 %
      L3/CR1           1          210 bp    2.13 %

LTR elements:          3         1237 bp   12.52 %
      ERVL             0            0 bp    0.00 %
      ERVL-MaLRs       1          368 bp    3.72 %
      ERV_classI       2          869 bp    8.80 %
      ERV_classII      0            0 bp    0.00 %

DNA elements:          0            0 bp    0.00 %
     hAT-Charlie       0            0 bp    0.00 %
     TcMar-Tigger      0            0 bp    0.00 %

Unclassified:          0            0 bp    0.00 %

Total interspersed repeats:     4782 bp   48.40 %


Small RNA:             0            0 bp    0.00 %

Satellites:            0            0 bp    0.00 %
Simple repeats:        6          291 bp    2.95 %
Low complexity:        0            0 bp    0.00 %
==================================================

* most repeats fragmented by insertions or deletions
  have been counted as one element
```

Figure 16: Snapshot from RepeatMasker result on 10kb promoter and coding regions of an *HCAR2* fragment.

3.10. Compiled sequencing results

Sequence readouts were visualized with the Mutation surveyor v3.4 software (Soft Genetics, Cambridge, UK) that additionally displayed sequence quality. Sequence variants were visually confirmed from the best quality fragments and validated by checking the corresponding reverse fragment. Variants from the deep resequencing from both genes are listed in Table 10.

In order to compare with the current NCBI dbSNP content for the sequenced region, I blasted the DNA stretch in question (4252bp for *HCAR2* and 2100bp for *HCAR3*) across the most current build (build 137, Jun 26, 2012). All the polymorphisms that I found in resequencing were already listed in the most current dbSNP. For stretches of sequence that failed in my hands or in which the variants could not be confirmed because of poor sequence quality, I included the location validated polymorphisms from dbSNP as underlined entries, along with the MAF listed in the database. My results also include a description on whether the polymorphism is unique to the gene in question or polymorphic in both, the corresponding minor allele frequency based on frequency in my cohort and validated when possible with results in dbSNP. Overall for the 4252bp stretch of *HCAR2* that was resequenced, dbSNP listed 24 SNPs, 16 of which I have validated in my resequencing with the sequence around the others being too poor for analysis. Five out of these 16 variants found for *HCAR2* were polymorphic in both *HCAR2* and *HCAR3* without any mention in dbSNP. Similarly, in the 2100bp stretch resequenced for *HCAR3*, dbSNP listed 18 SNPs, 14 of which I validated in my resequencing. Half of these validated SNPs for *HCAR3* were also found to be

polymorphic in both *HCAR2* and *HCAR3.* dbSNP had no mention of this dual polymorphic nature in these SNPs either.

	***HCAR2* Sequencing results**				
	Location to CDS	**Identity**	**GENE**	**MAF**	**Functionality**
HCAR2 4252 bp	-2870 T>A	rs9668547	HCAR2	0.16	Promoter region
	-2400 C>A	rs7974561	HCAR2	0.21	Promoter region
	-2254 G>A	rs61955028	HCAR2	0.04	Promoter region
	-1964 T>C	rs7133768	HCAR2	0.29	Promoter region
	-1848 C>T	rs488391	HCAR2	0.47	Promoter region
	-1729 G>A	rs12303524	HCAR2	0.01	Promoter region
	-1669 C>T	rs6489222	HCAR2	0.32	Promoter region
	-1455 G>A	rs112378089	HCAR2	0.03	Promoter region
	-1378 A>G	rs7305589	HCAR2	0.28	Promoter region
	-1238 C>T	rs55736428	HCAR2	0.01	Promoter region
	-901 C>T	rs587756	HCAR2	N/A	Promoter region
	-768 A>C	rs112400581	HCAR2	0.04	Promoter region
	-747 G>A	rs116950578	HCAR2	0.02	Promoter region
	-645T>G	rs56959712	poly in both	0.19	Promoter region
	-536 G>A	rs118110667	poly in both	0.1	Promoter region
	-296 A>G	rs590447	poly in both	0.01	Promoter region
	-225 C>T	rs545288	HCAR2	N/A	Promoter region
	324 T>C	rs115977736	HCAR2	0.01	Coding region Synonymous
	592 T>C	rs676823	poly in both	N/A	Coding region Synonymous
	931 C>T	rs7314976	HCAR2	0.06	R [Arg] ⇒ C [Cys]
	951 G>A	rs28682471	poly in both	0.29	M [Met] ⇒ I [Ile]
	1220 G>C	rs79685171	poly in both	0.14	3' UTR
	1221 C>T	rs76270247	poly in both	0.13	3' UTR
	1235 G>T	rs76850512	HCAR2	0.14	3' UTR

	***HCAR3* Sequencing results**				
	Location to CDS	**Identity**	**GENE**	**MAF**	**Functionality**
	-764 G>T	rs2257405	HCAR3	0.33	Promoter region

	-641 G>T	rs7145677	HCAR3	0.5	Promoter region
	-530 G>A	rs1179102	poly in both	0.21	Promoter region
	-442 C>T	rs111626900	HCAR3	0.3	Promoter region
	-292 C>T	rs55718746	poly in both	0.33	Promoter region
	-255 C>G	rs28710048	HCAR3	0.48	Promoter region
	-224 C>T	rs2256572	HCAR3	0.47	Promoter region
	-7 G>A	rs3825156	poly in both	0.4	Promoter region
	271 C>T	rs11059549	HCAR3	0.01	Coding region Synonymous
	348 C>A	rs1696352	HCAR3	0.3	Coding region Synonymous
HCAR3 2100bp	517 C>A	rs1798192	HCAR3	0.31	T [Thr] ⇒ P [Pro]
	592 C>T	rs17884481	HCAR3	0.34	F [Phe] ⇒ L [Leu]
	758 G>A	rs118091133	HCAR3	0.33	H [His] ⇒ R [Arg]
	951 C>T	rs116821988	poly in both	0.6	I [Ile] ⇒ M [Met]
	1038 C>G	rs56308926	poly in both	0.2	M [Met] ⇒ I [Ile]
	1215 G>C	rs579876	poly in both	0.01	3' UTR
	1216 C>T	rs579877	poly in both	0.01	3' UTR
	1341 C>T	rs61955034	HCAR3	0.48	3' UTR

Table 10: Polymorphisms from deep re-sequencing of *HCAR2* and *HCAR3*.
In the underlined entries, MAF was taken from dbSNP. N/A refers to currently undetermined MAF in the database. The start codon for every gene was considered as the frame of reference for the numbering of variants.

3.11. Variants then and today

When the sequencing efforts first began in 2009, dbSNP listings for *HCAR2* and *HCAR3* were not comprehensive. Following from Zellner *et al*'s lead, we suspected that the region was poorly defined particularly in the promoter regions, hampering any genotyping studies we would pursue in the OBB and possibly offering an explanation for the absence of GWAS hits at the time. Moreover, the early leads that we had established with HDL (described in 3.4) warranted further exploration in a larger cohort and required detailed knowledge of the sequence around the two variants for proper targeting on gDNA. Resequencing aimed to address all of these issues and potentially uncover missed rare variants in both genes.

Overall, the genomic complexity of the region around both genes affected the length and quality of the readouts and proved resequencing to be a demanding and laborious process. It was extremely challenging to unveil as much of the promoter region as I intended to, but quality control of the specificity at each step ensured that the insight I do have is important.

Compiling my initial targeted resequencing results in 2010 showed many discrepancies with the corresponding dbSNP listings (Builds 131 and 132). Certain polymorphisms listed in dbSNP at the time were found to be single nucleotide differences (SNDs) between the two genes in our specific resequencing – this has now been corrected in the latest build. Of more relevance, other variants were found to be polymorphic in both genes in my resequencing while the corresponding 2010 dbSNP build listed them as specific to one gene and not existing in the other. At the time, this was very useful information when designing

genotyping assays so off-target detection could be minimized and so that results reflected polymorphisms in the correct gene. An example of this, rs590447 in *HCAR2* did not have its alignment position equivalent, rs55718746 in *HCAR3,* recognized as a polymorphism at the time in dbSNP. Finally, no rare variants were uncovered in either genes.

Shortly after my resequencing results were compiled, the results of The 1000 Genomes Consortium were made public and their findings updated and merged with dbSNP (1000 Genomes Project Consortium et al., 2012). This allowed me to re-evaluate, validate and consolidate my results (combined as a final output in Table 10). In addition, this allowed me to confirm the unique advantages of my methodology in this region: the Next Generation Sequencing (NGS) platforms used in 1000 Genomes have only been able to characterize about 98% of accessible variants in the human genome (or 72.2% when using stricter criteria)(1000 Genomes Project Consortium et al., 2012). This is the result of the limited accessibility and reliability of the NGS' created short-paired end read data in duplicated and repeat rich genomic regions (1000 Genomes Project Consortium, 2010). Considering that my method was developed to deal with that exact problem by creating specific initial long reads, I was able to get valuable insight into the region. Indeed, a genomic accessibility track has been recently made available on the Ensembl Browser (September 2012, http://browser.1000genomes.org). When my two sequenced genes are questioned, the gaps of coverage highlighted in the 1000 Genomes' data justify the importance of my resequencing in getting a clear view of the variation in the region (Figure 15). The accessibility mask's coverage

(highlighted in red) is seen to break in coding and promoter regions of both genes, proving that to this day these regions still lack appropriate characterization.

In summary, resequencing allowed me to create a validated inventory of variation for the two genes in a complex genomic region that has not been thoroughly questioned. As will be discussed in Chapter 4, the sequence assembly that I created was used as a technical template to help design challenging genotyping assays for dual polymorphic variants (specifically rs7314976 in *HCAR2* and rs116821988 in *HCAR3*, rs590447 in *HCAR2* and rs55718746 in *HCAR3*). Similarly, knowing about the presence of such variants in the immediate proximity of a polymorphism of interest also allows for a better targeting in genotyping assays. In fact, most of the genotyping assays in the region were henceforth custom made with LGC Genomics (Hoddeston, UK) by using the resequencing data to anchor challenging polymorphisms and question nearby sequence features. As a result, resequencing allowed a better understanding of the region around the two SNPs in *HCAR2* with the HDL associations (as introduced in 3.4) and the subsequent design of a genotyping assay that works on gDNA for one of them. These results will be discussed in detail in Chapter 4.

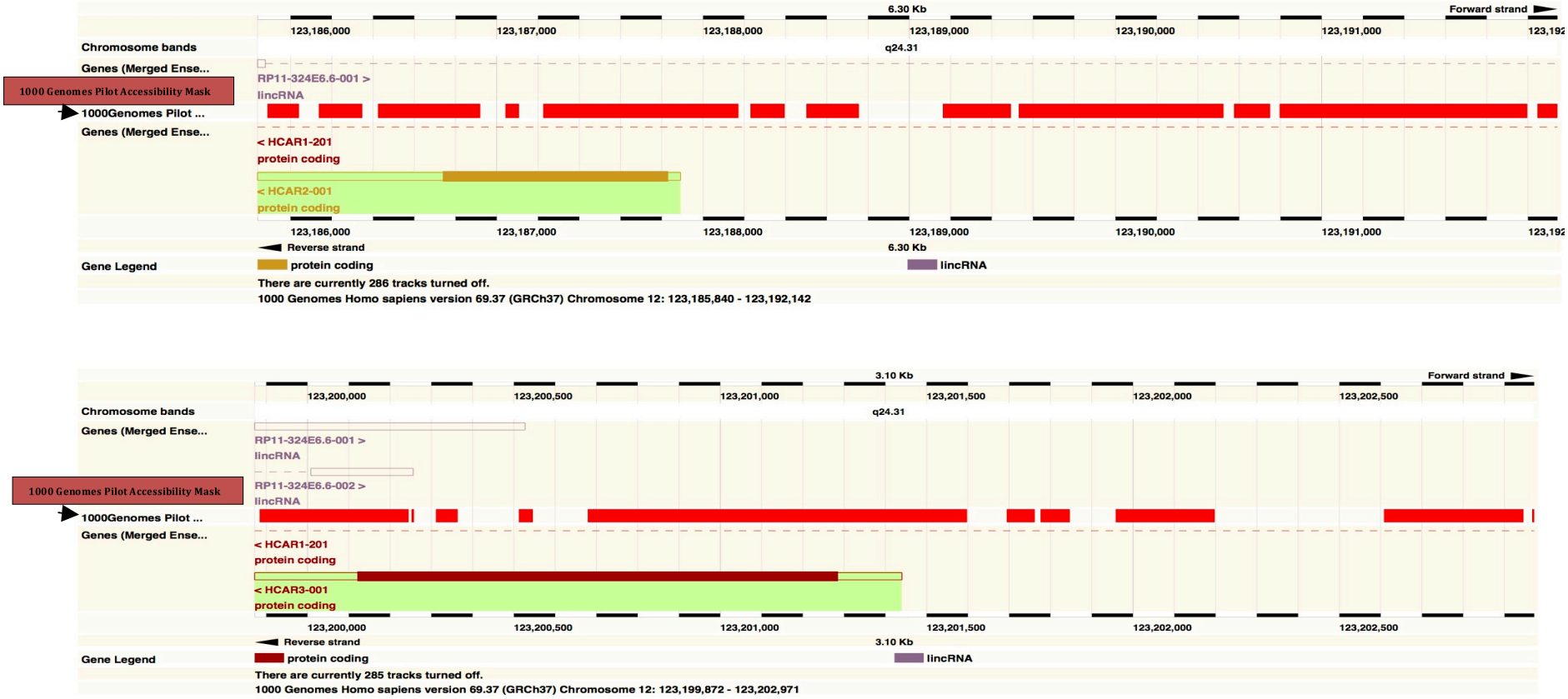

Figure 17: 1000 Genomes Ensembl Browser sequence visualization of *HCAR2* and *HCAR3* with the accessibility tracks.
This figure shows the extent of the regions I resequenced in both genes superimposed to the region that was accessible to NGS with 1000 Genomes (seen as red blocks) and the gaps within this track that were missed by NGS (seen as white rectangles) on the newly included 1000Genomes Accessibility Mask Track (http://browser.1000genomes.org).

Chapter 4 Exploring polymorphisms in *HCAR2* and *HCAR3*

4.1. Exploring the coding region after resequencing

As previously described, the genomic region covering *HCAR2* and *HCAR3* is riddled with sequence homology and complexity. This makes it challenging to explore polymorphisms and identify genotype-phenotype associations with a candidate gene approach. Therefore it came as no surprise that in the beginning of my DPhil in 2009, very few variants had been previously typed or tagged by association studies in the genomic duplicated area encompassing both genes.

Following the resequencing (Chapter 3), I was able to confirm the validity of polymorphisms and gain relevant insights into the DNA sequence around them. This served as an important tool enabling me to design genotyping assays that target the exact variant in the appropriate gene by customizing the primers and probes to differences in sequences uncovered during resequencing.

Using the candidate-gene approach, I predicted that certain genetic variants; specifically protein-modifying ones, would influence measurable traits in the population. Although currently disproven, at the time of the investigations, the receptor was thought to modulate HDL levels through its anti-lipolytic mechanisms (as introduced in section 1.3.1). I hypothesized that a variant that affects function of HCAR2 could have measurable HDL differences between different genotypes. Similarly, with evidence linking HCAR2 to anti-inflammatory chemokine modulation of IL-6 (Zandi-Nejad et al., 2013), and CRP (J. M. S. Lee et al., 2009; Plaisance et al., 2008) and introduced in section 1.3.2, I hypothesized that protein-modifying variants in HCAR2 could have measurable differences in measured CRP parameters in the OBB. CRP measurements in the OBB were

particularly useful as they are also indicative of IL-6 fluctuations (a variable that is not measured in our cohort) since IL-6 induces CRP production in the liver through activation of Janus kinases (Pepys & Hirschfield, 2003).

Non-synonymous coding region variants that could affect putative HCAR2 protein function were obvious initial choices for genotyping. The two main variants of interest (rs7314976 and rs28682471) are the only identified coding region variants in *HCAR2* that lead to an amino acid change in the protein. These were previously genotyped on PCR products (introduced in section 3.4) and revealed a relationship with HDL levels (Figures 7 and 8) that needed to be verified in a larger cohort.

4.1.1. Genotyping rs7314976 (931C>T)

rs7314976 (931C>T) is a non-synonymous variant in *HCAR2* coding for an Arginine to Cysteine substitution. This substitution is predicted to have a benign effect on protein function by Polyphen-2 – an online tool for annotating non-synonymous coding SNPs and predicting their effect on protein function (http://genetics.bwh.harvard.edu/pph2/)(Adzhubei et al., 2010). Resequencing in the OBB revealed that this variant was only polymorphic in *HCAR2* therefore making it easier to design a conventional genotyping assay that could target it in gDNA.

The region that encompassed the SNP was a particularly challenging homologous region between *HCAR2* and *HCAR3* with a high density of neighbouring polymorphisms that can be seen in Figure 16. Designing the assay took into account polymorphisms identified in Chapter 3 that featured in the immediate vicinity by inserting the corresponding IUPAC code. This ensured that all possible

existing variants in the population were accounted for. Three different custom assays were designed and validated with the assistance of LGC Genomics (Hoddeston, UK) assay-on-demand team. The sequences of the successful assay that showed conventional allelic distribution pattern as tested by LGC Genomics are shown in Table 11.

Polymorphism	Primer Sequence(5'-3')
rs7314976 in *HCAR2*	FAM- CAACTTCTTCTCCACTTTGATCAACT VIC- CAACTTCTTCTCCACTTTGATCAACC Common- ACAATGTCCCTTCTTGGCATGGTTATTTA

Table 11: Primer sequences of successful custom designed genomic assay for rs7314976.

Genotyping was performed on gDNA samples from the OBB cohort that had grown to almost 3500 individuals at the time (Details in Table 12).

	Mean (± s.d.)	
	Female (N=1741)	Male (N=1741)
Age (years)	41.71 (±6.0)	42.27 (±5.7)
BMI (kg/m^2)	25.54 (±4.73)	26.78 (±4.11)
Glucose (mmol/L)	5.11(±0.48)	5.47 (±0.72)
HDL Cholesterol (mmol/L)	1.52(±0.37)	1.22(±0.3)

Table 12: Details of rs7314976 genotyped individuals in the OBB.

Genotyping followed the methods previously described in section 2.2.1 with a modified touchdown protocol provided by LGC Genomics to account for specific sequence feature of the designed assay (Table 13).

Step	Temperature	Time
1) Activation	94°C	15 minutes
2) Denaturation	94°C	20 seconds
3) Annealing	61°C	60 seconds
Drop - 0.6°C/per cycle and repeat steps 2-3 for a total of 10 cycles reaching 55°C		
5) Denaturation	94°C	10 seconds
6) Extension	57°C	60 seconds
Repeat steps 5-6 for a total of 25 cycles.		

Table 13: Touchdown protocol for rs7314976 genotyping assay designed by LGC Genomics (Hoddeston, UK).

Figure 18: UCSC Genome Browser (GRCh37/hg19) Screenshot of the coding and promoter regions of *HCAR2*
The common variants are identified and the coding region rs7314976 variants picked for genotyping highlighted in black. The SNPs are colour-coded depending on their effect with red SNPs representing coding non-synonymous, Green SNPs represent coding synonymous variants and blue and black are in the un-translated region. These SNPs are a collective assembly from various validated and un-validated sources and ancestries and only a fraction of them was found in our resequencing.

4.1.2. rs7314976 (931C>T) genotyping results

I was looking to investigate the initial HDL relationship that was outlined in section 3.4 with an increased sample size from 1500 to 3482 individuals from the OBB by conveniently genotyping on genomic DNA with a new assay design (section 4.1.1).

After increasing the sample size, the previous trend with HDL did not gain any statistical significance (Figure 17) even when looking for gender effects and correcting for BMI (p=0.239, N=3116, Kruskal-Wallis analysis of variance, Figure 18). However, the trend of the dose-dependant decrease in HDL values with the rare allele (introduced in section 3.4) was still present.

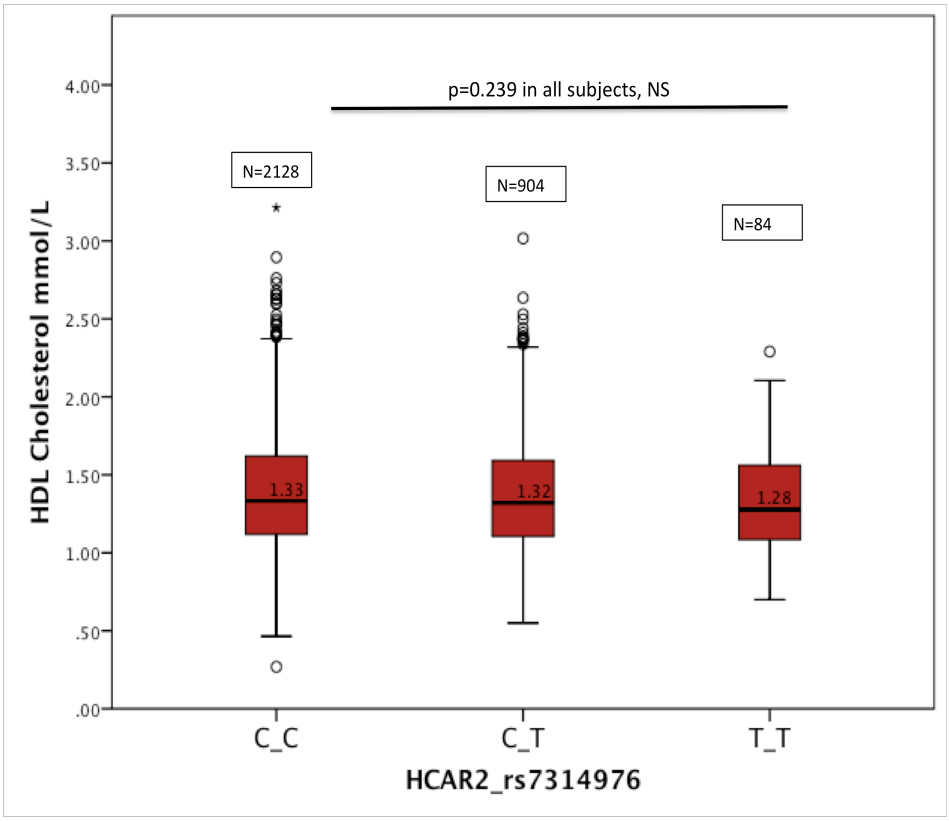

Figure 19: Median levels of HDL cholesterol in relation to genotypes in rs7314976.

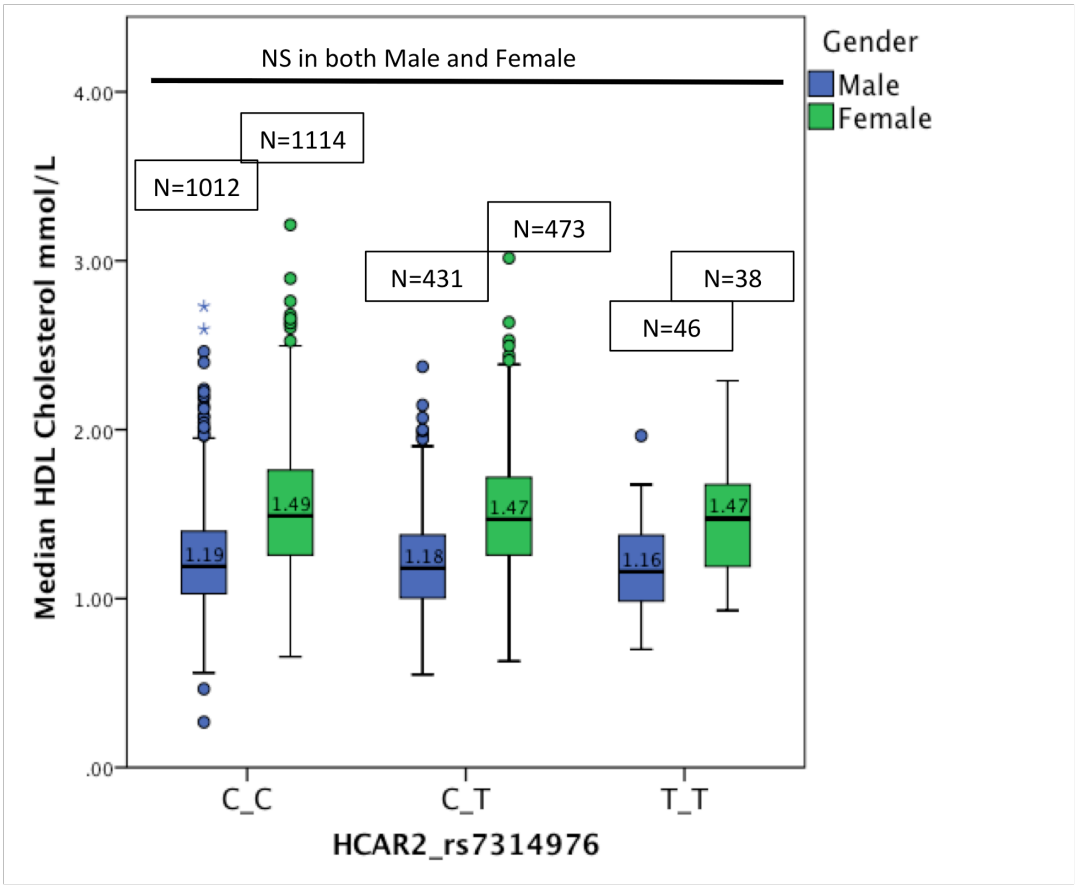

Figure 20: Median HDL levels in Males and females in relation to their rs7314976 genotypes (Differences are non-significant as tested by Kruskal-Wallis analysis of variance).

4.1.3. Targeting rs28682471 (951 G>A)

Resequencing in Chapter 3 (results in Table 10) confirmed the dual polymorphic nature of the 951G>A variant in both *HCAR2* and *HCAR3*. This variant codes for a Methionine to Isoleucine substitution in *HCAR2* (rs28682471) and an Isoleucine to Methionine substitution in *HCAR3* (rs116821988), both predicted to have a benign effect on both protein functions with Polyphen-2 (http://genetics.bwh.harvard.edu/pph2/)(Adzhubei et al., 2010).

Even with specific knowledge of the sequence around this variant in post-resequencing, the targeted genotyping of each locus on genomic DNA proved a significant challenge. With the help of the design team at LGC Genomics

(Hoddeston, UK), two different designs were assessed and run with different parameters. The custom designed assays were showing a genotyping spread with a co-localized mixture of calls, indicative of lack of specificity with the primers and probes and therefore amplification at both gene loci. After extensive testing it was concluded that it was impossible to target this locus (rs28682471) in one of the genes, and not the other, in gDNA.

However, this region has previously been characterized to be in strong linkage disequilibrium (LD) and the variant alleles of rs28682471 in *HCAR2* and its homologous equivalent rs116821988 in *HCAR3* were known not be on the same haplotypes (Zellner et al., 2005). Therefore, a possible way around directly genotyping these loci was to identify a proxy polymorphism that targets the specific haplotype of each locus. With this objective, resequencing data was assembled into genotypes and analyzed using PHASE v2.0.2 to construct haplotypes for the 64 individuals (Stephens, Smith, & Donnelly, 2001). I was hoping to identify a haplotype that could specifically tag variation in 951G>A in *HCAR2*. This would allow me to impute 951G>A genotypes by genotyping another more accessible variant from gDNA on the said haplotype.

As simplified in Figure 19, I was not able to resolve a haplotype that individually tagged the variant allele in 951G>A in *HCAR2*. As seen in the region highlighted in red, the variant allele of 951G>A (rs28682471 in *HCAR2*, represented as a '1') most frequently segregated in haplotypes with the variant allele of 931C>T (rs7314976 in *HCAR2,* represented as a '1') at a haplotype frequency of 10.94% in the resequenced population (in the haplotype labelled 'B'). The other two haplotypes (labelled 'G' and 'H') where the variant allele for 951G>A was shown to be present

(at a frequency of 3.91% each in the resequenced population, Figure 19) comprise four unique variants that could, even if just partially, tag the 951G>A variant (identified in squares, Figure 19). Out of these four variants, two variants were annotated through my resequencing to be polymorphic in both genes therefore not allowing for easy specific access through genotyping. Those variants are -530 G>A (rs1179102) and -7G>A (rs3825156) both in *HCAR3* (shown as blue squares in Figure 19). Genotyping assays were designed for the remaining two variants -442 C>T (rs111626900) in *HCAR3* and -1964 T>C (rs7133768) in *HCAR2* as they were uniquely polymorphic to their gene (shown as red squares in Figure 19). However, after extensive trialling, both assays failed to amplify the region of interest and show the expected genotyping spread. The difficulties faced with the genotyping assays were not entirely surprising since both these variants were in the complex promoter region of *HCAR2* and *HCAR3* (complexity previously discussed in section 3.9).

Even without being able to directly target the tagging variants, the haplotype assembly indicates that the HDL relationship previously found with 951G>A (genotyped on PCR products in section 3.4) and questioned with 931C>T (initially in section 3.4 and on a larger cohort in section 4.1.2) might still stand and be stronger that previously thought. The variant allele of the 951G>A polymorphism figures in three haplotypes ('B', 'G' and 'H') while the variant allele of 931C>T only figures in haplotype 'B'. That means that the HDL association investigated in section 4.1.2 tags the 'B' haplotype (in 10.94% of the haplotypes identified in the population), but misses the 'G' and 'H' haplotypes (in a total 7.82% of the haplotypes) for the 951G>A variant. Therefore, only a little over half (10.94% out

of 18.76%) of the expanded OBB haplotypes with the 951>A variant has been tested for the HDL association indirectly by genotyping on 931C>T. In fact, it could be that the initial relationship with 951G>A and HDL (introduced in section 3.4) could have been diluted by the 'B' haplotype and the 931C>T variant, if the association between 931C>T and HDL were not true (as tested in section 4.1.2). Although the two leftover haplotypes that represent 951G>A are inaccessible with current genotyping methods and sequence knowledge to test this hypothesis, it may well be that the HDL relationship is its strongest there.

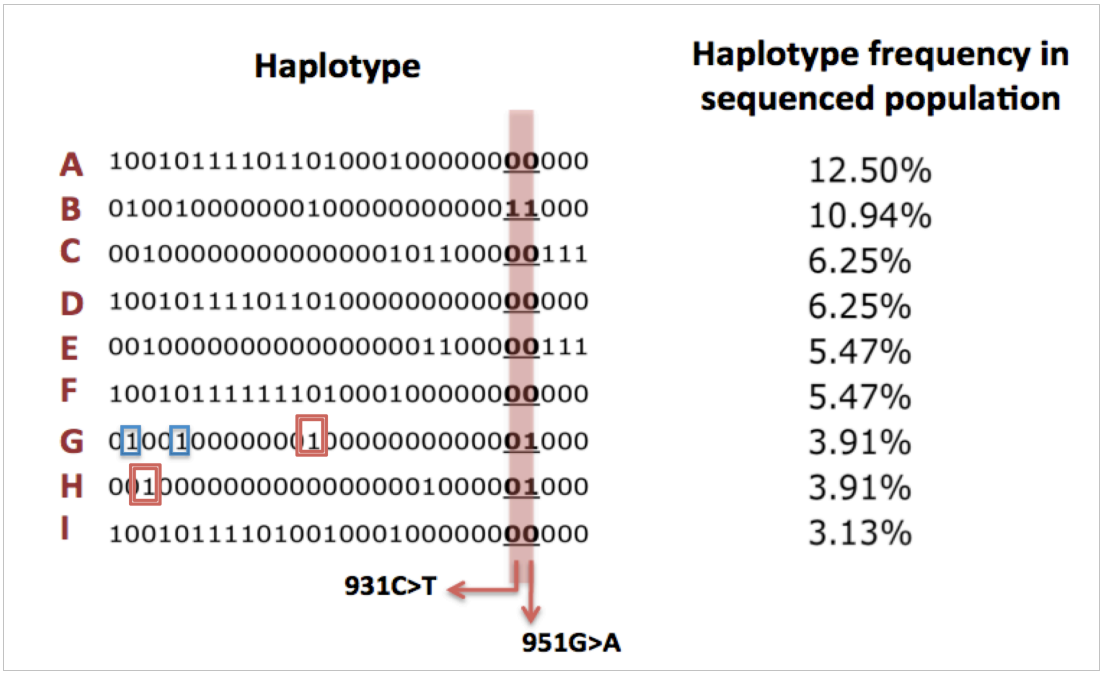

Figure 21: An assembly of haplotypes from polymorphisms in resequenced individuals
This figure is adapted from the analysis results from PHASE v2.0.2, haplotypes are constructed from genotype data: '0' refers to a polymorphism present in its wild-type form while '1' refers to the recessive allele. Each row represents a unique haplotype identified within the OBB population and the combination of alleles identified that make up that haplotype, along with its frequency, with each digit representing a SNP. Some further rare haplotypes with frequencies less than 3% were also uncovered but an element of uncertainty exists since the polymorphisms in question were only successfully sequenced in one direction. The variants highlighted in red represent the coding variants in *HCAR2* with the initial HDL association.

4.2. Exploring the promoter region after resequencing

4.2.1. Exploring rs590447 in *HCAR2*

I was also interested in identifying variants in the promoter region of *HCAR2* that could affect its expression and potentially translate into metabolic phenotypes. Specifically, the rs590447 variant in the promoter region of *HCAR2* had been previously predicted *in-silico* to have a functional effect on transcription factor binding sites and gene expression. This was identified as part of an effort to characterize SNPs with pharmaceutical relevant effects on G-protein coupled receptors (Mottagui-Tabar et al., 2005). Exploring the corresponding genomic location in light of the release of the Chromatin Immunoprecipitation and high-throughput DNA sequencing (ChIP-Seq) results by the ENCODE consortium (Landt et al., 2012) (Furey, 2012), showed that this SNP was within a region verified in a variety of cell lines to contain transcription factor binding sites (Figure 20).

Resequencing also showed that the corresponding genomic position for rs590447 (-296 A>G in H*CAR2*) was also polymorphic in *HCAR3* (rs55718746, -292C>T), with a MAF of 0.01 for rs590447 of in *HCAR2* in our population and a MAF of 0.33 for rs55718746 in *HCAR3* in my resequenced population (MAF=0.49 in 1000 Genomes). rs55718746 in *HCAR3* was also proven through ChIP-Seq results to be in a genomic region rich in transcription factor binding sites (Figure 21). Haplotype analysis of the resequencing results also showed that both these variants were on completely different haplotypes than the two coding region variants introduced in sections 4.1.1 and 4.1.3, adding impetus for genotyping these SNPs and probing for metabolic associations in the OBB. A genotyping

custom-made assay was synthesized with LGC Genomics (Hoddeston, UK) for rs590447 in *HCAR2.* Only three individuals out of the cohort of 4128 individuals carried the rare allele with no obvious drastic effect on their phenotypes.

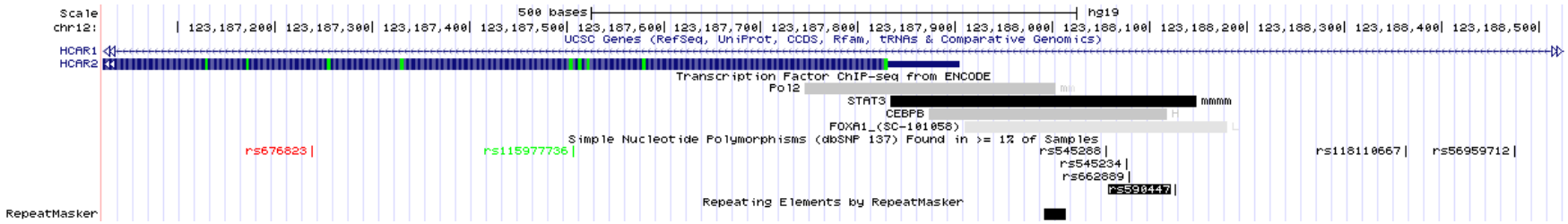

Figure 22: UCSC Genome Browser (GRCh37/hg19) Screenshot of the coding and promoter regions of *HCAR2*
The rs590447 variant is highlighted in black and the results from Chip-Seq in ENCODE showing the transcription factor binding sites in that specific region.

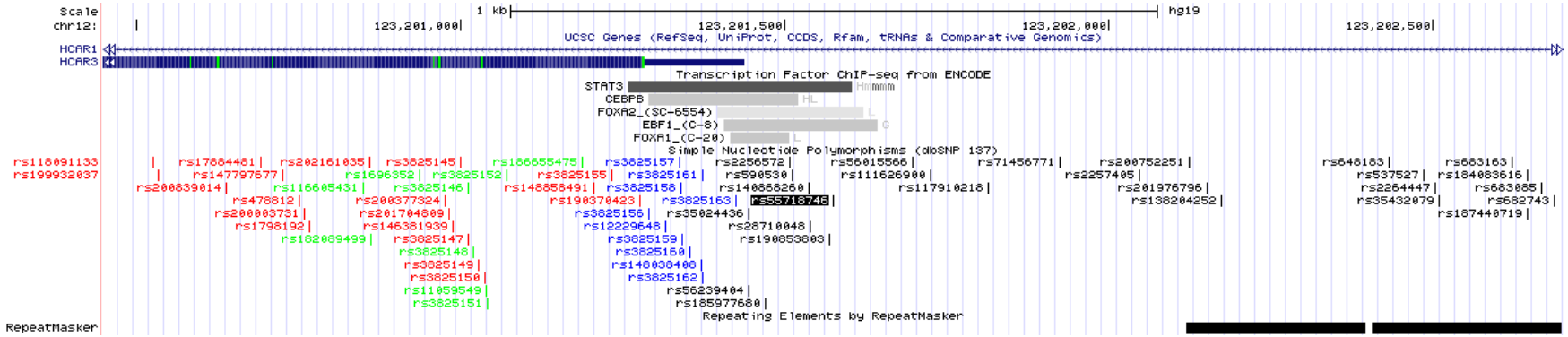

Figure 23:UCSC Genome Browser (GRCh37/hg19) Screenshot of the coding and promoter regions of *HCAR3*
The rs55718746 variant highlighted in black and the results from Chip-Seq in ENCODE showing the transcription factor binding sites in the same region.

4.2.2. Genotyping rs55718746 in *HCAR3*

Although *HCAR3'* s effects on metabolism are not as well understood as those of *HCAR2*, possibilities of co-regulation between the two genes (later discussed in Chapter 5) expanded my interest in exploring genetic variability in *HCAR3*'s promoter region. Furthermore, the location of the polymorphism within a hot spot for transcriptional regulation (as results from ChIP-Seq introduced in section 4.2.1) further warranted the investigation of rs55718746 in *HCAR3*.

The assay was custom designed and tested with LGC Genomics (Hoddeston, UK). A specific anchoring method had to be used to ensure that the assay differentiated between the two highly similar sequences of *HCAR2* and *HCAR3* promoters. This method makes use of a single unique base common to the region of interest to "anchor" the common primer to. The common primer is designed with this unique base at its 3' end and only the region containing this base or anchoring point will preferentially amplify (Sequences shown in Table 14).

Polymorphism	Primer Sequence(5'-3')
rs55718746 in *HCAR3*	FAM- TTCACTGATTTTCGAATGACAGTCG VIC- GTTTCACTGATTTTCGAATGACAGTCA Common- ATAAACAAYTAATAAGAATCCCCTGGGCA

Table 14: Primer sequences of successful custom designed genomic assay for rs55718746.

Genomic DNA samples from the OBB (details in Table 15) were genotyped under the same touchdown parameters as the ones introduced in Table 13 and following the protocol described in sections 2.2.1.1 and 2.2.1.2.

	Mean (± s.d.)	
	Female (N=2064)	Male (N=2064)
Age (years)	41.69 (±6.0)	42.02 (±5.7)
BMI (kg/m^2)	25.53 (±4.8)	26.63 (±4.02)
Glucose (mmol/L)	5.11 (±0.45)	5.45 (±0.68)
HDL Cholesterol (mmol/L)	1.52(±0.36)	1.22(±0.31)
CRP(mg/L)*	1.89 (±3.09)	2.02 (±4.8)

Table 15: Full details of genotyped individuals in the OBB. *The 99th percentile of CRP values is displayed with outliers removed.

4.2.3. rs55718746 (-292C>T) results

The MAF of rs55718746 in the OBB cohort was 0.42 (MAF=0.49 in 1000 Genomes), different to the MAF of 0.33 in the initial resequenced population. This is not surprising considering that the resequenced population was small (64 individuals) and selected for certain specific traits.

When looking at associations between genotypes in the rs55718746 polymorphism and lipid levels, no real patterns emerged with HDL, LDL or total cholesterol. However, a significant trend was observed with C-Reactive Protein (the inflammatory relevance of which has been introduced in section 1.3.2) measured with a high sensitivity CRP kit in the OBB. The hsCRP measurements considered for this relationship were lower than 10mg/L to exclude any individuals with an underlying pathogen-related inflammation. This association between hsCRP and rs55718746 in *HCAR3* was gender-specific and was statistically significant with a linear regression model adjusting for BMI (p=0.007 in Males, N=1808, Figure 22). The 20% reduction in hsCRP in the male homozygous recessive genotype was previously unreported so replication in a larger cohort was sought.

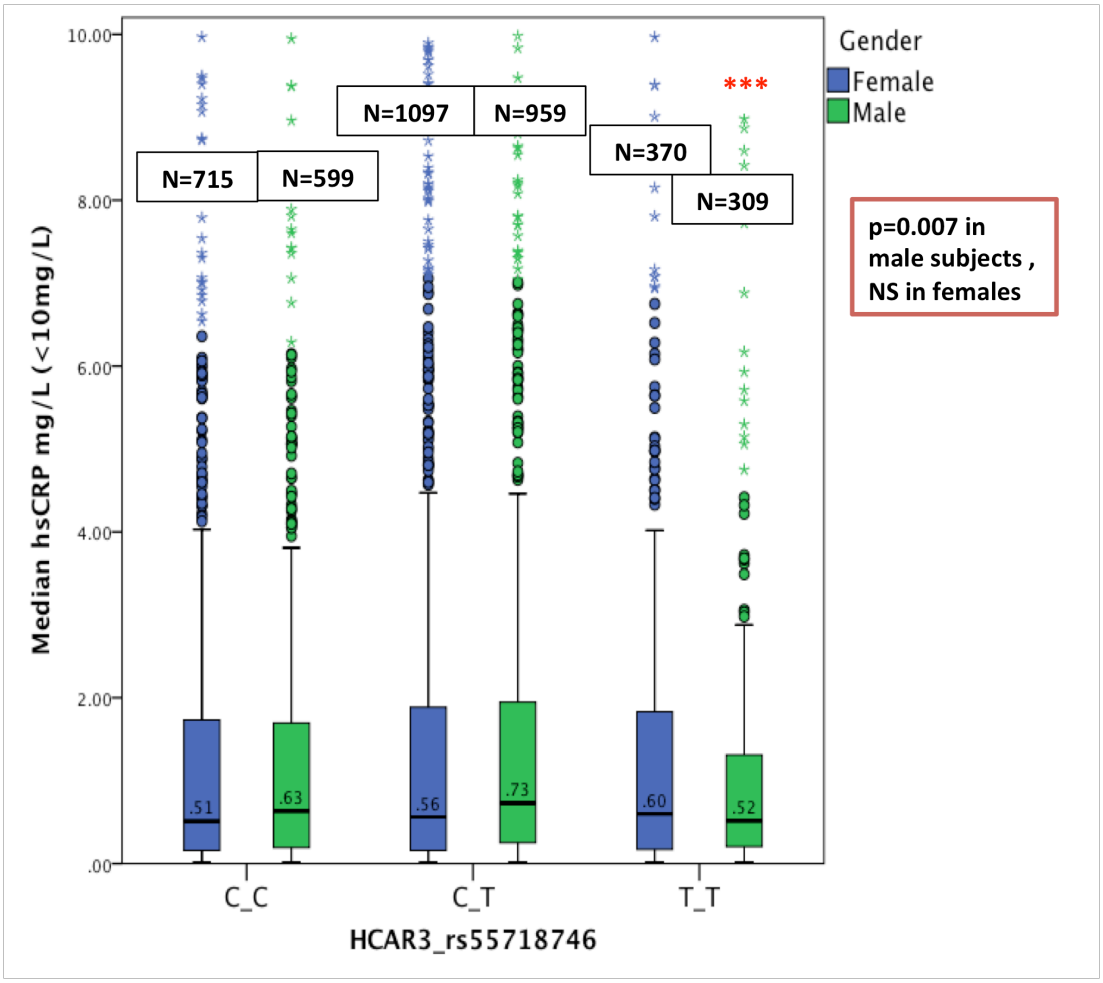

Figure 24: Median values of hsCRP in the OBB split by gender in rs55718746 genotypes (significant results in men p=0.007, N=1808, Kruskal-Wallis analysis of variance)

4.2.4. Replicating rs55718746 in *HCAR3* association

I sought to find a healthy matched cohort of a sufficiently large size to replicate the hsCRP association described above. I followed the standard measures to be considered for replication studies (Chanock et al., 2007) and ensured that a standardized methodology of genotyping and quality control existed by either having the possibility of the samples being sent over to our facility or to LGC Genomics (Hoddeston, UK) for genotyping.

4.2.4.1. *The NPHS-II study*

The prospective Second Northwick Park Heart Study (NPHS-II study) is a cohort of 3,052 healthy middle-aged men recruited in 1989 from general practices in the United Kingdom (Cooper et al., 2000). Information on lifestyle habits, height, weight, and blood pressure was recorded at baseline and after prospective follow-up with DNA samples were available for 2,778 of these men (details in Table 16). Since this cohort only comprised men, it was powered to replicate for the gender dependant hsCRP effect in rs57718746 genotypes.

	Mean (± s.d.)
	Male (N=2185)
Age (years)	55.7 (±3.2)
BMI (kg/m^2)	26.3 (±3.26)
HDL Cholesterol (mmol/L)	1.71(±0.58)
CRP(mg/L)	2.5 (±2.56)

Table 16: Details of the NPHS-II cohort on which I replicated my finding.

Of the 2,778 Caucasian men in the NPHS-II study, 2,236 were successfully genotyped for rs55718746 in *HCAR3* on gDNA using the designed assay described in section 4.2.2 and following the method described in sections 2.2.1.1 and 2.2.1.2. Since I was blinded for the variables, the genotyping results were quality checked and sent to my collaborator at University College of London (Professor Steve Humphries and his team) for unblinding and analysis. The research group's statistician (Ms. Jackie Cooper) performed the analysis (Table 17). Diabetic men and individuals with CRP levels out of the selected range for analysis (>0.02 and <10 mg/L) were excluded, bringing down the total number of genotyped males to 1677. This was done to match our sensitivity range and to remove outliers of underlying inflammatory conditions.

	Mean (± s.d.) CC (N=734)	TC (N=1032)	TT (N=419)	p value (Kruskal-Wallis test)	B (se) additive model, p value
Age	55.7 (±3.2)	55.8 (±3.2)	55.7 (±3.2)	0.54	0.060 (±0.096) p=0.53
BMI[1]	26.2 (±3.3)	26.3 (±3.4)	26.2 (±3.10)	0.996	-0.0001 (±0.004) p=0.98
HDL	1.71 (±0.59)	1.70 (±0.59)	1.72 (±0.58)	0.98	0.001 (±0.019) p=0.95
LDL	3.10 (±1.02)	3.10 (±1.00)	3.20 (±1.01)	0.18	0.040 (±0.033) p=0.23
hsCRP[1,2]	2.10 (±1.95) N=558	2.09 (±1.91) N=799	2.41 (±2.04) N=320	**0.05***	0.058 (±0.031) p=0.06

Table 17: Results from the NPHS-II cohort divided by rs55718746 genotypes.[1]b (se) is for log-transformed data, [2]any values <0.02 or >10 mg/L excluded.

The genotyped cohort displayed a slightly different minor allele frequency for the rs55718746 variant (MAF in NPHS-II is 0.49, MAF in OBB is 0.42). The results showed a significant increase in hsCRP values in the recessive genotype for men (p=0.05, N=1778) going in the opposite direction of our initial results in the OBB, where the recessive homozygous men displayed a lower level of hsCRP (shown in Table 19). Seeing that this replication resulted in a contradicting association with hsCRP, and since the final number of men was lower than expected after applying our exclusion criteria, a third cohort was sought to clarify the discrepancies.

4.2.4.2. The Whitehall cohort

The Whitehall cohort (Marmot & Brunner, 2005) is a high-profile comprehensive collection of over 10,000 civil servants in the UK that have been followed since 1985 for a range of clinical and metabolic variables as well as health-related questionnaires (relevant cohort details in Table 18), from which various findings have been published (Hamer et al., 2013; Talmud et al., 2013).

	Mean (± s.d.)	
	Female (N=998)	Male (N=3230)
Age (years)	61 (±6.13)	60.7 (±5.9)
BMI (kg/m^2)	27.1 (±5.6)	26.6 (±3.78)
Glucose (mmol/L)	5.27 (±1.24)	5.50 (±1.25)
HDL Cholesterol (mmol/L)	1.86(±0.51)	1.48(±0.39)
CRP(mg/L)*	2.72 (±3.29)	2.05 (±2.72)

Table 18: Details of the Whitehall cohort on which I replicated my findings. The 99th percentile of CRP values is displayed with outliers removed.

The previously designed assay for rs55718746 was used following the same conditions (described in section 4.2.2) with genotyping performed on gDNA at LGC Genomics facilities where the Whitehall dried-down gDNA samples are stored (Hoddeston, UK).

This cohort displayed a very similar MAF for rs55718746 as the one seen in the OBB (MAF=0.43). These small discordances in minor allele frequencies' are not surprising considering the allele's abundance and population sampling.

In this cohort, I found no significant associations between the genotypes and hsCRP. This was also true when the groups were split for gender and corrected for BMI and further adjusted for age differences (Figure 23). The hsCRP measurements in the Whitehall cohort were taken at a different phase, when the mean age of the individuals was about 20 years older than those in the OBB, a point which was not initially apparent when choosing this replication cohort.

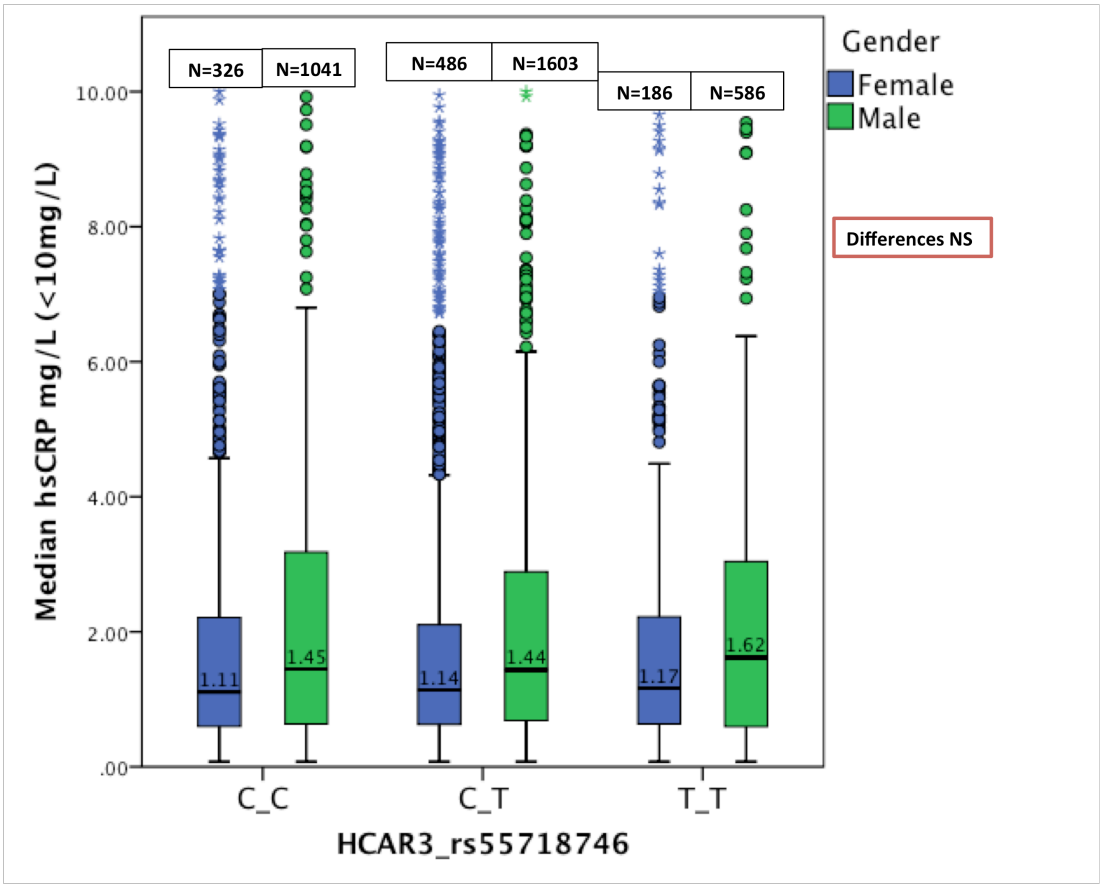

Figure 25: Median values of hsCRP in the Whitehall cohort in rs55718746 genotypes in *HCAR3* split by gender (p=0.831 for females and p=0.859 for males, Kruskal- Wallis test)

4.3. Summary of genetic associations after resequencing

The laborious effort of resequencing promoter and coding regions of both genes was valuable for the exploration of *HCAR2*- and *HCAR3*-specific genetic associations. It not only proved necessary for designing specific assays that targeted complicated polymorphisms (from which the relevant results with rs7319476, rs590447 and rs55718746 are shown), but it also allowed the construction of haplotypes (shown in section 4.1.3) that extended beyond the previously described coding region (Zellner et al., 2005).

When looking at specific genetic associations, the initial HDL association with rs7314976 (introduced in section 3.4) was tested on gDNA with a newly designed genotyping assay and significance was lost when OBB numbers were expanded. However, the trend of dose-dependant reduction in HDL with the rare allele of rs7314976 remained (section 4.1.2). The other HDL-relevant polymorphism rs28682471 could not be directly targeted with genotyping (described in section 4.1.3), but haplotype analysis from resequencing proved insightful (introduced in section 3.4). The haplotype assembly showed that there was a renewed interest in pursuing the HDL relationship with rs28682471 as well since rs7314976 might be diluting the strength of the association. To confirm whether one or both of these two coding region variants affects HDL, a larger cohort to genotype is needed for rs7314976. As for rs28682471, improved assays designs for variants that tag the haplotypes 'G' and 'H' of interest are needed to selectively target it (Figure 19, as explained in section 4.1.3). Indeed, a recent GWAS study in 45,981 individuals looking at loci that influenced circulating adiponectin levels (Dastani et al., 2012)

has added new hope to the rs7314976 and HDL story. This study initially uncovered another polymorphism, rs601339 (MAF=0.18), that is situated over 10kb further downstream of *HCAR2* beyond the reach of my resequencing, to be highly correlated with both adiponectin ($p=7.94 \times 10^{-10}$) and HDL ($p=5.59 \times 10^{-7}$). The researchers also coincidentally genotyped rs7314976 (MAF=0.14) in *HCAR2* in different cohorts of European descent and confirmed the HDL association with a larger number of individuals (n= 18,425, $p = 2.9 \times 10^{-8}$) and adding a new adiponectin association to the same variant (n= 8,285, $p = 4.6 \times 10^{-8}$)(Dastani et al., 2012). This example benefits of a large sample size but since no data were made available about the considerations for designing neither the genotyping assays nor any issues with homology for both these variants, it should be considered with a degree of caution.

The other intriguing genetic association that was uncovered was the significant 20% reduction in hsCRP levels in males with rs55718746 in *HCAR3*. This association in homozygous recessive men in the OBB (section 4.2.3) was tested in two rounds of replication. The first replication in the NPHS-II cohort produced results that went in the opposite direction of our association (section 4.2.4.1) while the Whitehall cohort lost the association altogether (section 4.2.4.2). Overall, the field of genetic associations is teeming with reports that fail to replicate previous findings. Consequently, the failure to replicate genotype-phenotype associations in different cohorts has been extensively reviewed and corresponding standards have been developed (Cardon & Bell, 2001) (Chanock et al., 2007). Drawing up from these reviews and the limits of association studies, the lack of success of replication of the hsCRP association with rs55718746 in *HCAR3* can be attributed

to several interpretations. The variants chosen could have been uninformative for both the lipid and the inflammation variables. Alternatively, this could be a simple instance of a Type I error in my initial significant associations, possibly as a factor of gender stratification. The Whitehall cohort was certainly more powered to detect associations in men since it comprised three times more men than women (detailed in Table 18). However, digging into cohort demographics, the age of the individuals in the Whitehall cohort might have played a large role in the loss of association. HsCRP levels are shown to increase with age and certain environmental confounding factors (Wener, Daum, & McQuillan, 2000), so a twenty year difference between mean age in the OBB and the Whitehall cohort could be a major confounder. When attempting to adjust for this age difference by combining cohorts and using a statistical multivariate regression model that accounts for age, the hsCRP association with rs55718746 is still found to be insignificant (N=8367, p=0.519). However, this difference in age is not necessarily statistically adjustable since other metabolic co-variables are also confounded by age. Ultimately, this highlights the difficulties of finding appropriate replication cohorts for a healthy young population (such as the OBB) and the need for another replication cohort test the hsCRP association with rs55718746.

It is clear that following the adiponectin and HDL associations described, the unanswered questions with the two coding region variants in *HCAR2* (rs7314976 and rs28682471), and the unfinished appropriate replication of the hsCRP findings, that further exploration for metabolic associations should take place. However as I have shown, all of these results should be interpreted with care,

assays custom-designed for genotyping and haplotypes rebuilt for analysis. It turns out genetically exploring this simple one-exon gene is not so simple.

Chapter 5 *HCAR2* and *HCAR3* Gene Expression in Human Adipose Tissue

5.1. Studying depot differences

Beyond its function as a storage depot, adipose tissue (AT) is recognized as having further immune, endocrine, mechanical, regenerative and thermal roles (Leff & Granneman, 2010). These roles are fulfilled to varying extents since factors such as energy status, location of the depots, gender and adiposity levels influence AT's responses (Arner, 2005a; Berg & Scherer, 2005; Frayn, 2002). Since expansion of AT can have a major impact on metabolic health (Willett, Dietz, & Colditz, 1999), understanding the differences and the fine-tuned molecular processes that fulfil AT roles can lead to better predicting the balance between a healthy and diseased metabolism.

Much of the initial reports on detrimental metabolic effects of AT focused on its expansion in the visceral depot (Björntorp, 1992),(Wajchenberg, 2000). The contributions of the subcutaneous adipose tissue (SAT) and its regional importance have recently been evaluated from clinical and epidemiological studies (Manolopoulos, Karpe, & Frayn, 2010). The review comprehensively compiled *in vitro* and *in vivo* evidence of differences between SAT depots in fatty acid handling, adipokine formation and release and the consequences of gluteo-femoral SAT loss or dysfunction. Interestingly, the gluteo-femoral depot was confirmed to be associated with improved metabolic and cardiovascular outcomes, the properties of which are interesting from a therapeutic perspective.

Much of the general cellular factors for differentiation and expansion of adipose tissue have been extensively studied (Gregoire, 2001), shifting the current focus to understanding AT differences at a genetic level (Gesta, 2006). In particular, exploring the transcriptome of adipose tissue has uncovered distinct

developmental origins for different depots (Gesta et al., 2011; Karastergiou et al., 2013; n.d.; Tchkonia et al., 2007) along with differences between humans and mice, justifying the relevance of investigations on human adipocytes (Gesta, 2006). Studying adipose gene expression has also allowed the investigation of the effects of obesity on inflammation and lipid metabolic pathways (Laurila et al., 2013; Soronen et al., 2012) and differences in microRNA regulation between depots (Rantalainen et al., 2011). The genome-wide expression microarrays used in these studies comprehensively evaluated thousands of genes' transcript levels. As a result, the literature has many reports and new investigations that follow up on transcript differences previously seen.

Accounts of *HCAR2* and *HCAR3* gene expression in adipose tissue have mainly been for *in vivo* and *in vitro* treatment with nicotinic acid (Kang, Kim, & Youn, 2011), with no specific mention in any of the transcriptomic studies. To explore whether the genes had been comprehensively covered in the expression microarrays, I investigated the two main arrays that are most commonly used: the Sentrix® Human-6 and HumanRef-8 Expression BeadChips by Illumina (most recently used in(Karastergiou et al., 2013)) and GeneChip Human Genome U133 Plus 2.0 Array by Affymetrix (used in (Min et al., 2012) and (Rantalainen et al., 2011)). These microarrays contain probes for over 40,000 genes that have been selected with bioinformatics algorithms to avoid highly homologous sequences, areas with repeats and complex sequences. Both arrays provided sequence information for the probes sequences and genes they have covered. This allowed me to look up and blast the sequences to see whether they adequately covered the region of interest. In the case of the Illumina array, it was possible to contact technical support and

obtain their annotation files (http://www.switchtoi.com/annotationfiles.ilmn) and directly look up the gene of interest and probe sequence were provided. I blasted those across the latest NCBI dbSNP (build 137, Jun 26, 2012) and the identity matches (Table 19) indicated that the probes were not necessarily specific enough to detect either transcript independently.

Gene	Probe Sequence (5'-3')	Identity match
HCAR2	GGTGAGCCATGGAGCCCCTCTTATCTGGGCCCAACCTCTCCTTA AATAAC	100% *HCAR2* 86.7% *HCAR3*
HCAR3	CTCCGGTGAGCCATGGAGCCCCTCTTATCTGGGCCCAACCTCAA ATAACC	100% *HCAR2* 100% *HCAR3*

Table 19: Illumina Sentrix Human-6 V2 Expression BeadChip Probe sequences and gene identity match

Similarly, I accessed Affymetrix' annotation files to look for gene names and their corresponding probes (http://www.affymetrix.com/analysis/netaffx/xmlquery.affx?netaffx=netaffx4_annot). The GeneChip Human Genome U133 Plus 2.0 Array only covered *HCAR1* and *HCAR3* and no probes were available for *HCAR2*.

Therefore, considering that both genes had not been adequately covered in transcriptome studies and following from *HCAR2's* interesting range of effects, questions about depot distribution of transcripts warranted further investigation.

5.2. Gene Expression considerations and methods

5.2.1. Ensuring assay specificity

In light of the high sequence similarity between *HCAR2* and *HCAR3*, reservations about detecting a combination of both transcripts in off-target amplification needed to be addressed. I therefore began by testing the specificity of the commercial assays for each gene with specific positive control PCR products that I created with sequence similarities in mind (Figure 24). Several primer pairs were tested to make the positive controls (sequences in Table 20) and their identity was confirmed with the MfeI genotyping assay (as described in section 2.2.1.1).

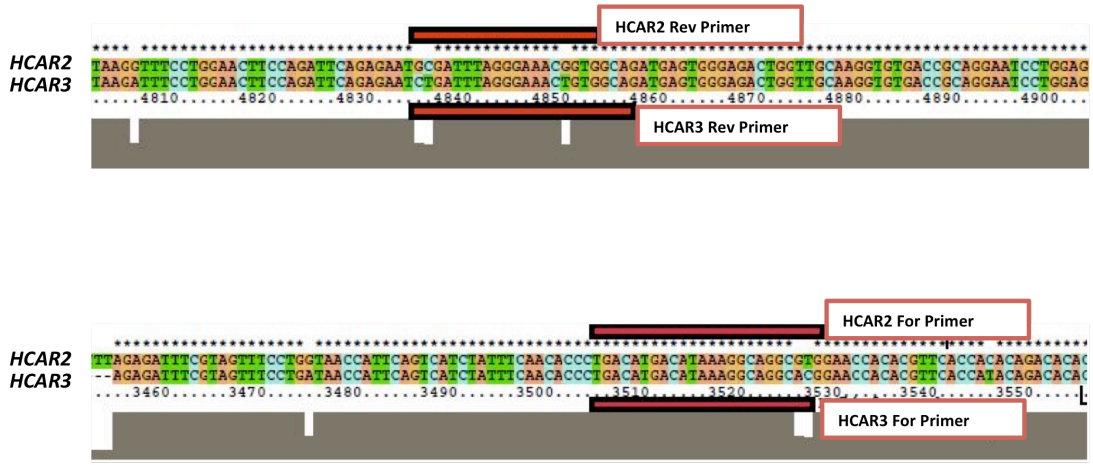

Figure 26: Snapshot from Clustal X (1.83) Multiple Sequence Alignment Software showing an alignment of *HCAR2* and *HCAR3* and the mismatch considerations when designing each primer.

Gene	Primer Sequence (5'-3')	Tm°	Product size bp
HCAR2	F- ACA TGA CAT AAA GGC AGG CGT	61.8	1451
	R- AGC GTC AGA GAT GAA GCA AAA G	61.1	
HCAR3	F- TGA CAT GAC ATA AAG GCA GGC AC	64.4	1446
	R- AGC GTC AGA GAT GAA GCA AGT T	60.6	

Table 20: Primer sequences for positive controls

These positive reference products were diluted 1:10,000 and were run as reference controls with both *HCAR2* and *HCAR3* commercial Taqman gene expression assays. The generic *HCAR2* assay (Hs00271958_s1) provided by Life Technologies (Paisley, UK) showed non-specific amplification and detection of both HCAR2 and HCAR3 PCR reference positive controls (Figure 25, A). Consequently, a custom designed assay was created with Life Technologies (Paisley, UK) that showed specific detection of HCAR2 reference controls (Figure 25, B). Similarly, a custom assay was also designed and tested for *HCAR3* (details in Table 21).

Following my concerns that were reported to Life Technologies (Paisley, UK), the off-target amplification issue has been revaluated in Taqman assays and they then issued a disclaimer noting the specificity issues and designed revised versions of their assays.

Gene	**Primer and Probe Sequences (5'-3')**
HCAR2	F- CCATGGAGCCCCTCTTATCTG R- AATGTCCCTTCTTGGCATGG Probe- CCAACCTCTCCTTAAAT
HCAR3	F- CCATGGAGCCCCTCTTATCTG R- TGACAATGTCCCTTCTTGGAATG Probe- CCCAACCTCAAATAA

Table 21: Primer and Probe sequences of custom-made gene expression assays

A.

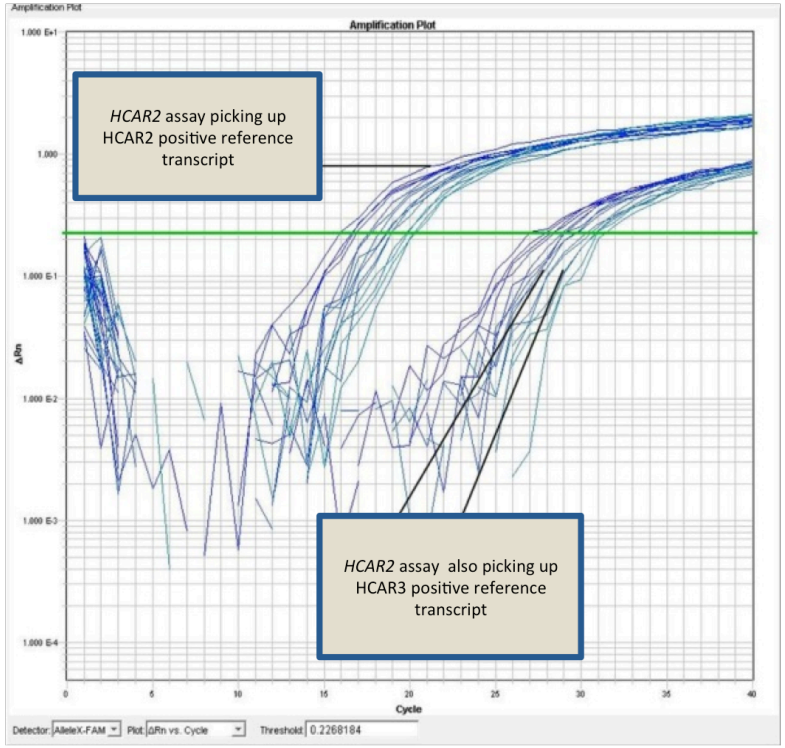

B.

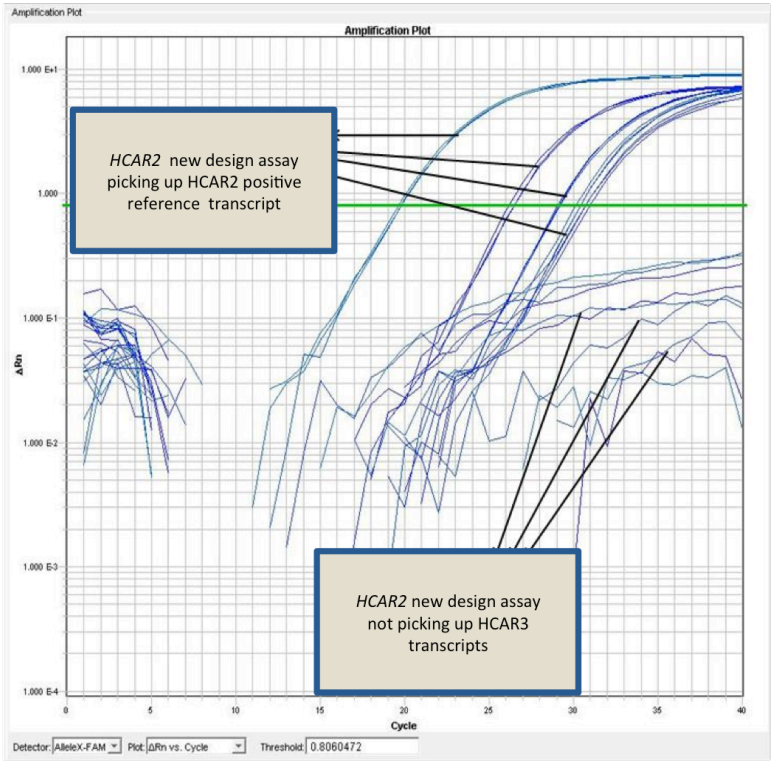

Figure 27: Screenshot from ABI Sequence Detection Systems Software (SDS) signal intensity detection with increasing cycles
This clearly shows two different signals being amplified by the assay in the first screenshot corresponding to the PCR positive reference controls for *HCAR2* and *HCAR3*. The custom made new design assay for *HCAR2* only amplifies dilutions of the *HCAR2* PCR positive reference controls. This assay was deemed to be specific and is the one used for the expression assays in the results section reaching the limits of detection between 29 and 32 cycles with variation between samples less than 5%.

5.2.2. Determining gene expression

Abdominal and gluteal adipose tissue samples were made available from the OBB (described in section 2.3.1) and their mRNA was extracted and reverse transcribed into cDNA (described in sections 2.3.2 and 2.3.2). A total of 213 paired abdominal/gluteal biopsies with an even gender representation was used. As seen in Table 22, many significant metabolic differences existed in the biopsied panel between female and male samples, so further analysis was done on male and female samples separately. Taqman gene expression was run on the cDNA samples, normalized to housekeeping genes and analyzed as described in section 2.3.3.

	Mean (± s.d.)		
	Female (N=106)	Male (N=107)	Significance
Age (years)	44.18 (±5.28)	44.5 (±4.5)	p=0.67
BMI (kg/m^2)	26.29 (±4.71)	28.4 (±5.04)	p=0.002
WHR	0.937 (±0.06)	0.82 (±0.08)	p<0.001
Glucose (mmol/L)	5.09 (±0.56)	5.36 (±0.48)	p<0.001
HOMA-IR	3.28 (±3.5)	3.59 (±2.3)	p=0.009
HDL Cholesterol (mmol/L)	1.42 (±0.32)	1.15 (±0.27)	p<0.001
hsCRP (mg/L)	2.73 (±4.37)	2.15 (±2.84)	p=0.260
Waist circumference (cm)	84.9 (±12.9)	98.8 (±13.13)	p<0.001
Hip circumference (cm)	103.2 (±8.9)	105.3 (±8.9)	p=0.083
Suprailiac skinfold thickness (mm)	22.26 (±10.62)	24.61(±13.01)	p=0.340

Table 22: Details of the abdominal/gluteal paired biopsy panel, anthropometric differences tested with the Wilcoxon Sign-Rank t tests.

5.3. *HCAR2* and *HCAR3* transcript levels in adipose tissue

5.3.1. Depot associations

As mentioned in 5.2.2, analysis was performed on male and female samples separately as the well documented differences in metabolic parameters and fat distribution between the genders (Regitz-Zagrosek, Lehmkuhl, & Weickert, 2006; Wells, 2007), were indeed seen in the biopsied panel (Table 22).

In females, *HCAR2* transcript differences reached significance between the subcutaneous abdominal and the gluteal depots, with female abdominal relative expression of *HCAR2* being 18% higher than that of the corresponding gluteal depot (Table 23, Figure 28, N=106, p<0.0001, Wilcoxon Signed Ranks Test). No differences in *HCAR2* transcript levels were seen in males between depots (Table 23, Figure 28, N=107, p=0.402, Wilcoxon Signed Ranks Test).

Gender	Depot	*HCAR2* Mean ΔΔCt (±se)	Significance
Female	Abdominal	1.19 (±0.04)	p<0.0001
	Gluteal	1.01 (±0.03)	N=106
Male	Abdominal	0.94 (±0.05)	p=0.402
	Gluteal	0.96 (±0.03)	N=107

Table 23: Details of mean ΔΔCt levels of *HCAR2* in the adipose tissue from different depots corresponding to Figure 28

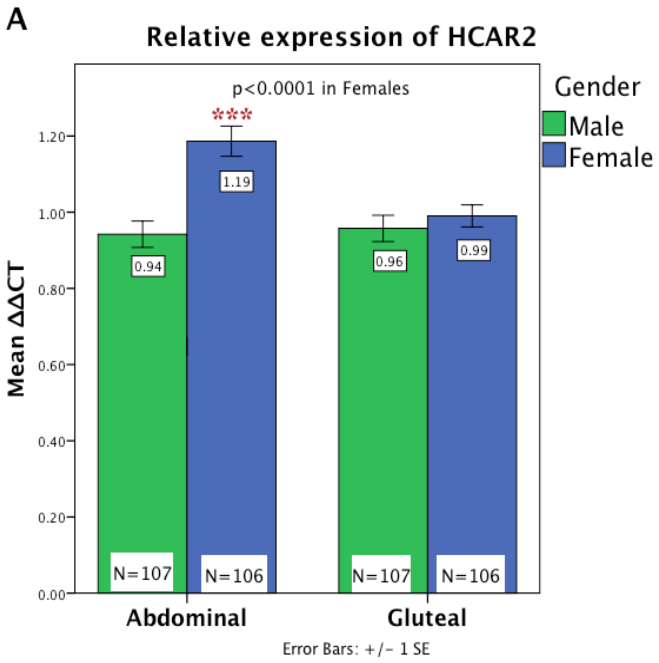

Figure 28: Differences in relative expression of HCAR2 between genders

HCAR3 transcript levels, on the other hand, were constant across biopsies and no differences were seen between depots (Table 24, p=0.055 in males, p=0.838 in females, Wilcoxon Signed Ranks Test).

Gender	Depot	*HCAR3* Mean ΔΔCt (±se)	Significance
Female	Abdominal	1.13 (±0.06)	p= 0.838
	Gluteal	1.12 (±0.05)	N=106
Male	Abdominal	1.03 (±0.06)	p=0.055
	Gluteal	0.90 (±0.05)	N=107

Table 24: Details of mean ΔΔCt levels of *HCAR3* in the adipose tissue from different depots

5.3.2. Increasing adiposity

The effect of increasing adiposity on *HCAR2* and *HCAR3* transcript levels, as tested with a regression model, showed depot-specific predictors. An increasing waist circumference, traditionally seen in an android model of obesity, predicted abdominal *HCAR2* transcript levels strongly in male (β=-0.373, p<0.001) and female subjects (β=-0.251, p=0.01, Table 25). An increasing hip circumference, on the other hand, only predicted Gluteal *HCAR2* in males (β=-0.209, p=0.036, Table 25). Increasing adiposity had no effects on *HCAR3* across genders and depots (results not reported as no significance was seen).

Increasing	**Gender**	***HCAR2* transcript levels in**	**β**	**Significance p**
Waist Circumference	*Female*	Abdominal	-0.251	0.01
	Male	Abdominal	-0.37	<0.001
Hip Circumference	*Female*	Gluteal	0.026	0.798
	Male	Gluteal	-0.209	0.036

Table 25: Regression analysis showing the effect of an increasing adiposity on *HCAR2* expression in genders and depots

5.3.3. Associations with metabolic phenotypees

Associations between transcript levels and metabolic phenotypes were also investigated. Following from NA's receptor-mediated effect on inflammation parameters and CRP in particular (introduced in 1.3.2 and seen in 4.2.3), I hypothesized that *HCAR2* transcript levels may predict measured levels of circulating CRP. After adjusting for Waist-Hip Ratio, a strong predictor of CRP levels in both females and males (β=0.4, p<0.001), *HCAR2* expression in both depots and genders was not found to predict CRP levels (Table 26). Metabolic phenotypes, such as HOMA-IR and HDL cholesterol, were also tested for associations with transcript levels while also correcting for gender and obesity.

The regression model showed no predictors for these variables either (results not shown). The implications of all of these findings will further be discussed in section 5.5.

Gender	*HCAR2* transcript levels predicting CRP levels in	β	Significance p
Female	Abdominal	-0.184	0.231
	Gluteal	0.220	0.124
Male	Abdominal	0.007	0.956
	Gluteal	-0.034	0.778

Table 26: Regression analysis results of *HCAR2* transcript levels and CRP associations

5.3.4. *HCAR2* and *HCAR3* regulation

Considering the homology in the promoter region of both the genes and consequently suspecting similar gene expression regulation, I investigated transcript correlation between these two genes. As predicted, transcript levels in both depots positively correlated with each other ($p<0.0001$ for both depots, $\rho=0.451$ for the abdominal depot and $\rho=0.371$ for the gluteal depot, Figures 31, 32).

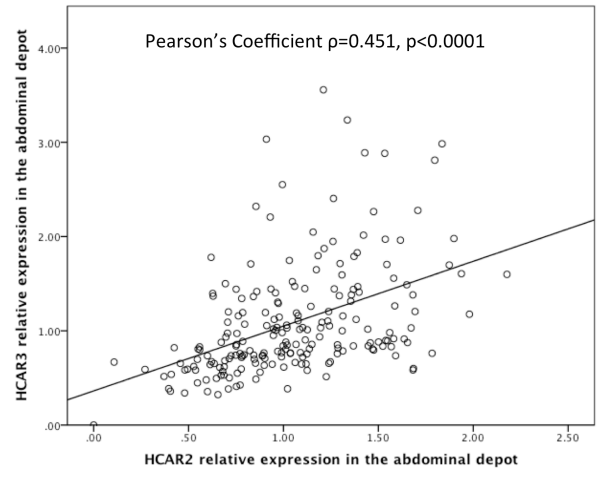

Figure 29: Correlations between *HCAR2* and *HCAR3* transcript levels in the abdominal depot.

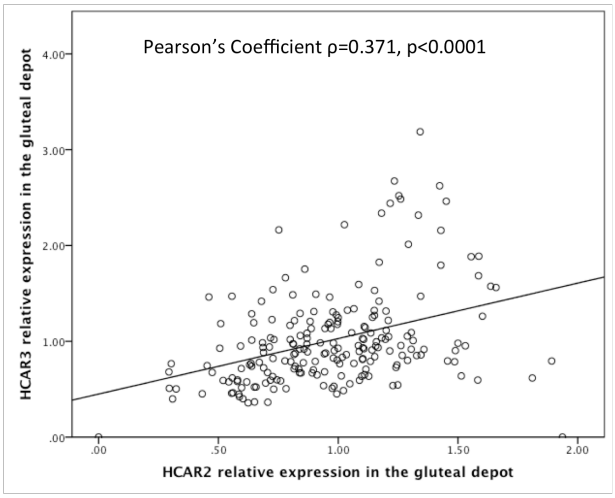

Figure 30: Correlations between *HCAR2* and *HCAR3* transcript levels in the gluteal depot.

5.4. Polymorphisms and gene expression

Measuring relative gene expression was also useful to investigate whether previously discussed polymorphisms that fall within a putative transcription factor-binding site in *HCAR2* and *HCAR3* (introduced in section 4.2) had any effects on transcript levels of both genes. As mentioned in section 4.2.1, and due to the small minor allele frequency of rs590447 in *HCAR2* (in the OBB, MAF<0.01), the lack of individuals that carried the rare allele meant that the analysis on this polymorphism could not be followed-up on this panel.

On the other hand, the variant alleles of rs55718746 (MAF=0.43 in the OBB) in *HCAR3* were present in the biopsied panel (N=210).

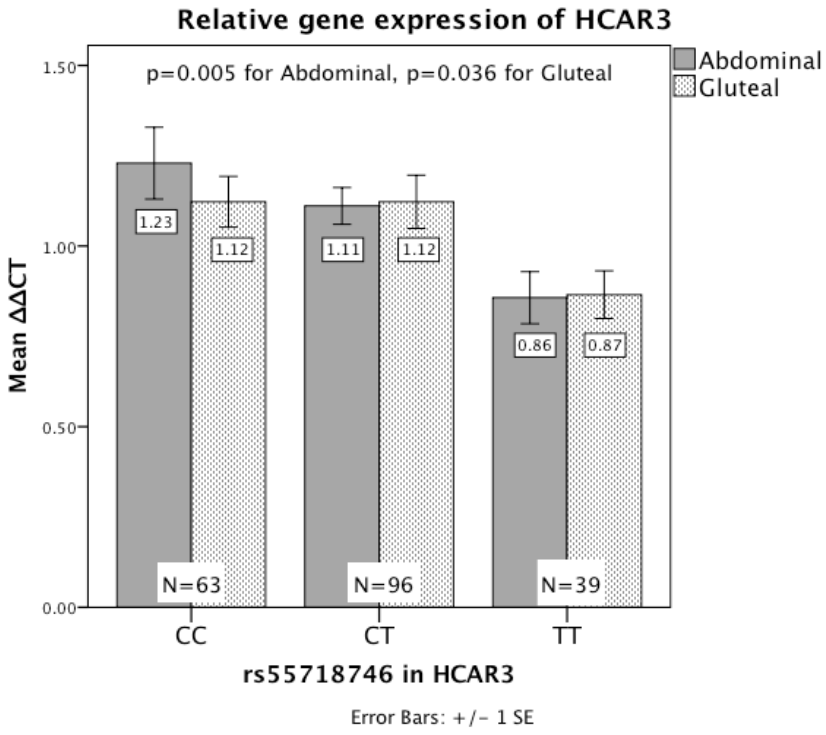

Figure 31: Relative gene expression of *HCAR3* corresponding to different rs55718746 genotypes.

Mean relative expression of *HCAR3* between rs55718746 genotypes was found to be significantly different in both abdominal and gluteal depots in a dose-dependant manner (p=0.006 for abdominal, p= 0.03 for gluteal, N=183, Figure 30). This almost 30% total dose-dependant decrease in mean ΔΔCt (from 1.23±0.06 to 0.86±0.06 in the abdominal depot), is likely to expose a true effect since the finding is internally replicated and the effect is in both depots based on two separate analyses.

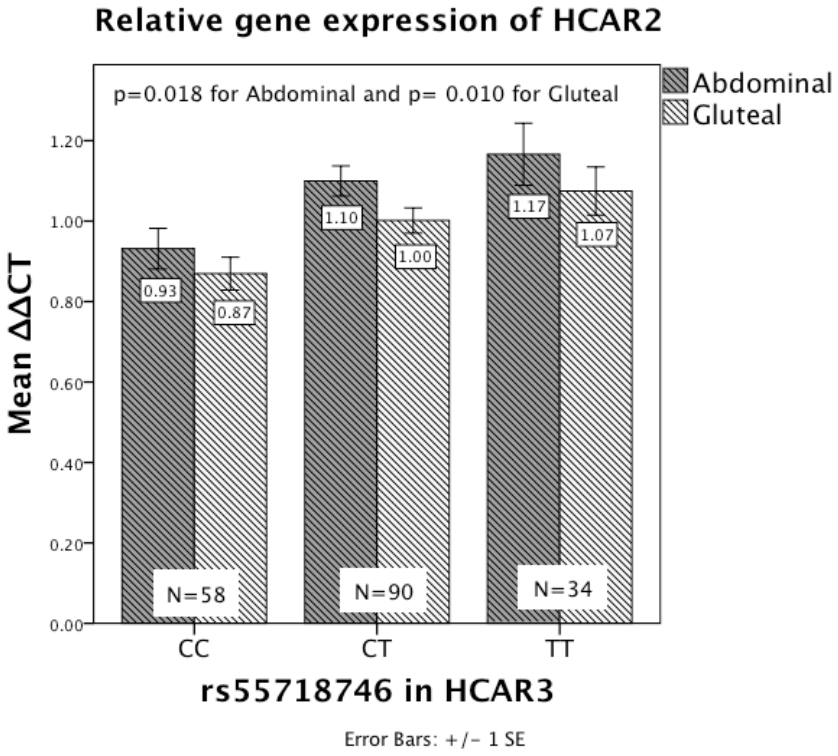

Figure 32: Corresponding Relative gene expression of *HCAR2* in different rs55718746 genotypes

The rs55718746 polymorphism in *HCAR3* was also associated with a significant change in transcript levels of *HCAR2.* However, this effect was in the opposite direction than the change seen with *HCAR3* (p=0.018 for abdominal, p= 0.01 for gluteal, N=183, Figure 31). Similarly, this 20% total increase (from 0.93±0.02 to

1.17±0.02 in the abdominal depot) was dose-dependant. This was a paradoxical effect considering that transcript levels of *HCAR2* and *HCAR3* were positively correlated in both depots (shown in section 5.3.2.).

In light of the association with rs55718746 and hsCRP introduced in section 4.2.3, the physiological significance of this dose-dependant increase in relative expression of *HCAR2* with rs55718746 was considered. Although it is known that *HCAR2* gene expression is upregulated in reponse to both hypoxia and inflammatory stimuli (TNFα, LPS and INFγ) in particular cells (Knowles et al., 2006; Zandi-Nejad et al., 2013), regulation of expression in relation to ligand exposure is not properly understood (Offermanns et al., 2011). However in theory, individuals with higher gene expression of *HCAR2* and following activation by the corresponding ligand, could show more of the positive lipid and anti-inflammatory profiles of NA administration. The levels of *HCAR2*'s endogenous ligand, β-hydroxybutyrate, required to activate the receptor are around its EC_{50} of 1.6mM. Genotyped individuals from the OBB were therefore split into quartiles based on their fasting β-hydroxybutyrate levels, with the top quartile having a concentration range from 0.101mM to 1.2mM. The top quartile (N=1053) was tested for any differences in lipid or hsCRP levels between the rs55718746 genotypes. No significant differences or trends were found in any of the parameters (in particular, N=375, p=0.194, Kruskal-Wallis for males and hsCRP). Considering that the range of β-hydroxybutyrate is potentially at the lower end required for receptor activation, this finding is not surprising. Furthermore, the differences in relative expression of *HCAR2* in adipose tissue do not necessarily translate onto other tissues where *HCAR2* is expressed. There might be different forms of regulation

and compensation to account for in immune cells for example. Similarly, the elevated expression of the receptor could be due to physiological signals shown to affect it (hypoxia and inflammation) and not necessarily translate into differences in receptor activation and further signalling cascades. Also, it is not completely understood how much HCAR2 in adipose tissue, compared to the receptor in other cell types, contributes to the overall range of effects. Ultimately, it would be interesting to test the same hypothesis in individuals where the receptor is known to be activated, as is the case with NA therapy, to see whether the differences in expression levels with rs55718746 leads to any observable phenotypic differences.

5.5 Summary of expression results

Differences in adipose tissue lipolysis and fatty acid uptake in the abdominal and gluteal depots have been documented in both isolated adipocytes and *in vivo*. Depot-differences exist in stimulated lipolysis across both genders, with the gluteo-femoral depot having a lower response (Leibel & Hirsch, 1987; Wahrenberg, Lönnqvist, & Arner, 1989). Furthermore, depot and gender differences are seen in mechanisms that regulate glucose and fatty acid uptake, with better insulin sensitivity and greater adipocyte size seen in the gluteal depot of women (Fried & Kral, 1987; Johnson, Fried, Pi-Sunyer, & Albu, 2001). In addition, the gluteo-femoral depot in women is more adept at taking up circulating fatty acids after a meal compared to both the abdominal depot in women and to both depots in men (Koutsari, Ali, Mundi, & Jensen, 2011). *In vivo*, lipolytic activity, as driven by catecholamines, is higher in the abdominal adipocytes (Wahrenberg et al., 1989) and corresponds to the higher levels of beta-adrenoreceptor transcripts in the abdominal depot (Arner, Hellström, Wahrenberg, & Brönnegård, 1990). Further differences exist at the level of adipose tissue differentiation and growth with femoral adipose tissue of women being able to expand by hyperplasia in response to overfeeding, while the abdominal sc AT responds with a hypertrophic growth (Tchoukalova et al., 2010). Most of these differences are transcript-based and have physiological significances that are being uncovered. The therapeutic applications from these can be very relevant.

Correspondingly, *HCAR2* transcript differences were seen in the isolated biopsies. Presented in section 5.3, relative gene expression of *HCAR2* was different between

depots in females specifically, with abdominal biopsies having about 18% higher mean relative expression than corresponding gluteal biopsies (Figure 28). Since *HCAR2* expression is shown to increase in hypoxic conditions and following inflammatory stimuli (Knowles et al., 2006; Zandi-Nejad et al., 2013), it is possible that the abdominal depot which harbours these conditions more so than the gluteal depot (Manolopoulos et al., 2010), contributes to this difference. It is however unclear why male samples do not exhibit the same behaviour.

Following this rationale, an increase in adiposity that increases hypoxic conditions and inflammation, would have been predicted to increase *HCAR2* expression. Instead, increased abdominal adiposity as measured in waist circumference, negatively predicted relative expression of abdominal *HCAR2* both in males and females (shown in 5.3.2). These observations fit with several studies examining the downregulation of gene expression in human adipose tissue *in vivo* driven by obesity (Tan, Goossens, Humphreys, Vidal, & Karpe, 2004),(McQuaid et al., 2011),(Karastergiou et al., 2013), and inflammation (Shah et al., 2012). The genes studied encompass lipolysis and metabolism-related genes (Karastergiou et al., 2013; McQuaid et al., 2011; Tan et al., 2004), and cell development and differentiation genes (Shah et al., 2012). This depot-specific downregulation warrants further interest since it contrasts with the constant gene expression in the expanding gluteal depot (female only). In the gluteal depot, *HCAR2's* constant expression in females with increasing hip adiposity, corresponds well with the 'protective sink' proprieties of gynoid obesity, where the constant *HCAR2* expression can be considered an example of the receptor's protective role in overall metabolism. This finding does not translate into male adipose tissue as

seen with the negative correlation with *HCAR2* in gluteal depot in men with increasing hip circumference, and in general (β=-0.209, p=0.036, Table 25) (Manolopoulos et al., 2010).

On the whole, *HCAR2*'s transcript differences between depots, genders and obesity status in AT strengthen the receptor's role in metabolism and obesity-related pathologies, considering they follow the trends of other AT relevant genes. This is particularly important in light of the recent report (Lauring et al., 2012) discrediting the receptor's profound lipid effects to be a result of its anti-lipolytic role in adipose tissue (described in Chapter 1). As a result since then, most of the investigation into the receptor's mode of action and involvement in anti-inflammatory signals have focused on studying immune cells (Digby, Ruparelia, & Choudhury, 2012b; Joshua T Chai, 2013). Previous evidence of *HCAR2* gene expression in immune cells show gene up-regulation in hypoxic conditions and after 'activation' with inflammatory stimuli (Knowles et al., 2006; Zandi-Nejad et al., 2013), unlike the evidence shown in 5.3. This further illustrates the need to explore the function of both HCAR2 and HCAR3 in human adipose tissue independently than that in immune cells, as the gene expression in response to inflammation (either with a stimulus or obesity-induced) seems different. This gap in knowledge and the specific targeting of *HCAR2* and *HCAR3* transcript in human adipose tissue makes this effort unique and relevant.

When looking at associations with metabolic phenotypes and specifically hypothesizing an effect on hsCRP of varying levels of *HCAR2* transcript, no significance was detected (section 5.3.1). This is not surprising considering the various levels of regulation and signalling involved in hsCRP protein modulation

and secretion. Perhaps a better future measure would be to test the associations of these metabolic phenotypes with *HCAR2* by measuring gene expressions of known direct precursors alongside *HCAR2* and *HCAR3*, as less post-transcriptional and signalling events are involved.

HCAR3 on the other hand, seems to have constant transcript levels across all measured parameters, even when *HCAR2* and *HCAR3* transcript are found to be positively correlated (shown in section 5.3.2). However, before dismissing the role this gene plays, some intriguing questions remain unanswered about the regulation of both genes at a transcript level. While at first glance, the results fit into the predicted 'homologous promoter – homologous regulation' correlation pattern (Figures 31, 32), the lack of depot or gender-based difference and the dose-dependant opposite effect on transcripts with rs55718746, suggests this to be more complex (Figures 33, 34). This could be an effect of transcription factor binding site compensation or an unexplored form of fine-tuning of regulation that requires further exploration. The rs557718746 polymorphism in *HCAR3* can therefore be classified as an unreported expression quantitative trait loci acting on *HCAR2* and *HCAR3* in cis (cis-eQTL) (reviewed in (Franke & Jansen, 2009)) considering its immediate location to *HCAR3*. Not much is known about eQTLs around *HCAR2* and *HCAR3* gene regions as the most recent GTEx (Genotype-Tissue Expression) eQTL Browser (http://www.ncbi.nlm.nih.gov/gtex/GTEX2/gtex.cgi) holds no records for the region. This reveals the need to further explore transcription factors and gene expression for both genes, along with post-translational handling and protein expression. This is particularly interesting from

a pharmaceutical perspective, as tapping into regulation of these genes could prove useful in designing future therapeutic options.

Finally, as specific as the gene expression assay has been designed to be, it is not necessarily showing the full picture of *HCAR2*'s role in adipocytes. To begin with, the biopsies comprise other cells from the stromovascular fraction, including immature adipocytes and infiltrated immune cells. Both of these cell fractions are known to express *HCAR2* and *HCAR3* and are potentially contributing the total levels we are detecting. Furthermore, levels of HCAR2 protein have not been reliably measured in human adipocytes but rather in human macrophages (Chai, Digby, Ruparelia, Jefferson, et al., 2013b). In their attempt to overcome homology issues, Digby et al. tested HCAR2 protein levels and the antibody specificity in a system where *HCAR2* has been knocked down – but one that does not specify whether *HCAR3* and therefore the HCAR3 protein has been knocked out as well (Digby, Martinez, Jefferson, Ruparelia, et al., 2012a). Most of the other published protein results are from mice mature adipocytes or murine cell lines, which don't express *HCAR3*. Along with the expected species differences between mice and humans in metabolism (Demetrius, 2005), these studies bypass the issue of homology in antibody design and HCAR2 protein detection and ignore any role HCAR3 could play. One study that did address the relationship between levels of *HCAR2* transcript and protein in humans, did so in brain tissue, and found that the levels were not correlated (Miller & Dulay, 2008). Although this study is not relevant to metabolic research, it acknowledges the gap in knowledge in post-translational regulation and processing for *HCAR2* transcripts. Consequently, not much is known about the post-transcriptional regulation and activity of HCAR2.

Both of these are necessary to better understand the impact of transcript differences on adipose tissue. Overall, these results combined with those from the previous chapter (in relation to CRP as presented in section 4.2.2) justify the need to explore the role that HCAR2 and HCAR3 play at functional level in human adipocytes.

Chapter 6 Functional interrogation of the involvement of *HCAR2* and *HCAR3* in modulating inflammation

6.1. From adipose tissue to adipocytes

As introduced in Chapter 1, mounting evidence describes adipose tissue's role in modulating systemic inflammation and its influence on overall metabolic health (Berg & Scherer, 2005). Adipokine secretion by adipose tissue, notably that of adiponectin, has been shown to increase in response to treatment with NA, with evidence of the involvement of HCAR2 (Digby et al., 2010). However, more is known about the role of HCAR2 in mediating inflammatory signals in adipose tissue-associated macrophages than in adipocytes. In fact, the bulk of the investigations of the receptor's role in modulating inflammation has focused on immune cells in view of their importance in the progression of atherosclerosis, as introduced in 1.3.2.2 (Digby, Martinez, Jefferson, Ruparelia, et al., 2012a; Knowles et al., 2006; Kostylina et al., 2008; Maciejewski-Lenoir et al., 2006; Zandi-Nejad et al., 2013). In murine macrophages in particular, HCAR2 – the mRNA of which is up-regulated in response to LPS exposure which 'activates' the macrophage – responds to NA and leads to a reduced secretion of IL-6 and TNFα, with promising anti-inflammatory applications (Zandi-Nejad et al., 2013). Although HCAR2 is expressed in adipocytes and immune cell components of adipose tissue, an interrogation of the anti-inflammatory role of HCAR2 in the human adipocyte has not been properly conducted.

Only one study clearly set out to investigate the anti-inflammatory role of HCAR2 in the adipocyte, but did so in 3T3-L1 cells *in vitro* (Digby et al., 2010). The 3T3-L1 cell line, established in the 1970s from murine preadipocytes, is a widely used model of adipose tissue (Green & Kehinde, 1974; 1975). Although this cell line is

reproducible and has been widely characterized, occurrences in rodent models do not always translate to humans. A notable example is the insulin-resistance linked adipokine resistin which is released by the adipocytes of obese mice but not produced by human adipocytes (Arner, 2005b). Furthermore, and of more relevance to investigations with nicotinic aid, the 3T3-L1 cells only express *HCAR2* and do not express *HCAR3* (Offermanns, 2006). My findings from Chapter 4 suggest that a polymorphism in *HCAR3* (rs55718746) is associated with CRP levels (described in section 4.2.2) and affects gene expression of both *HCAR3* and *HCAR2* (described in section 5.4). This, along with the evidence that *HCAR2* and *HCAR3* gene expression is positively correlated (shown in section 5.3.2), reinforces the need to explore both of these genes' involvement and interplay in inflammation in human adipose tissue *in vitro*.

Following recent evidence indicating that the isolated human adipocyte was capable of independently synthesizing and expressing a range of biologically active inflammatory cytokines such as IL-6, IL-18 and CRP (Meijer et al., 2011), I chose to investigate whether *HCAR2*'s expression and exposure to its ligand could affect these inflammation parameters. In particular, Meijer *et al*. showed that the mature adipocyte synthesized biologically active IL-6 protein that has a chemotactic importance for macrophage infiltration. IL-6 secretion from adipose tissue could account for a third of systemic levels and is an important signalling protein that modulates hepatic synthesis of CRP (Bataille & Klein, 1992; Yudkin, Kumari, Humphries, & Mohamed-Ali, 2000). In light of my findings associating rs55718746 in HCAR3 with CRP levels (described in section 4.2.3) and the gene expression results (described in Chapter 5), I therefore decided to establish a pilot study to

investigate *IL-6* transcript and protein levels in isolated human adipocytes and question *HCAR2* and *HCAR3*'s involvement in inflammation.

6.2. Developing the experimental setup in primary adipocytes

Human adipose tissue biopsies from the OBB allowed convenient access to a source of preadipocytes to setup my *in vitro* experiments. Although mature human adipocytes can also be obtained and cultured from the biopsies, they are buoyant and need to be cultured in suspension and only for a short period. Furthermore, they are fragile and get damaged during isolation so are not suitable for inflammation studies. Therefore, isolating human preadipocytes from adipose tissue and their subsequent differentiation in vitro provides the best means by which the adipocyte may be studied (RODBELL, 1964),(Hauner, Skurk, & Wabitsch, 2001).

6.2.1. Human adipocyte isolation and differentiation

Preadipocytes differentiated *in vitro* retain the characteristics of the adipose depot from which they were taken (Tchkonia et al., 2006). Following from results in section 5.3 that showed the female abdominal depot to express higher levels of *HCAR2* transcript, abdominal subcutaneous biopsies were obtained from six female volunteers. Human preadipocytes were isolated (as described in section 2.4.1) then differentiated as explained in section 2.4.2. The differentiating adipocytes were morphologically monitored until considered mature at day 14 (as seen in Figures 32 A and B). Adipocyte differentiation from three biopsies was terminated as one did not show any signs of differentiation at day 14 and the two others had signs of unexplained cell death – the implications of this will be further

discussed in section 6.4. Adipocytes from the three remaining biopsies came from females with an average BMI of 23.5± 1.7 and an average age of 32± 2.6 years.

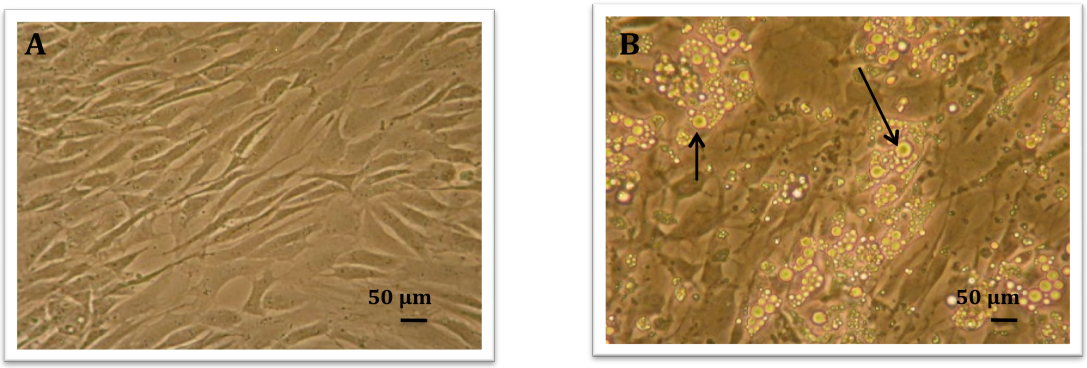

Figure 33: Abdominal preadipocytes seen at day 0 before differentiation (A) and at day 14 with lipid droplets visible (B) as indicated by the arrows.

6.2.2. HCAR2 and HCAR3 in cultured adipocytes

Adipocyte RNA was extracted from cell culture at days 0 and 14 to assay for transcript levels of both *HCAR2* and *HCAR3* following the method described in section 2.3.2 and using the specific designed assays described in section 5.2. The highest levels of transcript for both genes were found at day 14 when the cells were fully differentiated (Figure 33). It was noted that there was a large variability between levels of transcript between the three individuals due to inconsistencies in the degree of differentiation between them and the limited number of samples.

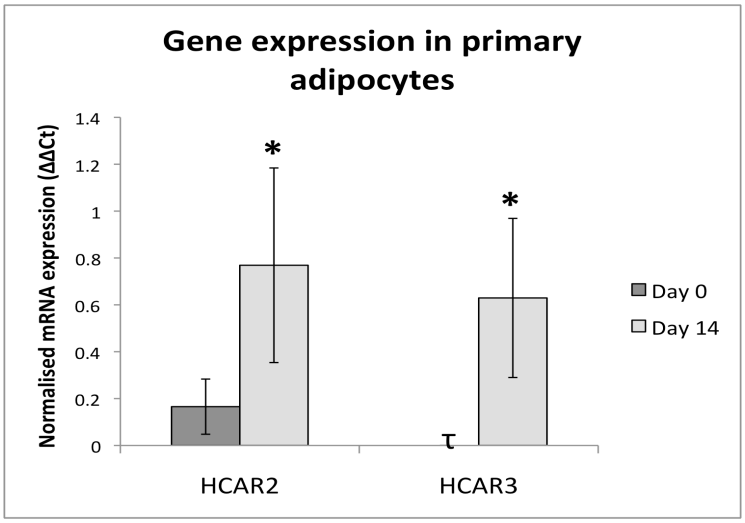

Figure 34: Levels of *HCAR2* and *HCAR3* transcript in isolated preadipocytes (day 0) and mature adipocytes (day 14) (p=0.01, N=3).

6.2.3. IL-6 in cultured adipocytes

Adipocytes were grown in six-well plates at a starting seeding density of approximately 200,000 cells. At day 14, a subset of the cells was extracted for basal *IL-6* transcript and protein measurements following the method described in sections 2.3.2 and 2.3.3. When cell numbers allowed it, a separate well for a protein fraction for each condition was seeded at day 0 and extracted as described in section 2.4.4. This was used to normalize protein measurements from the ELISA.

Measured *IL-6* mRNA at day 0 and day 14 showed a great variability between the biopsies of origin with day 0 preadipocytes expressing more of *IL-6* transcript compared to day 14 of the same biopsy (seen in Figure 34). Again, the small number of samples along with their unsimilar differenatiating behaviour could explain these inconsistencies.

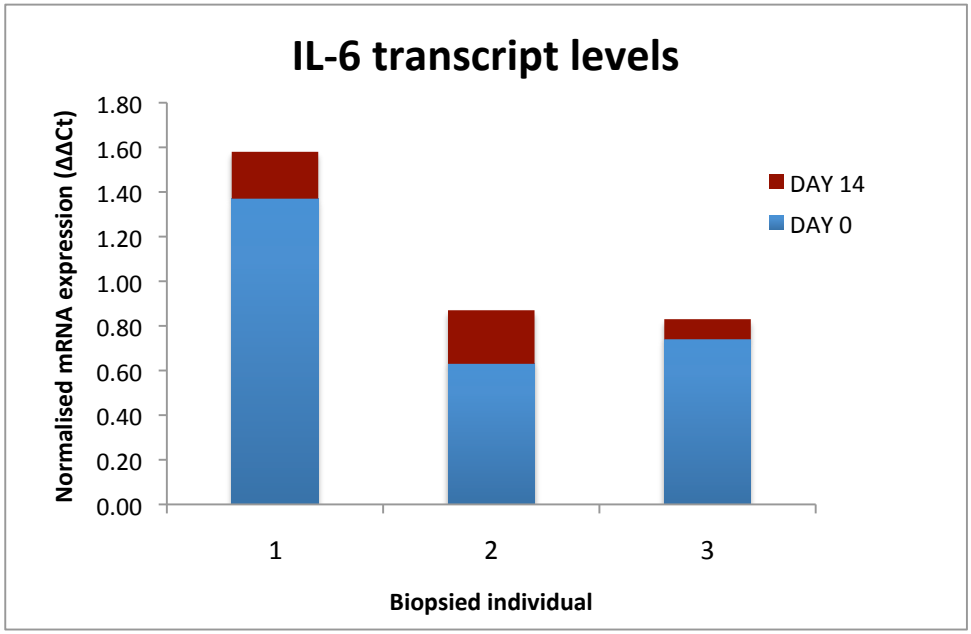

Figure 35: Inter-individual variability in IL-6 relative gene expression at day 0 and day 14.

The high sensitivity IL-6 ELISA kit conventionally used for measuring protein levels in supernatants of cultured adipocytes proved to be too sensitive for measurements of day 14. Even when a 1:100,000 dilution of the supernatant was attempted, the media was too saturated with IL-6 protein for the measurement to be trusted. No exact measurement for these days was therefore available.

6.2.4. Modulating IL-6 levels with nicotinic acid

Seeing that cultured adipocytes expressed *IL-6* transcript at a basal level without any added inflammatory stimulus, I decided to test whether nicotinic acid in the media could directly alter those transcript levels. Day 14 mature adipocytes were chosen since they expressed the highest level of *HCAR2* and *HCAR3* and a range of concentration of NA was tested modelled on previous cell culture inflammation work on 3T3-L1 cells (Digby et al., 2010).

At day 14, the differentiation medium was removed and the cells were serum-starved for 4 hours and insulin-starved for 24 hours following the same protocol (Digby et al., 2010). After that, the media were replaced with either a fresh DMEM (NIL) or DMEM supplemented with dissolved nicotinic acid (Sigma-Aldrich, Gillingham, UK) at a final concentration of 50, 100 and 500μM (NA50, NA100, NA500). Cells were left in the described conditions for 4 hours before assaying the supernatant for *IL-6* (described in section 2.4.3) and extracting protein and mRNA (described in sections 2.4.4 and 2.3.2).

Similarly, the response was variable between the cultured adipocytes from the three biopsies, so the results are shown independently. As seen in Figure 34, there seems to be a dose-dependent response to varying levels of NA compared to baseline at day 14 (marked as NIL) in cultured mature adipocytes from biopsied individuals 1 and 2 (Figures 35 A and B). Cultured mature adipocytes from biopsied Individual 3 on the other hand, exhibit a somewhat different response, with varied levels of transcripts that do not seem to respond to NA as much (Figure 35 C). Again, the variability between individuals and the small sample size could explain this unexpected result.

Measuring protein levels again proved unreliable, whereby measurements seemed to fluctuate and could only be reliably measured in mature cultured adipocytes from biopsied individual 2 (Figure 35 D). These levels do not seem to correspond to transcript levels of *IL-6* in the mature adipocytes from the same biopsied individual.

In retrospect, two ELISA kits at different sensitivity ranges should have been used. The choice of the sensitivity of the used kit (0.156 - 10 pg/mL) was guided by

previous experiments in which a 2pg/ml sensitivity kit was used to measure LPS-induced up-regulation of IL-6 (Hoch et al., 2008). Since their measurements were in response to a strong inflammatory stimulus, I had decided that a more sensitive kit would be more suitable to my conditions that did not include any stimulus.

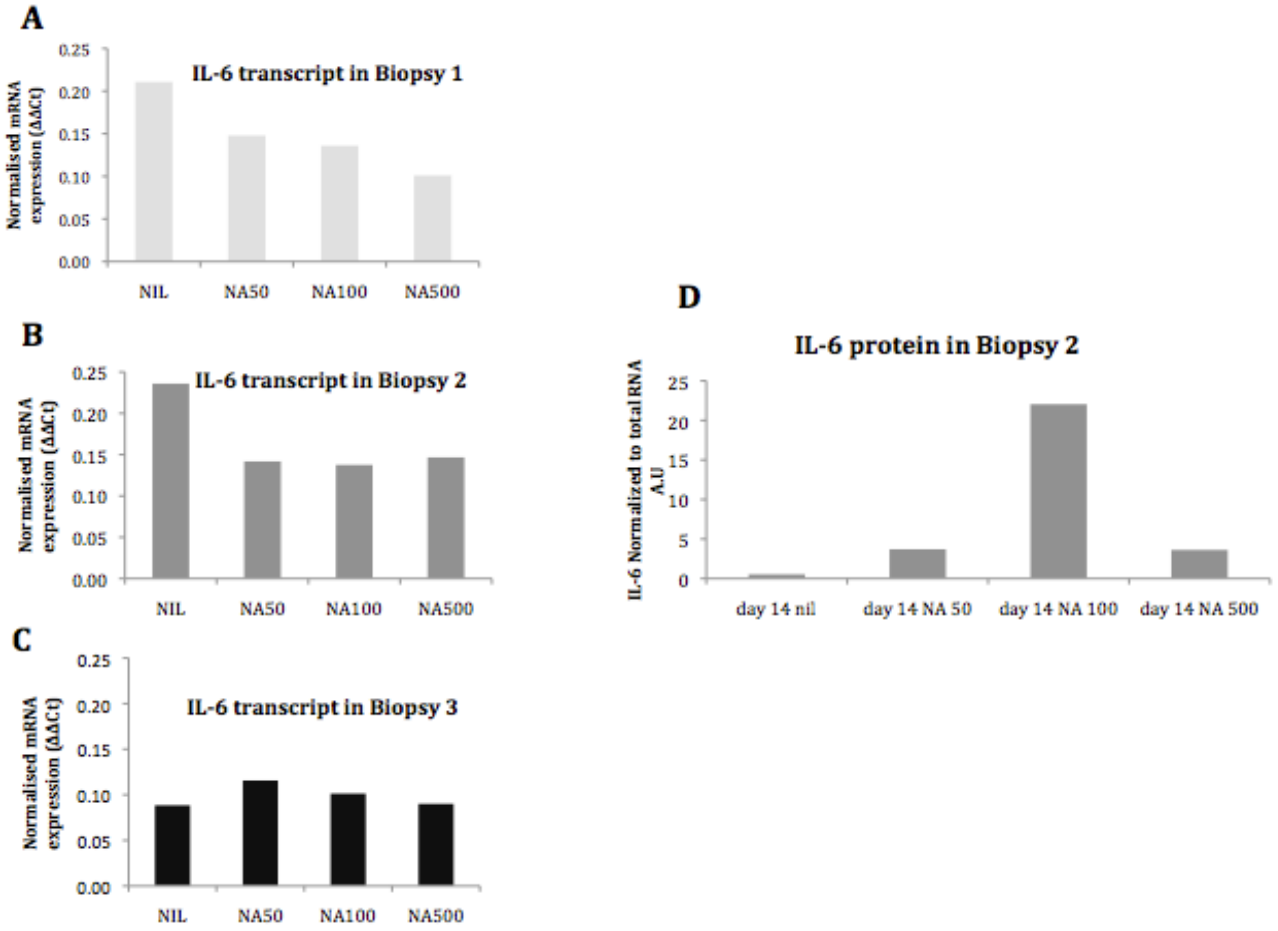

Figure 36: Levels of IL-6 transcript in cultured mature adipocytes (day 14) from three female volunteers
No exposure to NA is presented as NIL or exposure to varying concentrations of NA is presented as 50µM (NA50), 100µM (NA100) and 500µM (NA500). In D, measured IL-6 protein levels for the same conditions from the supernatant of adipocytes from individual 2.

6.3. Gene expression knockdown

In parallel to the inflammation experiments, I attempted to knockdown gene expression of both *HCAR2* and *HCAR3* with small interfering RNA to test whether they play a role in the inflammatory process.

Introducing synthetic double-stranded RNA molecules (siRNAs) into cultured cells leads to efficient gene silencing through the degradation of the complimentary endogenous mRNA (Caplen, Parrish, Imani, Fire, & Morgan, 2001). The delivery methods for introducing these siRNAs differ, e.g. by transfection, electroporation or viral gene transfer, and two were trialled in the cultured human primary adipocytes. Commercial siRNA (Invitrogen, Paisley, UK) that targeted *HCAR2* and *HCAR3* was first introduced into the mature primary adipocytes using Lipofectamine™ transfection reagent following the manufacturer's instructions. Since both *HCAR2* and *HCAR3* had highest levels of expression at day 14 and the transfected siRNAs reaches optimal silencing around 2 days post-transfection as per manufacturer's recommendations, gene knockdown was attempted at day 12 of the differentiation process. Multiple rounds of optimization did not prevent the transfected cells from showing signs of cell death. Despite significant expertise in this technique in the laboratory, doubts about the toxicity of Lipofectamine™ agent and documented evidence about difficulties of transfecting mature adipocytes (Kilroy, Burk, & Floyd, 2009), led me to abandoning this method .

As an alternative, I attempted lentiviral transfection with DNA expression plasmids. The pre-assembled lentiviral particles generate a stable stem-loop structure (short hairpin RNA, shRNA) connecting two siRNA molecules that are recognized and cut by the DICER complex in the cells. The resulting siRNA

molecules are then able to target complementary mRNA for degradation (Stewart et al., 2003). MISSION® TRC lentiviral constructs and appropriate controls (Sigma-Aldrich, Gillingham, UK) were added to 80% confluent at day 0 since the lentiviral particles express the shRNA in a stable manner, following the manufacturer's protocol. The transfected cells were expanded and then differentiated as described in section 2.4.2. Similarly, accounts of cell death and lack of differentiation was observed in all transfected cells possibly due to the toxicity of the transfected constructs, leading to this effort being put on hold. Future attempts at gene knockdown in the primary cells should be optimized in cells that show consistent robust differentiation and perhaps with a different set of less toxic constructs such as the recent inducible lacO shRNA vectors pLKO-puro-IPTG-1xLacO (Sigma Aldrich, Gillingham, UK). An inducible system might bypass toxicity issues at critical points of the cell's development and differentiation by turning on the shRNA expression when the target genes are highly expressed. In the case of HCAR2 and HCAR3, this could be done after day 10. This method was not available at the time of this pilot study and could be an interesting lead to follow.

6.4. Lessons learnt from primary cells

There lacks an experimental setup that interrogates the roles of both *HCAR2* and *HCAR3* in modulating inflammation in human primary adipocytes. In this chapter, I aimed to develop a pilot study to test the effects of nicotinic acid on IL-6 levels in cultured primary adipocytes as a proxy of adipocyte inflammation.

6.4.1. Inconsistencies with primary cells

Firstly, an inconsistency in cell viability, growth rate and differentiation potential was seen in the primary cells coming from different individuals. The differences in rates of cell growth between individuals hindered the ability to have similar cell numbers, so some conditions of the experiments could not afford corresponding protein fractions. Furthermore, as mentioned in section 6.2.1, half of the biopsied cells were lost to either lack of differentiation or unexplained cell death. Although the cells were grown in presence of antibiotics in the media (described in section 2.4.2) and tested negative for presence of mycoplasma, undetected pathogens could have caused these problems.

From a genetic aspect, levels of transcripts varied between individuals both for *HCAR2* and *HCAR3* (with the levels at their highest at day 14 of differentiation seen in Figure 33) and for *IL-6* (with the levels highest at day 0 seen in Figure 34). The variability in these levels, seen as a large standard error if the measurements were averaged, was exacerbated by the small sample size and the differences in cell behaviour in both differentiation and some cell death.

IL-6 transcript levels were seen to decrease with differentiation for all three individuals with levels lower at day 14 than they are at day 0 (seen in Figure 34). Although this finding corresponds to previous observations in a differentiating 3T3-L1 cell line (Yudkin et al., 2000), it goes against the most recent evidence in human primary adipocytes (Meijer et al., 2011). Meijer *et al.* used two independent sources of subcutaneous human primary adipocytes that they purchased commercially, without specifying the depot nor the obesity status. Using an Illumina (mRNA) Bead Array to assay levels of various cytokines and proteomic analysis to validate protein levels, they found that levels of *IL-6* transcript increased with differentiation in their human primary cells and corresponding protein levels decreased. They therefore concluded a negative correlation existed between mRNA and protein levels for *IL-6* (Meijer et al., 2011).

This negative correlation does not correspond to my analysis, in which IL-6 protein levels measured reliably in biopsied individual 2 do not seem to show any consistent trend with the corresponding transcript levels (Figure 35 B and D). Although similarly sourced from subcutaneous human preadipocytes, these results cannot be generalized without knowing the BMI and depot from which the cells came from since differences in IL-6 secretion and transcript exist between depots and are BMI-dependant (Fried, Bunkin, & Greenberg, 1998) (unpublished results from our group).

Furthermore, at a transcriptional regulation level, IL-6 is a multifunctional cytokine in humans known to be induced transiently when exposed to an inflammatory stimulus (Matsusaka et al., 1993), and constitutively in viral-induced inflammation and auto-immune diseases and malignancies (Kishimoto, Akira, &

Taga, 1992; Matsusaka et al., 1993). *In vivo* evidence of IL-6 protein secretion from adipose tissue shows patterns to fluctuate throughout the day and to depend on adiposity (Mohamed-Ali et al., 1997), while noting that the resulting plasma IL-6 is known to be short-lived (Flick & Gifford, 1986). The combination of all of these factors makes it almost impossible to have a standardized baseline IL-6 measurement in primary adipocytes between individuals since the initial systemic contributions in terms of transcriptional regulation, added onto the cell stress incurred during the biopsy itself and inter-individual genetic differences could confuse all measurements. Similar experiments investigating the effects of NA on inflammation in macrophages used an inflammatory stimulus (LPS) to 'activate' macrophages into secreting IL-6 (Zandi-Nejad et al., 2013). This approach was not used here as the adipocytes exhibited IL-6 secretion without any stimulation (due to the stress of in *vitro* culturing) and *HCAR2* expression was present at the day of the experiment with NA (day14). However this could have been a limiting factor for the results shown in 6.2.4. and future trials should similarly consider LPS-sensitization before NA exposure.

In summary, considering the inconsistencies in my results and the inability to compare with previous findings, combined with difficulties in measuring protein levels, IL-6 might not be the most reliable proxy for assessing inflammation in cultured human adipocytes. Furthermore, the genetic and cell variability seen between the three independent human adipocytes in my experiment along with the unsuccessful attempts at genetic manipulation of knocking out *HCAR2* and *HCAR3* in them, casts doubts on their suitability as a model to investigate inflammation in the adipocyte. Following from this, an immortalized human

adipocyte model that was being developed in my laboratory was considered as a possible experimental alternative.

6.4.2. Possible solutions with immortalized cells

This immortalized human adipocyte cell line was created and being characterized by a group of postdoctoral fellows in our group based on previous similar protocols (Darimont & Macé, 2003). Abdominal and gluteal preadipocytes isolated from a healthy male volunteer were transfected to over-express hTERT (Human telomerase reverse transcriptase) and HPV16-E7 (Human papillomavirus 16) both of which allow cells to survive continuously *in vitro* (Darimont et al., 2003). The resulting cells were still being properly characterized but displayed increased rates of proliferation, retained robust adipogenic capacity and accumulated lipid droplets upon differentiation (unpublished data from our group).

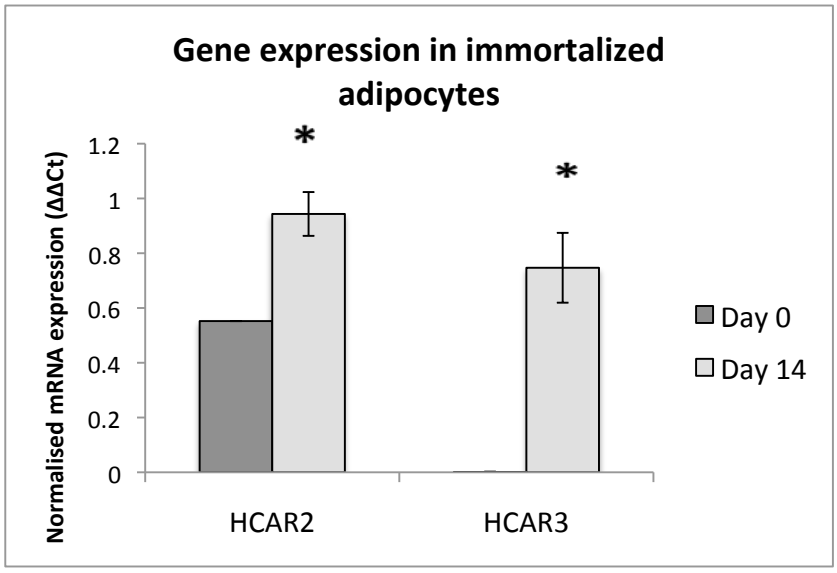

Figure 37: Relative gene expression of *HCAR2* and *HCAR3* primary and immortalized adipocytes (B) at day 0 and day 14 of differentiation (N=3, passages 8, 12, 14).

When three different passages of abdominal immortalized cells were assayed for gene expression of *HCAR2* and *HCAR3* (similarly to section 6.2), the cells showed similar differences between days 0 and 14 in both transcripts, albeit with less variability in results (Figure 36). Experiments are still underway to determine how suitable this cell line for experiments on mature adipocytes and inflammation, but they show promising leads to follow especially in the possibe gene knockdown of *HCAR2* and *HCAR3*.

Chapter 7 Final

Discussion

There existed a gap in genetic knowledge for *HCAR2* that could increase our understanding of the mechanism of action of NA. Therefore, the main focus of this project was to gain genomic insight on poorly defined polymorphisms in *HCAR2* and its 96% homologue *HCAR3* and to ascertain how they may translate into relevant phenotypes. Deep resequencing in Chapter 3 was meticulously undertaken for this aim, with numerous steps of specificity checks to guarantee that the right gene was targeted. This ensured that the polymorphisms uncovered corresponded to *HCAR2* and not *HCAR3*, and vice versa. This resequencing also extended the reach of validated variants into the promoter region, allowing the construction of new haplotypes that proved informative for genotyping studies (with the specific example outlined in section 4.1.3). Furthermore, by getting a detailed and simultaneous view of the variants (as shown in Table 12), it was possible to see which variant was polymorphic in both genes, knowledge that is invaluable when designing genotyping assays so that only the wanted variant/gene is targeted. My findings showed that about 30% of the variants listed in dbSNP from the 4252bp fragment of *HCAR2* are polymorphic in both genes and thus inaccessible to current high throughput genotyping technology. Similarly, around 38% of the variants in the 2100bp *HCAR3* fragment are polymorphic in both genes. The implications are noteworthy: dbSNP does not indicate this dual polymorphic status and subsequently designed genotyping assays could capture variation in both genes. Ultimately, although the findings described in Chapter 3 do not encompass the full extent of the genomic area aimed for at the onset of this project (10Kb) because of sequence complexity, they were further proven valuable after recent next generation sequencing (NGS) releases. Introduced in section 3.11,

these NGS releases highlighted that some areas of the genomes are still being 'skipped' in the latest sequencing because of their complexity. As expected *HCAR2* and *HCAR3* fit within this area and are therefore inadequately covered by the short read resequencing efforts, adding value to my results and making the method adopted here an essential approach for genes of a similar nature, of which there are many examples in the human genome.

Insights gained from deep resequencing were applied in Chapter 4 to design specific assays for interesting variants to genotype in the OBB. An early trend seen of a coding region variant in *HCAR2* (rs7319476) with HDL initiated the genotyping efforts with a specific assay developed to successfully target the variant on gDNA. Although the association with HDL did not reach significance after expansion of numbers in the OBB, the trend was still observable and needs further follow-up with an increased sample size (sections 4.1.1 and 4.1.2). This follow-up is more crucial following independent reports that flagged the rs7314976 and HDL association in a larger cohort (mentioned in section 4.3)(Dastani et al. 2012). Dastani *et al.* did not specify the appropriate measures taken to overcome the homology issues introduced in section 3.4. Therefore, an attempt to validate the genotyping assay they used and test it on the OBB for the same association is required.

The HDL story with *HCAR2* gains further momentum with the second coding region variant associated with HDL (rs28682471) initially genotyped on HCAR2 PCR products (section 3.4). This SNP is in LD with rs7314976 but was not being completely captured by the rs7314976 genotyping (performed in section 4.1.2 and explained in Figure 19). Unfortunately, after extensive trialling of custom-designed

assays, combined efforts from resequencing and the haplotype assembly proved unsuccessful at targeting a proxy SNP for the challenging rs28682471 variant to be directly genotyped on gDNA. However, close examination of haplotypes assembled in the resequenced population showed that there is still merit in pursuing this variant – or others that could tag it. As mentioned above, examining the haplotypes showed that only half of the haplotypes containing the rare allele of rs28682471 in the resequenced population cosegregated with haplotypes with the rare allele of rs7314976. Consequently, the association of HDL with either variant could be confounded by the other variant since only about half of the variation in either variant has been targeted so far. In order to test this, genotyping rs7314976 on a larger cohort is required along with further trials of genoytping rs28682471 or its tagging SNPs (as described in section 4.1.3.). These genotyping efforts will offer another avenue to understand the HDL and NA story, specifically if these variants could further be characterized at a functional level.

Amongst the other interesting variants I investigated, a promoter variant in *HCAR3* located in a hotspot for transcription factor binding sites (predicted and validated with Chip-Seq in the ENCODE consortium) showed an interesting association with inflammation. The rs55718746 polymorphism in *HCAR3* was associated with an approximate 20% decrease in hsCRP levels in rare homozygotes in the OBB, warranting two rounds of replication in different cohorts. While the overall association was inconsistent between the chosen replication cohorts, this polymorphism highlighted the importance of not overlooking *HCAR3* in studies of the nicotinic acid receptor *HCAR2*. The interest of pursuing this variant in a cohort with less hsCRP confounders is further confirmed from findings in Chapter 5 that

showed the rs55718746 variant appears to impact the expression levels of both genes in AT, although paradoxically in opposite directions. Difficulties in finding suitable cohorts for replication studies might have exacerbated the results with the OBB being a healthy relatively young control population. This will hopefully be facilitated in the future with the further expansion of the National NIHR Bioresource network, of which the OBB is part, that will allow access to a larger number of individuals with closer matching phenotypes.

The characterization of transcript levels in different adipose tissue depots (Chapter 5) showed that the gene expression assays for *HCAR2* and *HCAR3* present at the time were not specific, detecting transcripts from both genes. Another round of method development followed to successfully design assays that targeted each gene independently. The resulting gene expression analysis showed that *HCAR2* transcript levels differed between depots. Relative expression of *HCAR2* was around 18% higher in the female abdominal depot compared to the gluteal one. Increasing abdominal adiposity, as measured with waist circumference, was seen to drive down *HCAR2* abdominal expression significantly in both males and females (details in section 5.3.1). This trend fits within several lines of reported evidence of down-regulated genes with obesity and inflammation in adipose tissue (Shah et al., 2012), although it is also opposite to what is known about *HCAR2* gene expression in macrophages with inflammatory stimuli and hypoxic conditions which increases with increasing adiposity (Zandi-Nejad et al., 2013). No direct metabolic associations were found with *HCAR2*, but depot-specific transcript differences with increasing adiposity fall within the protective proprieties of

gluteal adipose tissue in a gynoid model of obesity. Altogether, HCAR2 seems to be involved in the pathophysiology of obesity.

Unsurprisingly, since sharing highly homologous sequences in their promoter regions, *HCAR2* and *HCAR3* were found to have correlated expression patterns, even though they do not share the same range of effects nor transcript levels in different depots. *HCAR3*'s relative gene expression was not different across gender, obesity status and depots. The importance of the method development is therefore evident, since previous assays could have easily missed this difference by targeting both transcripts and getting interferences from both genes. Following from these findings, it becomes clear that information about the potential co-regulation of both genes is lacking.

This is further evident when the paradoxical inverse correlation of expression levels of HCAR2 and HCAR3 when related to the hsCRP-associated rs55718746 promoter variant in *HCAR3* (section 5.5). A future setup to test the physiological implications of this new cis-eQTL is required. This was attempted with the endogenous ligand β-hydroxybutrate in section 5.5 with no clear results since the concentrations required to activate *HCAR2* were possibly not met in our healthy cohort. In future work, it would be interesting to see whether the higher relative expression of *HCAR2* in AT (in individuals with the rare allele for rs55718746) translates into any measurable phenotypes in conditions where HCAR2 is known to be signalling, such during NA therapy.

With questions around the function of HCAR2 in AT, I set out in Chapter 6 to establish a pilot study that interrogates the role HCAR2 plays in modulating inflammation in the human adipocyte, along with any potential interplay with

HCAR3. The vast amount of current litterature looking at the role of NA in inflammation do so through either the 3T3-L1 cell model, that does not account for HCAR3, or look at adipose tissue as a whole thereby including other cell types – such as infiltrated macrophages – that also express *HCAR2*. As described in section 6.4, it proved difficult to reach my aim because of complications in measuring the chosen proxy of inflammation IL-6, as well as difficulties in knocking down gene expression of *HCAR2* and *HCAR3* in the primary adipocytes. However, based on previous findings from chapters 4 and 5, the importance of continuing this research and accounting for HCAR3 is evident. Further investigations in the immortalized human adipocyte cell line are therefore needed to clarify the co-regulation and specific roles of both genes.

In conclusion, my project set out to understand the gap in genetic variability in the nicotinic acid receptor HCAR2 and build upon initial observations with HDL. My findings have determined the need to pursue specific genotyping for both rs7314976 and rs28682471 as they both show trends with HDL levels, with potential future functional characterizations of the variants. Similarly, the previously unreported hsCRP association with rs55718746 in *HCAR3* will require further replication in a suitable cohort. Furthermore, the functional implications of this variant on HCAR2 and any physiological effects need to be clarified, as this is the first cis-eQTL described for *HCAR3* and this genomic region. General studies of post-transcriptional and post-translational regulation for both *HCAR2* and *HCAR3* are required as they could have therapeutic relevance. Finally, the differences in *HCAR2* expression in different human adipose tissue depots suggest a potential role for HCAR2 in AT that cannot be dismissed. While this project set out to explore

the role of 'The nicotinic acid receptor in human adipose tissue' it has become clear that future work should focus on both HCAR2 and HCAR3 in human adipose tissue. Although the genetic gap in *HCAR2* has been patched up, a bigger gap in our understanding of the interaction between *HCAR2* and *HCAR3* in human adipose tissue has been revealed.

APPENDIX

ClustalW 2.1 alignment readout of *HCAR2* and *HCAR3* coding regions + 2kb upstream promoter sequence. The stars represent matches in sequence, while gaps indicate mismatches. The start codon in both genes is highlighted in red. Retrieved on the 17th September 2013.

```
HCAR2_dna       -CGAAAGCTCGGAGTGAGGCATGAAACATTTTCCCTTAGCCTCCAGATGGAACCAACCCT 59
HCAR3_dna       CCGAAAGCTCGGAGTGAGGCATGAAACATTTTCCCTTAGCCTCCAGATGGAACCAACCCT 60
                 ************************************************************

HCAR2_dna       GCCAACACCTTGATTCTGCACTTCTAGCTTCTAGATCTGTGGGAGAATACATTTCTATTG 119
HCAR3_dna       GCCAACACCTTGATTCTGCACTTCTAGCTTCTAGATCTGTGGGAGAATACATTTCTATTG 120
                ************************************************************

HCAR2_dna       TTCCAAGCCACCCAGCCACAGGAAATGAACACGCAGTCACCAACCTAATTCTCACCTCAG 179
HCAR3_dna       TTCCAAGCCACCCAGCCACAGGAAATGAACATGCAGTCACCAACCTAATTCTCACCTCAG 180
                ****************************** ***************************

HCAR2_dna       GGCCTTTGCACTTACCATTCCCTCTGCTTGGCGTGTCTTTCCCCCAGACTTTTGCATTGC 239
HCAR3_dna       GGCCTTTGCACTTACCATTCCCTCTGCTTGGCGTGTCTTTCCCCCAGACTTTTGCATTGC 240
                ************************************************************

HCAR2_dna       TTTTCTGTTTAGTCATTCATGGCTCAGCTCAGGGTCAATGCCTCATAGAAGCCATCCCAG 299
HCAR3_dna       TTTTCTGTTTAGTCATTCATGGCTCAGCTCAGGGTCAATGCCTCATAGAAGCCATCCCAG 300
                ************************************************************

HCAR2_dna       TCACCCCAGCCCCGGTTACTTTTTATCCCCATTGTCCCACTCCACCATAGTCATGACACC 359
HCAR3_dna       TCACCCCAGCCCCGGTTACTTTTTATCCCCATTGTCCCACTCCACCATAGTCATGACACC 360
                ************************************************************

HCAR2_dna       CATAGCCACCCCAAGGCTCCTTTTTATTCCTGCCTGTCTCCCCACTCCAAAAGTCAGCTC 419
HCAR3_dna       CATAGCCACCCCAAGGCTCCTTTTTATTCCTGCCTGTCTCCCCACTCCAAAAGTCAGCTC 420
                ************************************************************

HCAR2_dna       GATGAGAAGAGGACTGTGGCTGCCTTGTTTCTTGTTCTATCTCCACCACCCAGAACAGCG 479
HCAR3_dna       GATGAGAAGAGGACTGTGGCTGCCTTGTTCCTTGTTCTATCTCCACCACCCAGAACAGCG 480
                ***************************** ****************************

HCAR2_dna       CCTGGCACACAGTTGGTGCTTAATACATAAAACTGATGGAATGAGGCTGGGCACAGTGGC 539
HCAR3_dna       CCTGGCACACAGTTGGCGCTTAATACATAAAACTGATGGAATGAGGCTGGGCACAGTGGC 540
                *************** ****************************************

HCAR2_dna       TCACACCTGTAATCCCAGCACTTTGGGAGGCTGAGGCAGGTGGATCACCTGAGGTCAGGA 599
HCAR3_dna       TCACACCTGTAATCCCAGCACTTTGGGAGGCTGAGGCAGGTGGATCACCTGAGGTCAGGA 600
                ************************************************************

HCAR2_dna       GTTCAAGACCAGCCTGGGCAACATGGCGAGACCCCACCTCTACTAAAAATACAAAAATTA 659
HCAR3_dna       GTTGGAGACCAGCCTGGGCAACACAGCGAAAGCCCATCTCTACTAAAAATACAAAAATTA 660
                ***  *****************  **** * **** **********************

HCAR2_dna       GCCAGGCATGGTGGTGCACACCTGTAATCCCAGCTACTGGGGGGGCTGAGGTAGGAGAAT 719
HCAR3_dna       GCCAGGCATGGTGGTGCACACCTGTAATCCCAGCTACTGGGGAGGCTGAGGTAGGAGAAT 720
                ****************************************** *****************

HCAR2_dna       CACTTGAACCCAGGAGGCAGAGGCTGCAGTGAACCCAGATCACACCACTGCACTCCAGCC 779
HCAR3_dna       CACTTGAACCCAGGAGGCAGAGGCTGCAGTGAACCCAGATCACACCACTGCACTCCAGCC 780
                ************************************************************

HCAR2_dna       TAGATGACAGAGTGAGACTCGGTCTCAAAAAAAAAAAAAAAAACAAAGAACTGATGGAATG 839
HCAR3_dna       TAGATGACAGAGTGAGACTCGGTCTCAAAAAAAAAAAAAAAAACAAAGAACTGATGGAATG 840
                ************************************************************

HCAR2_dna       CCTGAATCAGTGAATGAATGTGAGCTGTGGAGGTCCAAACACCCCAAACCACCTCATCCC 899
```

```
HCAR3_dna       CCTGAATCAGTGAATGAATGTGAGCTGTGGAGGTCCAAACACCCCAAACCACCTCATCCC 900
                ************************************************************

HCAR2_dna       TTGAACGAATCCGCGTTTCACAACGAGGCTCCCCACTGACTCATGCCTCCGAGGCTGGGG 959
HCAR3_dna       TTGAACGAATCCGCGTTTCACAACGAGGCTCCCCACTGACTCATGCCTCCGAGGCTGGGG 960
                ************************************************************

HCAR2_dna       AATCCCTATTTTCCTCTGAGCTCATCCCTGACATCTCTTCCTCTTTAAGGTGATCCTTGC 1019
HCAR3_dna       AATCCCTATTTTCCTCTGAGCTCATCCCTGACATCTCTTCCTCTTTAAGGTGATCCTTGC 1020
                ************************************************************

HCAR2_dna       TTTTGGCTTTTTACCTGTACATTGCTTGGTGATACAGACAAGCCAACTGCTCTGAAAGCA 1079
HCAR3_dna       TTTTGGCTTTTTACCTGTACATTGCTTGGTGATACAGACAAGCCAACTGCTCTGAAAGCA 1080
                ************************************************************

HCAR2_dna       CAGAGGTAATTCCAGAGCATCCACCTTTCTTCATTTACTGTCATTCACCCAGAGCTGGGA 1139
HCAR3_dna       CAGAGGTAATTCCAGAGCATCCACCTTTCTTCATTTACTGTCATTCACCCAGAGCTGGGA 1140
                ************************************************************

HCAR2_dna       GCCTGTCTCTAAATTCCTTATCTGTGTTCATGTCAGGAGGTTGAAGCAAGCCTCGTCTTG 1199
HCAR3_dna       GCCTGTCTCTAAATTCCTTATCTGTGTTCATGTCAGGAGGTTGAAGCAAGCCTCGTCTTG 1200
                ************************************************************

HCAR2_dna       CCAAATAATCAAGGACTGACAGAGTTAGAAATGAAAGCGTAACAGAAACTTGGACTGATC 1259
HCAR3_dna       CCAAATAATCAAGGACTGACAGAGTTAGAAATGAAAGCGTAACAGAAACTTGGACTGATC 1260
                ************************************************************

HCAR2_dna       ACAGACTCAAACCAGTACATCTCCTTTCCTTCTCTGAATTGGGAACTGAAACCATTCCAT 1319
HCAR3_dna       ACAGACTCAAACCAGTACATCTCCTTTCCTTCTCCGAATTGGGAACTGAAACCATTCCAT 1320
                ********************************** ************************

HCAR2_dna       AGGAAGCTCGCTCTTCCCCCTCCTATGGAAAAATATCTGCCTGGCTTGATTCCCTTTTTA 1379
HCAR3_dna       AGGAAGCTCGCTCTTCCCCCTCCTATGGAAAAATATCTGCCTGGCTTGATTCCCTTTTTA 1380
                ************************************************************

HCAR2_dna       TATTATTTATTATTATTATTTGAGATGAAGTCTTGCTCTGTCCCCCAGGCTGGAGTGCAG 1439
HCAR3_dna       TATTATTTATTATTATTATTTGAGATGAAGTCTTGCTCTGTCCCCCAGGCTGGAGTGCAG 1440
                ************************************************************

HCAR2_dna       GCACACCACCTCGGCTCACTGCAACCTCCGCCTCCTGGGTTCAAGCAATTCTTCTTCCCC 1499
HCAR3_dna       GCACACCACCTCGGCTCACTGCAACCTCCGCCTCCCGGGTTCAAGCAATTCTTCTTCTCC 1500
                ********************************** ********************* **

HCAR2_dna       CAGCCTTCCCAGTAGCTGGGACTACAAGCGGCCGCCACCATGCCTGGCTAATTTTTCTTG 1559
HCAR3_dna       CAGCCTTCCCAGTAGCTGGGACTACAAGCGGCCGCCACCATGCCTGGCTAATTTTTCTTG 1560
                ************************************************************

HCAR2_dna       TATTTTTAGTAGAAGTGGGGTTTCGCCATGTTGTCCAGGCTGGTCTCAAACTCCTGACCT 1619
HCAR3_dna       TATTTTTAGTAGAAGTGGGGTTTCACCATTTTGTCCAGGCTGGTCTCAAACTCCTTACTT 1620
                ************************ **** ************************** ** *

HCAR2_dna       CAGGGTGATCTGCCCACCTCGGTCCCCTCAAAGTGCTGGGATTACAGGCATGAACCATTG 1679
HCAR3_dna       CAGG-TGATCTGCCCGCCTTGGCTCCCCCAAAGTGCTGGGATTACAGGCATGAACCATTG 1679
                **** ********** *** **  *** ********************************

HCAR2_dna       CACCTGGCCTTGATTCCCTGTTTAATGCACAAATACTAAGAGCAATATTCACCAAACTCT 1739
HCAR3_dna       CACCTGGCCTTGATTCCCTTTTTAATGCACAAATATGAAGAGCAATATTCACCAAACTCT 1739
                ******************* ***************  ************************

HCAR2_dna       AATAAAATGTAAGTGCTCTTGCGATCCTATCTGTACTATCCTTCCAAATTATTTTTAATC 1799
HCAR3_dna       AATAAAATGTAAGTGCTCTTGCAATCCTATCTGTACTATCCTTCCAAATTATTTTTAATC 1799
                ********************** ***********************************

HCAR2_dna       CCAGCTCTTTCTATCTTTGTTTAGACACAGGTGTAATTTCTGCTTAGTTGTTTCATGATG 1859
HCAR3_dna       CCAGCTCTTTCTATCTTTGTTTAGACACAGGTGTAATTTCTGCTTAGTTGTTTCATGATG 1859
                ************************************************************

HCAR2_dna       TAGCTCAGTGTCTGTGTCTCTTTCTTACTTTGCAGTGTGGAGTAGTTTTCTACCAGGACA 1919
HCAR3_dna       TAGCTCAGTGTCTGTGTCTCTTTCTTACTTTGCAGTGTGGAGTAGTTTTCTACCAGGACA 1919
                ************************************************************

HCAR2_dna       GAGTTAACAACCCATAAAGGTCTCTGCTTAAGTAAGAAGTCCATTTCTGTGAACCATAAC 1979
HCAR3_dna       AAGTTAACAACCCATAAAGGTCTCTGCTTAAGTAAGAAGTCCATTTCTGTGAACCATAAC 1979
                 ***********************************************************

HCAR2_dna       CCAGATATAGCAACGCCAGACTGTCTCCTATCAAAATTTATTGAAATGGTAGATTTTTGG 2039
HCAR3_dna       CCAGATATAGCAACGCCAGACTGTCTCCTATCAAAATTTATTGAAATGGTAGATTTTTGG 2039
                ************************************************************
```

```
HCAR2_dna       TAAGTACAGAAACACAAGCGAAGGAACCAGGAGGAACGTGCACCCCTCTAACTGTGGGGC 2099
HCAR3_dna       TAAGTACAGAAACACAAGCGAAGGAACCAGGAGGAACGTGCACCCCTCTACCCGTGGGGC 2099
                ********************************************** * *******

HCAR2_dna       AGAGGCACATTTCCCTTTTAATGTTAAAAGCAAACAGAGGTGGGAAACAGCTTTCTATCC 2159
HCAR3_dna       AGAGGCACGTTTCCCTTTTAATGGTAAAAGCAAACA--GGTGGGAAACAGCTTTCTATCC 2157
                ******** ************** ************  **********************

HCAR2_dna       TGAAGCCGTTTTAACTGCCCAACCCTTAGATTACTATAAACAAGAGAGGAATGGATTGCA 2219
HCAR3_dna       TGAAGCCGTTTTAACTGTTCAACCCTTAGATTACTATAAACAAGAGAGGAATGGATTGCA 2217
                *****************  ****************************************

HCAR2_dna       TTAGTCGCTGGTTGAAAGCAGCAATGCCATTTCCTTTCCCATAATAACACTGTTTAGCTC 2279
HCAR3_dna       TTAGTCGCTGGTTGAAAGCAGCAATGCCATTTCCTTTCCCATAATAACACTGTTTAGCTC 2277
                ************************************************************

HCAR2_dna       AGTCCCTTCTGGGGCTAATCCCCTATTACACCCACCGGAAACACAGATATTAACCAAAGC 2339
HCAR3_dna       AGTCCCTTCTGGGGCTAATCCCCTATTACACCCACCGGAAACACAGATACTAACCAAAGC 2337
                ********************************************** **********

HCAR2_dna       GTGTGAGTCTCTTCCCTGAGTCCATTTCTGCTAAAGCTTGTCTGAAAGATGAATTGGTCC 2399
HCAR3_dna       ATGTGAGTCTCTTCCCTGAGTCCATTTCTGCTAAAGATTGTCTGAAAGATGAATTGGTCC 2397
                 ********************************** **********************

HCAR2_dna       ACGGAAGCCAGGTGACCTACTGGCTTGTTTAATGATGCCTGGGCTCCCTCCAGGAGCAAC 2459
HCAR3_dna       ACGGAAGCCAGGTGACCTACTGGCTTGTTTAATGATGCCTGGGCTTCCTCCAGGAACAAC 2457
                ********************************************* ********* ****

HCAR2_dna       ACAATTCCCTCCAATCTCAGCTCTCCTTATCCCTGCTAGAGCTCACAAGCAGGCTAGATA 2519
HCAR3_dna       ACAATTCCCTCCAATCTCAGCTCTCCTTATCCCTGCTAGAGCTCACAAGCAGGCTAGATA 2517
                ************************************************************

HCAR2_dna       TCACCCCAGGAGCTGAGCCCCCTCCAGTCTGAGGCAGATGTGGGAAGAAGGCCAACAAGT 2579
HCAR3_dna       TCACCCCAGGAGCTGAGCCCCCTCCAGTCTGAGGCAGATGTGGGAAGAAGGCCAACAAGT 2577
                ************************************************************

HCAR2_dna       CACAAGTAGATCTCTGGCTCCAACTCTGCTCAGCAGAAATGCCTACAATTTGCCCATCTT 2639
HCAR3_dna       CACAAGTAGATCTCTGGCTCCAACTCTGCTCAGCAGAAACGCCTACAATTTGCCCATCTT 2637
                ************************************* ********************

HCAR2_dna       CAGTCCTGCGAGCGTCAGAGATGAAGCAAAAGTTTCAGATGCCTAGAAGCTTTACTCTCT 2699
HCAR3_dna       CAGTCCTGCGAGCGTCAGAGATGAAGCAA--GTTTCAGATGCCTAGAAGCTTTACTCTCT 2695
                ****************************  ****************************

HCAR2_dna       ATTCCTCCAGGATTCCTGCGGTCACACCTTGCAACCAGTCTCCCACTCATCTGCCACCGT 2759
HCAR3_dna       GTTCCTCCAGGATTCCTGCGGTCACACCTTGCAACCAGTCTCCCACTCATCTGCCACAGT 2755
                 ************************************************************ **

HCAR2_dna       TTCCCTAAATCGCATTCTCTGAATCTGGAAGTTCCAGGAAACCTTAGGCCGAGTCCAGTG 2819
HCAR3_dna       TTCCCTAAATCAGATTCTCTGAATCTGGAAGTTCCAGGAAATCTTAGGCCGAGTCCAGTG 2815
                ***********  **************************** ******************

HCAR2_dna       ACATTACTCGATGCAACAGCCCAACTGTTTCTCCAGAGATCCTGGTTCTTGGTGACAATG 2879
HCAR3_dna       ACATTACTCGATGCAACAGCCCAACTGTTTCTCCAGAGATGCTGGTTCTTGGTGACAATG 2875
                ************************************* ******************

HCAR2_dna       TCCCTTCTTGGCATGGTTATTTAAGGAGAGGTTGGGCCCAGATAAGAGGGGCTCCATGGC 2939
HCAR3_dna       TCCCTTCTTGGAATGGTTATTT-----GAGGTTGGGCCCAGATAAGAGGGGCTCCATGGC 2930
                *********** **********     *********************************

HCAR2_dna       TCACCGGAGTTGGCCATTAACGCCTCTGGAGCGCCTCTGGTTTTGTTGGGGTCCCCTGTG 2999
HCAR3_dna       TCACCGGAGTTGGCGATTAACGCCTCTGGAGCGCCTCTGGTTTTGTTGGGGTCCCCTGTG 2990
                ************** ********************************************

HCAR2_dna       AGCTCGACGCTCGTGCTGCGGTTATTATCTGGCTCACCTGTCATCTTCCTCTGGAGGCAG 3059
HCAR3_dna       AGCTCGACGCTCGTGCTGCGGTTATTATCTGGCTCACCTGTTATCTTCCTCTGGAGGCAG 3050
                ************************************* ******************

HCAR2_dna       CGGTTGATCAAAGTGGAGAAGAAGTTGGGAAAGGATGGGCTGGAGAAGTAGTACACCACG 3119
HCAR3_dna       CGGTTGATCAAAGTGGAGAAGAAGTTGGGAAAGGATGGGCTGGAGAAGTAGTACACCACG 3110
                ************************************************************

HCAR2_dna       GGGTCCAGCATGCTGTTCATGTAGGTGAAGCTGAGAGTGATAAAGAACGCCAGGTCCACC 3179
HCAR3_dna       GGGTCCAGCATGCTGTTCATGTAGGTGAAGCTGAGAGTGATAAAGAACGCCAGGTCCACC 3170
                ************************************************************

HCAR2_dna       GAGCGGTACACTTCACAATTCTGCGTGCCCGAAGTGTGCAGGAGCCAGAAGATGCGGATC 3239
HCAR3_dna       GAGCGGTACACTTCACAATTCTGCGTGCCCGAAGTGTGCAGGAGCCAGAAGATGTGGATC 3230
                ************************************************** *****
```

```
HCAR2_dna       CGCACAACCACGCTGGGAAGGAAGCAGATGACAAAGACGATGGCCACCACCATGATGAAG 3299
HCAR3_dna       CGCACAACCACGCTGGGAAGGAAGCAGATGACAAAGACGATGGCCACCACCATGATGAAG 3290
                ************************************************************

HCAR2_dna       GTGATGGCTCTCTTGATCTTGGCATGCCGGTCCATTTGTCTCTGCCGCAGGCTCCAGATA 3359
HCAR3_dna       GTGATGGCTCTCTTGATCTTGGCATGCCGGTCCATTTGTCTCTGCCGCAGGCTCCAGATA 3350
                ************************************************************

HCAR2_dna       ATTCTGGCTGAGCAGAACAGGATGATGCCCAGGGGCAGGAAGAACTCCAGGAGGAACATG 3419
HCAR3_dna       ATTCTGGCTGAGCAGAACAGGATGATGCCCAGGGGCAGGAAGAACTCCAGGAGGAACATA 3410
                ************************************************************

HCAR2_dna       GCTTCGTGCCACTGGAAGGTATGGCAGATGCTGAAGCTGCTGCACAAATTTGCACCGCCA 3479
HCAR3_dna       GCTTCGTGCCACCGGAAGGTATGGCAGATGCTGAAGCTGATGCACACATTTGCAGTGCCA 3470
                ************ ************************* ****** *******  ****

HCAR2_dna       TTCTGGATCGGCATCTTCTTCTTCAGGAGGTGGACTGTCAGGCCAATAGTGATGCCCCAC 3539
HCAR3_dna       TTCTGGATCAGCAACTTCTTCTTCAGGAGGTGGACTGTTAGGCCAACAGTGATGCCCCAC 3530
                ********* *** ************************ ******* *************

HCAR2_dna       AGAAGGCAAGAGATGATGGCTGCTGTCCGATTGGAGATCTTGTTCAGGGCGTGGTGGGGA 3599
HCAR3_dna       AGAAGGCAAGAGATGATGGCTGCTGTCCAATTGGAGATCTTGTTCAGGGCGTGGTGGGGA 3590
                ***************************** ********************************

HCAR2_dna       TGGACCACCCGGAAATACCTGTCTACCGCCACCACCGTGAGGAAGATGATGCTGCCCTGG 3659
HCAR3_dna       TGGACCACCCGGAAATACCTGTCTACCGCCACCACCGTGAGGAATATGATGCTGCCCTGG 3650
                ****************************************** ***************

HCAR2_dna       CGGTTCATAGCCAACATGAAGAGCATCAGCCGGCAAGGGATGTCCCCAAACTTCCAGTCC 3719
HCAR3_dna       CGGTTCATGGCAAACATGAAGAGCACCAGCCGGCAAGGGATGTCCCCAAACTTCCAGTCT 3710
                ******** ** ************* ********************************

HCAR2_dna       CAACGCCTCACATAGTTGTCCATCAGGAAGGGCAGGCAGATGATCAGTAGAAAGTCAGCC 3779
HCAR3_dna       GAACGCCGCACATAGTAGTCCATCACGAACGGCAGGCAGATGATCAGTAGAAAGTCAGCT 3770
                 ****** ******** ******** *** *****************************

HCAR2_dna       ACTGCCAGGTTGAACAGGAAAATCCGGCTGGATTTCCAGGACTTGAGGTGGAAACAGAAA 3839
HCAR3_dna       ACTGCCAGGTTGAACAGGAAAATCCGGCTGGATTTCCAGGACTTGAGGTGGAAACAGAAA 3830
                ************************************************************

HCAR2_dna       ATCCACAGGGCAAGGCCATTGCCCAGAAGCCCGAAGATAAACTCCAGCCCCAACACCGGC 3899
HCAR3_dna       ATCCACAGGGCAAGGCCATTGCCCAGAAGCCCAAAGATAAACTCCAGCCCCAACACCGGC 3890
                ******************************** ***************************

HCAR2_dna       GGCAACACCTTGACAATGAAGTCATCTCGGAACACACAGCAGTTCTTCTTGTCTATTTCC 3959
HCAR3_dna       GGCAACACCTTGGCAATGAAGTCATCTCGGAACACACAGCAGTTCTTCTTGTCTATTTCC 3950
                ************ ********************************************

HCAR2_dna       AGAAAGTGATCCTGCAGATGGTGCCGATTCATGAGTGCGGCTAGTGAGTCCGATGGAGCG 4019
HCAR3_dna       AGAAAGTGATCCTGCAGATGGTGCCGATTCATGAGTGCAGCTAGTGAGTCCGATGGAGCG 4010
                ************************************ ********************

HCAR2_dna       CCTCGCCTAGTGAATGCTCCAGCAAGGAGGTGTGTGTCTGTGTGGT-------------- 4065
HCAR3_dna       CCTCGCCTAGTGAATGCTCCAGCAAAGTGGCGTGTGTCTGTATGGTGAACGTGTGGTTCC 4070
                ************************ * ** ********** ****

HCAR2_dna       ------------------------------------------------------------
HCAR3_dna       GTGCCTGCCTTTATGTCATGTCAGGGTGTTGAAATAGATGACTGAATGGTTATCAGGAAA 4130


HCAR2_dna       -------
HCAR3_dna       CTACGAA 4137
```

REFERENCES

1000 Genomes Project Consortium. (2010). A map of human genome variation from population-scale sequencing. *Nature*, *467*(7319), 1061–1073. doi:10.1038/nature09534

1000 Genomes Project Consortium, Abecasis, G. R., Auton, A., Brooks, L. D., DePristo, M. A., Durbin, R. M., et al. (2012). An integrated map of genetic variation from 1,092 human genomes. *Nature*, *491*(7422), 56–65. doi:10.1038/nature11632

Adzhubei, I. A., Schmidt, S., Peshkin, L., Ramensky, V. E., Gerasimova, A., Bork, P., et al. (2010). A method and server for predicting damaging missense mutations. *Nature Methods*, *7*(4), 248–249. doi:10.1038/nmeth0410-248

Ahmed, K., Tunaru, S., & Offermanns, S. (2009a). GPR109A, GPR109B and GPR81, a family of hydroxy-carboxylic acid receptors. *Trends Pharmacol Sci*, *30*(11), 557–562. doi:10.1016/j.tips.2009.09.001

Ahmed, K., Tunaru, S., Langhans, C.-D., Hanson, J., Michalski, C. W., Kölker, S., et al. (2009b). Deorphanization of GPR109B as a receptor for the beta-oxidation intermediate 3-OH-octanoic acid and its role in the regulation of lipolysis. *J Biol Chem*, *284*(33), 21928–21933. doi:10.1074/jbc.M109.019455

AIM-HIGH Investigators, Boden, W. E., Probstfield, J. L., Anderson, T., Chaitman, B. R., Desvignes-Nickens, P., et al. (2011). Niacin in patients with low HDL cholesterol levels receiving intensive statin therapy. *The New England Journal of Medicine*, *365*(24), 2255–2267. doi:10.1056/NEJMoa1107579

Aktories, K., Jakobs, K. H., & Schultz, G. (1980). Nicotinic acid inhibits adipocyte adenylate cyclase in a hormone--like manner. *FEBS Letters*, *115*(1), 11–14.

Altschul, R., Hoffer, A., & Stephen, J. (1955). INFLUENCE OF NICOTINIC ACID ON SERUM CHOLESTEROL IN MAN. *Archives of Biochemistry and Biophysics*, *54*(2), 558–559.

Arner, P. (2005a). Human fat cell lipolysis: biochemistry, regulation and clinical role. *Best Practice & Research. Clinical Endocrinology & Metabolism*, *19*(4), 471–482. doi:10.1016/j.beem.2005.07.004

Arner, P. (2005b). Resistin: yet another adipokine tells us that men are not mice. *Diabetologia*, *48*(11), 2203–2205. doi:10.1007/s00125-005-1956-3

Arner, P., Hellström, L., Wahrenberg, H., & Brönnegård, M. (1990). Beta-adrenoceptor expression in human fat cells from different regions. *J Clin Invest*, *86*(5), 1595–1600. doi:10.1172/JCI114880

Bailey, J. A., Gu, Z., Clark, R. A., Reinert, K., Samonte, R. V., Schwartz, S., et al. (2002). Recent segmental duplications in the human genome. *Science (New York, N.Y.)*, *297*(5583), 1003–1007. doi:10.1126/science.1072047

Barter, P., Gotto, A. M., LaRosa, J. C., Maroni, J., Szarek, M., Grundy, S. M., et al. (2007). HDL cholesterol, very low levels of LDL cholesterol, and cardiovascular events. *The New England Journal of Medicine*, *357*(13), 1301–1310. doi:10.1056/NEJMoa064278

Bataille, R., & Klein, B. (1992). C-reactive protein levels as a direct indicator of interleukin-6 levels in humans in vivo. *Arthritis and Rheumatism*, *35*(8), 982–984.

Benyo, Z., Gille, A., Bennett, C., Clausen, B., & Offermanns, S. (2006). Nicotinic acid-induced flushing is mediated by activation of epidermal langerhans cells. *Mol Pharmacol*, *70*(6), 1844–1849. doi:mol.106.030833 [pii]
10.1124/mol.106.030833

Berg, A. H., & Scherer, P. E. (2005). Adipose tissue, inflammation, and cardiovascular disease. *Circulation Research*, *96*(9), 939–949. doi:10.1161/01.RES.0000163635.62927.34

Björntorp, P. (1992). Abdominal fat distribution and disease: an overview of epidemiological data. *Annals of Medicine*, *24*(1), 15–18.

Bodor, E., & Offermanns, S. (2008). Nicotinic acid: an old drug with a promising future. *Br J Pharmacol*, *153 Suppl 1*, S68–75. doi:0707528 [pii]
10.1038/sj.bjp.0707528

Brinton, E. A., Kashyap, M. L., Vo, A. N., Thakkar, R. B., Jiang, P., & Padley, R. J. (2011). Niacin extended-release therapy in phase III clinical trials is associated with relatively low rates of drug discontinuation due to flushing and treatment-related adverse events: a pooled analysis. *American Journal of Cardiovascular Drugs : Drugs, Devices, and Other Interventions*, *11*(3), 179–187. doi:10.2165/11592560-000000000-00000

Butcher, R. W., Baird, C. E., & Sutherland, E. W. (1968). Effects of lipolytic and antilipolytic substances on adenosine 3“,5-”monophosphate levels in isolated fat cells. *J Biol Chem*, *243*(8), 1705–1712.

Canner, P. L., Berge, K. G., Wenger, N. K., Stamler, J., Friedman, L., Prineas, R. J., & Friedewald, W. (1986). Fifteen year mortality in Coronary Drug Project patients: long-term benefit with niacin. *Journal of the American College of Cardiology*, *8*(6), 1245–1255.

Caplen, N. J., Parrish, S., Imani, F., Fire, A., & Morgan, R. A. (2001). Specific inhibition of gene expression by small double-stranded RNAs in invertebrate and vertebrate systems. *Proc Natl Acad Sci U S A*, *98*(17), 9742–9747. doi:10.1073/pnas.171251798

Cardon, L. R., & Bell, J. I. (2001). Association study designs for complex diseases. *Nature Reviews Genetics*, *2*(2), 91–99. doi:10.1038/35052543

Carlson, L. (2005). Nicotinic acid: the broad-spectrum lipid drug. A 50th anniversary review. *J Intern Med*, *258*(2), 94–114. doi:JIM1528 [pii]
10.1111/j.1365-2796.2005.01528.x

Carlson, L. A., & Orö, L. (1962). The Effect of Nicotinic Acid on the Plasma Free Fatty Acids Demonstration of a Metabolic Type of Sympathicolysis. *Acta Medica Scandinavica*, *172*(6), 641–645.

Carlson, L. A., & Rosenhamer, G. (1988). Reduction of mortality in the Stockholm Ischaemic Heart Disease Secondary Prevention Study by combined treatment with clofibrate and nicotinic acid. *Acta Medica Scandinavica*, *223*(5), 405–418.

Carlson, L., & Hanngren, A. (1964). Initial Distribution in Mice of 3h-Labeled Nicotinic Acid Studied with Autoradiography. *Life Sci*, *3*, 867–871.

Chai, J. T., Digby, J. E., & Choudhury, R. P. (2013a). GPR109A and Vascular Inflammation. *Curr Atheroscler Rep*, *15*(5), 325. doi:10.1007/s11883-013-0325-9
Chai, J. T., Digby, J. E., Ruparelia, N., Jefferson, A., Handa, A., & Choudhury, R. P. (2013b). Nicotinic acid receptor GPR109A is down-regulated in human macrophage-derived foam cells. *PloS One*, *8*(5), e62934. doi:10.1371/journal.pone.0062934
Chanock, S. J., Manolio, T., Boehnke, M., Boerwinkle, E., Hunter, D. J., Thomas, G., et al. (2007). Replicating genotype–phenotype associations. *Nature*, *447*(7145), 655–660. doi:doi:10.1038/447655a
Cholesterol Treatment Trialists. (2010). Efficacy and safety of more intensive lowering of LDL cholesterol: a meta-analysis of data from 170 000 participants in 26 randomised trials. *The Lancet*, *376*(9753), 1670–1681. doi:10.1016/S0140-6736(10)61350-5
Choudhury, R. P., Lee, J. M., & Greaves, D. R. (2005). Mechanisms of Disease: macrophage-derived foam cells emerging as therapeutic targets in atherosclerosis. *Nature Clinical Practice Cardiovascular Medicine*, *2*(6), 309–315. doi:10.1038/ncpcardio0195
Cooper, J. A., Miller, G. J., Bauer, K. A., Morrissey, J. H., Meade, T. W., Howarth, D. J., et al. (2000). Comparison of novel hemostatic factors and conventional risk factors for prediction of coronary heart disease. *Circulation*, *102*(23), 2816–2822.
Costa, C. G., Dorland, L., Holwerda, U., de Almeida, I. T., Poll-The, B. T., Jakobs, C., & Duran, M. (1998). Simultaneous analysis of plasma free fatty acids and their 3-hydroxy analogs in fatty acid beta-oxidation disorders. *Clinical Chemistry*, *44*(3), 463–471.
Creider, J. C., Hegele, R. A., & Joy, T. R. (2012). Niacin: another look at an underutilized lipid-lowering medication. *Nature Reviews. Endocrinology*. doi:10.1038/nrendo.2012.22
Daar, A. S., Singer, P. A., Persad, D. L., Pramming, S. K., Matthews, D. R., Beaglehole, R., et al. (2007). Grand challenges in chronic non-communicable diseases. *Nature*, *450*(7169), 494–496. doi:10.1038/450494a
Darimont, C., & Macé, K. (2003). Immortalization of human preadipocytes. *Biochimie*, *85*(12), 1231–1233.
Darimont, C., Zbinden, I., Avanti, O., Leone-Vautravers, P., Giusti, V., Burckhardt, P., et al. (2003). Reconstitution of telomerase activity combined with HPV-E7 expression allow human preadipocytes to preserve their differentiation capacity after immortalization. *Cell Death and Differentiation*, *10*(9), 1025–1031. doi:10.1038/sj.cdd.4401273
Dastani, Z., Hivert, M.-F., Timpson, N., Perry, J. R. B., Yuan, X., Scott, R. A., et al. (2012). Novel loci for adiponectin levels and their influence on type 2 diabetes and metabolic traits: a multi-ethnic meta-analysis of 45,891 individuals. *PLoS Genetics*, *8*(3), e1002607. doi:10.1371/journal.pgen.1002607
Demetrius, L. (2005). Of mice and men. *EMBO Reports*, *6*, S39–S44. doi:10.1038/sj.embor.7400422
Digby, J. E., Martinez, F., Jefferson, A., Ruparelia, N., Chai, J., Wamil, M., et al. (2012a). Anti-inflammatory effects of nicotinic acid in human monocytes are mediated by GPR109A dependent mechanisms. *Arterioscler Thromb Vasc Biol*, *32*(3), 669–676. doi:10.1161/ATVBAHA.111.241836
Digby, J. E., McNeill, E., Dyar, O. J., Lam, V., Greaves, D. R., & Choudhury, R. P. (2010). Anti-inflammatory effects of nicotinic acid in adipocytes demonstrated by suppression of fractalkine, RANTES, and MCP-1 and upregulation of adiponectin. *Atherosclerosis*, *209*(1), 89–95. doi:10.1016/j.atherosclerosis.2009.08.045
Digby, J. E., Ruparelia, N., & Choudhury, R. P. (2012b). Niacin in cardiovascular disease: recent preclinical and clinical developments. *Arterioscler Thromb Vasc Biol*, *32*(3), 582–588. doi:10.1161/ATVBAHA.111.236315
Dunbar, R. L., & Gelfand, J. M. (2010). Seeing red: flushing out instigators of niacin-associated skin toxicity. *J Clin Invest*, *120*(8), 2651–2655. doi:10.1172/JCI44098
Elvehjem, C. A., Madden, R. J., Strong, F. M., & Woolley, D. W. (1938). THE ISOLATION AND IDENTIFICATION OF THE ANTI-BLACK TONGUE FACTOR
. *J. Biol. Chem. 1938, 123:137-149.*
Emerging Risk Factors Collaboration, Di Angelantonio, E., Sarwar, N., Perry, P., Kaptoge, S., Ray, K. K., et al. (2009). Major lipids, apolipoproteins, and risk of vascular disease. *JAMA : the Journal of the American Medical Association*, *302*(18), 1993–2000. doi:10.1001/jama.2009.1619
Estivill, X., Cheung, J., Pujana, M. A., Nakabayashi, K., Scherer, S. W., & Tsui, L.-C. (2002a). Chromosomal regions containing high-density and ambiguously mapped putative single nucleotide polymorphisms (SNPs) correlate with segmental duplications in the human genome.
Estivill, X., Cheung, J., Pujana, M. A., Nakabayashi, K., Scherer, S. W., & Tsui, L.-C. (2002b). Chromosomal regions containing high-density and ambiguously mapped putative single nucleotide polymorphisms (SNPs) correlate with segmental duplications in the human genome. *Human Molecular Genetics*, *11*(17), 1987–1995.
Fisher, E. A., Feig, J. E., Hewing, B., Hazen, S. L., & Smith, J. D. (2012). High-density lipoprotein function, dysfunction, and reverse cholesterol transport. *Arterioscler Thromb Vasc Biol*, *32*(12), 2813–2820. doi:10.1161/ATVBAHA.112.300133
Flick, D. A., & Gifford, G. E. (1986). Pharmacokinetics of murine tumor necrosis factor. *Journal of Immunopharmacology*, *8*(1), 89–97.
Franke, L., & Jansen, R. C. (2009). eQTL Analysis in Humans. In *Methods in Molecular Biology* (Vol. 573, pp. 311–328). Totowa, NJ: Humana Press. doi:10.1007/978-1-60761-247-6_17
Frayn, K. N. (2002). Adipose tissue as a buffer for daily lipid flux. *Diabetologia*, *45*(9), 1201–1210. doi:10.1007/s00125-002-0873-y
Fredman, D., White, S. J., Potter, S., Eichler, E. E., Dunnen, Den, J. T., & Brookes, A. J. (2004). Complex SNP-related sequence variation in segmental genome duplications. *Nature Genetics*, *36*(8), 861–866. doi:10.1038/ng1401
Fried, S. K., & Kral, J. G. (1987). Sex differences in regional distribution of fat cell size and lipoprotein lipase activity in morbidly obese patients. *International Journal of Obesity and Related Metabolic Disorders : Journal of the International Association for the Study of Obesity*, *11*(2), 129–140.
Fried, S. K., Bunkin, D. A., & Greenberg, A. S. (1998). Omental and subcutaneous adipose tissues of obese subjects release interleukin-6: depot difference and regulation by glucocorticoid. *The Journal of Clinical Endocrinology and Metabolism*, *83*(3), 847–850.
Furey, T. S. (2012). ChIP-seq and beyond: new and improved methodologies to detect and characterize protein-DNA interactions. *Nature Reviews Genetics*, *13*(12), 840–852. doi:10.1038/nrg3306
Ganji, S. H. (2004). Niacin noncompetitively inhibits DGAT2 but not DGAT1 activity in HepG2 cells. *J Lipid Res*, *45*(10), 1835–1845. doi:10.1194/jlr.M300403-JLR200
Gesta, S. (2006). Evidence for a role of developmental genes in the origin of obesity and body fat distribution. *Proceedings of the National Academy of Sciences*, *103*(17), 6676–6681. doi:10.1073/pnas.0601752103

Gesta, S., Bezy, O., Mori, M. A., Macotela, Y., Lee, K. Y., & Kahn, C. R. (2011). Mesodermal developmental gene Tbx15 impairs adipocyte differentiation and mitochondrial respiration. *Proceedings of the National Academy of Sciences*, *108*(7), 2771–2776. doi:10.1073/pnas.1019704108

Ghani, M., Sato, C., & Rogaeva, E. (2013). Segmental duplications in genome-wide significant loci and housekeeping genes; warning for GAPDH and ACTB. *Neurobiology of Aging*, *34*(6), 1710.e1–1710.e4. doi:10.1016/j.neurobiolaging.2012.11.006

Green, H., & Kehinde, O. (1974). Sublines of mouse 3T3 cells that accumulate lipid. *Cell*, *1*(3), 113–116. doi:10.1016/0092-8674(74)90126-3

Green, H., & Kehinde, O. (1975). An established preadipose cell line and its differentiation in culture. II. Factors affecting the adipose conversion. *Cell*, *5*(1), 19–27.

Gregoire, F. M. (2001). Adipocyte differentiation: from fibroblast to endocrine cell. *Experimental Biology and Medicine (Maywood, N.J.)*, *226*(11), 997–1002.

Gut, I. G., & Lathrop, G. M. (2004). Duplicating SNPs. *Nature Genetics*, *36*(8), 789–790. doi:10.1038/ng0804-789

Hamer, M., Brunner, E., Bell, J., Batty, G., Shipley, M., Akbaraly, T., et al. (2013). Physical activity patterns over 10 years in relation to body mass index and waist circumference: The Whitehall II cohort study. *Obesity (Silver Spring, Md)*. doi:10.1002/oby.20446

Hanson, J., Gille, A., Zwykiel, S., Lukasova, M., Clausen, B. E., Ahmed, K., et al. (2010). Nicotinic acid- and monomethyl fumarate-induced flushing involves GPR109A expressed by keratinocytes and COX-2-dependent prostanoid formation in mice. *J Clin Invest*, *120*(8), 2910–2919. doi:10.1172/JCI42273

Hauner, H., Entenmann, G., Wabitsch, M., Gaillard, D., Ailhaud, G., Negrel, R., & Pfeiffer, E. F. (1989). Promoting effect of glucocorticoids on the differentiation of human adipocyte precursor cells cultured in a chemically defined medium. *J Clin Invest*, *84*(5), 1663–1670. doi:10.1172/JCI114345

Hauner, H., Skurk, T., & Wabitsch, M. (2001). Cultures of Human Adipose Precursor Cells (Vol. 155, pp. 239–247). New Jersey: Humana Press. doi:10.1385/1-59259-231-7:239

Heneghan, C., Blacklock, C., Perera, R., Davis, R., Banerjee, A., Gill, P., et al. (2013). Evidence for non-communicable diseases: analysis of Cochrane reviews and randomised trials by World Bank classification. *BMJ Open*, *3*(7). doi:10.1136/bmjopen-2013-003298

Ho, M.-R., Tsai, K.-W., Chen, C.-H., & Lin, W.-C. (2011). dbDNV: a resource of duplicated gene nucleotide variants in human genome. *Nucleic Acids Research*, *39*(Database issue), D920–5. doi:10.1093/nar/gkq1197

Hoch, M., Eberle, A. N., Peterli, R., Peters, T., Seboek, D., Keller, U., et al. (2008). LPS induces interleukin-6 and interleukin-8 but not tumor necrosis factor-α in human adipocytes. *Cytokine*, *41*(1), 29–37. doi:10.1016/j.cyto.2007.10.008

Holland, P. M., Abramson, R. D., Watson, R., & Gelfand, D. H. (1991). Detection of specific polymerase chain reaction product by utilizing the 5"----3" exonuclease activity of Thermus aquaticus DNA polymerase. *Proc Natl Acad Sci U S A*, *88*(16), 7276–7280.

HPS2-THRIVE Collaborative Group. (2013). HPS2-THRIVE randomized placebo-controlled trial in 25 673 high-risk patients of ER niacin/laropiprant: trial design, pre-specified muscle and liver outcomes, and reasons for stopping study treatment. *European Heart Journal*. doi:10.1093/eurheartj/eht055

Hu, M., Chu, W. C. W., Yamashita, S., Yeung, D. K. W., Shi, L., Wang, D., et al. (2012). Liver fat reduction with niacin is influenced by DGAT-2 polymorphisms in hypertriglyceridemic patients. *J Lipid Res*, *53*(4), 802–809. doi:10.1194/jlr.P023614

Irukayama-Tomobe, Y., Tanaka, H., Yokomizo, T., Hashidate-Yoshida, T., Yanagisawa, M., & Sakurai, T. (2009). Aromatic D-amino acids act as chemoattractant factors for human leukocytes through a G protein-coupled receptor, GPR109B. *Proc Natl Acad Sci U S A*, *106*(10), 3930–3934. doi:0811844106 [pii]
10.1073/pnas.0811844106

Jin, F., Kamanna, V., & Kashyap, M. (1999). Niacin accelerates intracellular ApoB degradation by inhibiting triacylglycerol synthesis in human hepatoblastoma (HepG2) cells. *Arterioscler Thromb Vasc Biol*, *19*(4), 1051–1059.

Johnson, J. A., Fried, S. K., Pi-Sunyer, F. X., & Albu, J. B. (2001). Impaired insulin action in subcutaneous adipocytes from women with visceral obesity. *American Journal of Physiology Endocrinology and Metabolism*, *280*(1), E40–9.

Jones, P. M., Tjoa, S., Fennessey, P. V., Goodman, S. I., & Bennett, M. J. (2002). Addition of quantitative 3-hydroxy-octadecanoic acid to the stable isotope gas chromatography-mass spectrometry method for measuring 3-hydroxy fatty acids. *Clinical Chemistry*, *48*(1), 176–179.

Joshua T Chai, J. E. D. R. P. C. (2013). GPR109A and Vascular Inflammation. *Current Atherosclerosis Reports*, *15*(5). doi:10.1007/s11883-013-0325-9

Kamanna, V. S., Ganji, S. H., & Kashyap, M. L. (2013). Recent advances in niacin and lipid metabolism. *Current Opinion in Lipidology*, *24*(3), 239–245. doi:10.1097/MOL.0b013e3283613a68

Kang, I., Kim, S.-W., & Youn, J. H. (2011). Effects of Nicotinic Acid on Gene Expression: Potential Mechanisms and Implications for Wanted and Unwanted Effects of the Lipid-Lowering Drug. *The Journal of Clinical Endocrinology and Metabolism*. doi:10.1210/jc.2011-1104

Karastergiou, K., Fried, S. K., Xie, H., Lee, M.-J., Divoux, A., Rosencrantz, M. A., et al. (2013). Distinct developmental signatures of human abdominal and gluteal subcutaneous adipose tissue depots. *The Journal of Clinical Endocrinology and Metabolism*, *98*(1), 362–371. doi:10.1210/jc.2012-2953

Karastergiou, K., Fried, S. K., Xie, H., Lee, M.-J., Divoux, A., Rosencrantz, M. A., et al. (n.d.). Distinct Developmental Signatures of Human Abdominal and Gluteal Subcutaneous Adipose Tissue Depots.

Karpe, F., & Chamas, L. (2010). Hyperlipidaemia and cardiovascular disease: nonantilipolytic effects of nicotinic acid in adipose tissue. *Current Opinion in Lipidology*, *21*(3), 282–283. doi:10.1097/MOL.0b013e32833965c5

Karpe, F., & Frayn, K. N. (2004). The nicotinic acid receptor–a new mechanism for an old drug. *The Lancet*, *363*(9424), 1892–1894. doi:10.1016/S0140-6736(04)16359-9

Kieleczawa, J. (2006). Fundamentals of sequencing of difficult templates--an overview. *Journal of Biomolecular Techniques : JBT*, *17*(3), 207–217.

Kilroy, G., Burk, D. H., & Floyd, Z. E. (2009). High efficiency lipid-based siRNA transfection of adipocytes in suspension. *PloS One*, *4*(9), e6940. doi:10.1371/journal.pone.0006940

Kishimoto, T., Akira, S., & Taga, T. (1992). Interleukin-6 and its receptor: a paradigm for cytokines. *Science (New York, N.Y.)*, *258*(5082), 593–597.

Knowles, H. J., Poele, te, R. H., Poole, Te, R., Workman, P., & Harris, A. L. (2006). Niacin induces PPARgamma expression and

transcriptional activation in macrophages via HM74 and HM74a-mediated induction of prostaglandin synthesis pathways. *Biochem Pharmacol*, *71*(5), 646–656. doi:10.1016/j.bcp.2005.11.019
Kostylina, G., Simon, D., Fey, M. F., Yousefi, S., & Simon, H. U. (2008). Neutrophil apoptosis mediated by nicotinic acid receptors (GPR109A). *Cell Death and Differentiation*, *15*(1), 134–142. doi:10.1038/sj.cdd.4402238
Koutsari, C., Ali, A. H., Mundi, M. S., & Jensen, M. D. (2011). Storage of circulating free fatty acid in adipose tissue of postabsorptive humans: quantitative measures and implications for body fat distribution. *Diabetes*, *60*(8), 2032–2040. doi:10.2337/db11-0154
Lai, E., De Lepeleire, I., Crumley, T. M., Liu, F., Wenning, L. A., Michiels, N., et al. (2007). Suppression of niacin-induced vasodilation with an antagonist to prostaglandin D2 receptor subtype 1. *Clinical Pharmacology and Therapeutics*, *81*(6), 849–857. doi:10.1038/sj.clpt.6100180
Landt, S. G., Marinov, G. K., Kundaje, A., Kheradpour, P., Pauli, F., Batzoglou, S., et al. (2012). ChIP-seq guidelines and practices of the ENCODE and modENCODE consortia. *Genome Research*, *22*(9), 1813–1831. doi:10.1101/gr.136184.111
Laurila, P.-P., Surakka, I., Sarin, A.-P., Yetukuri, L., Hyötyläinen, T., Söderlund, S., et al. (2013). Genomic, Transcriptomic, and Lipidomic Profiling Highlights the Role of Inflammation in Individuals With Low High-density Lipoprotein Cholesterol. *Arterioscler Thromb Vasc Biol*, *33*(4), 847–857. doi:10.1161/ATVBAHA.112.300733
Lauring, B., Taggart, A. K. P., Tata, J. R., Dunbar, R., Caro, L., Cheng, K., et al. (2012). Niacin lipid efficacy is independent of both the niacin receptor GPR109A and free fatty acid suppression. *Science Translational Medicine*, *4*(148), 148ra115. doi:10.1126/scitranslmed.3003877
Lee, D. K., Nguyen, T., Lynch, K. R., Cheng, R., Vanti, W. B., Arkhitko, O., et al. (2001). Discovery and mapping of ten novel G protein-coupled receptor genes. *Gene*, *275*(1), 83–91.
Lee, J. M. S., Robson, M. D., Yu, L.-M., Shirodaria, C. C., Cunnington, C., Kylintireas, I., et al. (2009). Effects of high-dose modified-release nicotinic acid on atherosclerosis and vascular function: a randomized, placebo-controlled, magnetic resonance imaging study. *Journal of the American College of Cardiology*, *54*(19), 1787–1794. doi:10.1016/j.jacc.2009.06.036
Leff, T., & Granneman, J. G. (2010). *Adipose Tissue in Health and Disease*. Wiley-Blackwell.
Leibel, R. L., & Hirsch, J. (1987). Site- and sex-related differences in adrenoreceptor status of human adipose tissue. *The Journal of Clinical Endocrinology and Metabolism*, *64*(6), 1205–1210.
Lukasova, M., Malaval, C., Gille, A., Kero, J., & Offermanns, S. (2011). Nicotinic acid inhibits progression of atherosclerosis in mice through its receptor GPR109A expressed by immune cells. *J Clin Invest*, *121*(3), 1163–1173. doi:10.1172/JCI41651
Maciejewski-Lenoir, D., Richman, J. G., Hakak, Y., Gaidarov, I., Behan, D. P., & Connolly, D. T. (2006). Langerhans cells release prostaglandin D2 in response to nicotinic acid. *The Journal of Investigative Dermatology*, *126*(12), 2637–2646. doi:10.1038/sj.jid.5700586
Mahboubi, K., Witman-Jones, T., Adamus, J. E., Letsinger, J. T., Whitehouse, D., Moorman, A. R., et al. (2006). Triglyceride modulation by acifran analogs: activity towards the niacin high and low affinity G protein-coupled receptors HM74A and HM74. *Biochemical and Biophysical Research Communications*, *340*(2), 482–490. doi:10.1016/j.bbrc.2005.12.022
Manolopoulos, K. N., Karpe, F., & Frayn, K. N. (2010). Gluteofemoral body fat as a determinant of metabolic health. *International Journal of Obesity (2005)*, *34*(6), 949–959. doi:10.1038/ijo.2009.286
Marmot, M., & Brunner, E. (2005). Cohort Profile: the Whitehall II study. *International Journal of Epidemiology*, *34*(2), 251–256. doi:10.1093/ije/dyh372
Matsusaka, T., Fujikawa, K., Nishio, Y., Mukaida, N., Matsushima, K., Kishimoto, T., & Akira, S. (1993). Transcription factors NF-IL6 and NF-kappa B synergistically activate transcription of the inflammatory cytokines, interleukin 6 and interleukin 8. *Proc Natl Acad Sci U S A*, *90*(21), 10193–10197.
McQuaid, S. E., Hodson, L., Neville, M. J., Dennis, A. L., Cheeseman, J., Humphreys, S. M., et al. (2011). Downregulation of adipose tissue fatty acid trafficking in obesity: a driver for ectopic fat deposition? *Diabetes*, *60*(1), 47–55. doi:10.2337/db10-0867
Meijer, K., de Vries, M., Al-Lahham, S., Bruinenberg, M., Weening, D., Dijkstra, M., et al. (2011). Human primary adipocytes exhibit immune cell function: adipocytes prime inflammation independent of macrophages. *PloS One*, *6*(3), e17154. doi:10.1371/journal.pone.0017154
Miller, C. L., & Dulay, J. R. (2008). The high-affinity niacin receptor HM74A is decreased in the anterior cingulate cortex of individuals with schizophrenia. *Brain Research Bulletin*, *77*(1), 33–41. doi:10.1016/j.brainresbull.2008.03.015
Min, J. L., Nicholson, G., Halgrimsdottir, I., Almstrup, K., Petri, A., Barrett, A., et al. (2012). Coexpression network analysis in abdominal and gluteal adipose tissue reveals regulatory genetic loci for metabolic syndrome and related phenotypes. *PLoS Genetics*, *8*(2), e1002505. doi:10.1371/journal.pgen.1002505
Mohamed-Ali, V., Goodrick, S., Rawesh, A., Katz, D. R., Miles, J. M., Yudkin, J. S., et al. (1997). Subcutaneous adipose tissue releases interleukin-6, but not tumor necrosis factor-alpha, in vivo. *The Journal of Clinical Endocrinology and Metabolism*, *82*(12), 4196–4200.
Mottagui-Tabar, S., Faghihi, M. A., Mizuno, Y., Engström, P. G., Lenhard, B., Wasserman, W. W., & Wahlestedt, C. (2005). Identification of functional SNPs in the 5-prime flanking sequences of human genes. *BMC Genomics*, *6*, 18. doi:10.1186/1471-2164-6-18
Musumeci, L., Arthur, J. W., Cheung, F. S. G., Hoque, A., Lippman, S., & Reichardt, J. K. V. (2010). Single nucleotide differences (SNDs) in the dbSNP database may lead to errors in genotyping and haplotyping studies. *Hum Mutat*, *31*(1), 67–73. doi:10.1002/humu.21137
Neville, M. J., Collins, J. M., Gloyn, A. L., McCarthy, M. I., & Karpe, F. (2010). Comprehensive Human Adipose Tissue mRNA and MicroRNA Endogenous Control Selection for Quantitative Real-Time-PCR Normalization. *Obesity (Silver Spring, Md)*. doi:10.1038/oby.2010.257
Nicholls, S. J. (2012). The AIM-HIGH (Atherothrombosis Intervention in Metabolic Syndrome With Low HDL/High Triglycerides: Impact on Global Health Outcomes) Trial. *Journal of the American College of Cardiology*, *59*(23), 2065–2067. doi:10.1016/j.jacc.2012.02.021
Nomura, H., Nielsen, B. W., & Matsushima, K. (1993). Molecular cloning of cDNAs encoding a LD78 receptor and putative leukocyte chemotactic peptide receptors. *International Immunology*.
Offermanns, S. (2006). The nicotinic acid receptor GPR109A (HM74A or PUMA-G) as a new therapeutic target. *Trends Pharmacol Sci*, *27*(7), 384–390. doi:S0165-6147(06)00132-5 [pii]
10.1016/j.tips.2006.05.008

Offermanns, S., Colletti, S. L., Lovenberg, T. W., Semple, G., Wise, A., & IJzerman, A. P. (2011). International Union of Basic and Clinical Pharmacology. LXXXII: Nomenclature and Classification of Hydroxy-carboxylic Acid Receptors (GPR81, GPR109A, and GPR109B). *Pharmacological Reviews*, *63*(2), 269–290. doi:10.1124/pr.110.003301
Owen, O. E., Felig, P., Morgan, A. P., Wahren, J., & Cahill, G. F. (1969). Liver and kidney metabolism during prolonged starvation. *J Clin Invest*, *48*(3), 574–583. doi:10.1172/JCI106016
Pedersen, T. R., Faergeman, O., Kastelein, J. J. P., Olsson, A. G., Tikkanen, M. J., Holme, I., et al. (2005). High-dose atorvastatin vs usual-dose simvastatin for secondary prevention after myocardial infarction: the IDEAL study: a randomized controlled trial. *JAMA : the Journal of the American Medical Association*, *294*(19), 2437–2445. doi:10.1001/jama.294.19.2437
Pepys, M. B., & Hirschfield, G. M. (2003). C-reactive protein: a critical update. *J Clin Invest*, *111*(12), 1805–1812. doi:10.1172/JCI18921
Perk, J., De Backer, G., Gohlke, H., Graham, I., Reiner, Z., Verschuren, W. M. M., et al. (2012, July). European Guidelines on cardiovascular disease prevention in clinical practice (version 2012): The Fifth Joint Task Force of the European Society of Cardiology and Other Societies on Cardiovascular Disease Prevention in Clinical Practice (constituted by representatives of nine societies and by invited experts). *Atherosclerosis*. doi:10.1016/j.atherosclerosis.2012.05.007
Pfaffl, M. W. (2001). A new mathematical model for relative quantification in real-time RT-PCR. *Nucleic Acids Research*, *29*(9), e45.
Plaisance, E. P., Grandjean, P. W., Brunson, B. L., & Judd, R. L. (2008). Increased total and high-molecular weight adiponectin after extended-release niacin. *Metabolism: Clinical and Experimental*, *57*(3), 404–409. doi:10.1016/j.metabol.2007.10.018
Poynten, A. M., Gan, S. K., Kriketos, A. D., O'Sullivan, A., Kelly, J. J., Ellis, B. A., et al. (2003). Nicotinic acid-induced insulin resistance is related to increased circulating fatty acids and fat oxidation but not muscle lipid content. *Metabolism: Clinical and Experimental*, *52*(6), 699–704.
Prospective Studies Collaboration, Lewington, S., Whitlock, G., Clarke, R., Sherliker, P., Emberson, J., et al. (2007). Blood cholesterol and vascular mortality by age, sex, and blood pressure: a meta-analysis of individual data from 61 prospective studies with 55,000 vascular deaths. *Lancet*, *370*(9602), 1829–1839. doi:10.1016/S0140-6736(07)61778-4
Qasim, A., & Rader, D. J. (2006). Human genetics of variation in high-density lipoprotein cholesterol. *Curr Atheroscler Rep*, *8*(3), 198–205.
Rantalainen, M., Herrera, B. M., Nicholson, G., Bowden, R., Wills, Q. F., Min, J. L., et al. (2011). MicroRNA Expression in Abdominal and Gluteal Adipose Tissue Is Associated with mRNA Expression Levels and Partly Genetically Driven. *PloS One*, *6*(11), e27338. doi:10.1371/journal.pone.0027338
Razzaghi, H., Santorico, S. A., & Kamboh, M. I. (2012). Population-Based Resequencing of LIPG and ZNF202 Genes in Subjects with Extreme HDL Levels. *Frontiers in Genetics*, *3*, 89. doi:10.3389/fgene.2012.00089
Regitz-Zagrosek, V., Lehmkuhl, E., & Weickert, M. O. (2006). Gender differences in the metabolic syndrome and their role for cardiovascular disease. *Clinical Research in Cardiology*, *95*(3), 136–147. doi:10.1007/s00392-006-0351-5
RODBELL, M. (1964). METABOLISM OF ISOLATED FAT CELLS. I. EFFECTS OF HORMONES ON GLUCOSE METABOLISM AND LIPOLYSIS. *J Biol Chem*, *239*, 375–380.
Rosen, E. D., & Spiegelman, B. M. (2000). Molecular regulation of adipogenesis. *Annual Review of Cell and …*.
Rosenblum, B. B., Lee, L. G., Spurgeon, S. L., Khan, S. H., Menchen, S. M., Heiner, C. R., & Chen, S. M. (1997). New dye-labeled terminators for improved DNA sequencing patterns. *Nucleic Acids Research*, *25*(22), 4500–4504.
Rosenson, R. S. (2012). Clinical trials of HDL cholesterol-raising therapy: what have we learned about the HDL hypothesis from AIM-HIGH? *Curr Atheroscler Rep*, *14*(3), 190–192. doi:10.1007/s11883-012-0236-1
Rosenson, R. S., & Gotto, A. M. (2013). When clinical trials fail to address treatment gaps: the failure of niacin-laropiprant to reduce cardiovascular events. *Curr Atheroscler Rep*, *15*(6), 332. doi:10.1007/s11883-013-0332-x
Sanger, F., Nicklen, S., & Coulson, A. R. (1977). DNA sequencing with chain-terminating inhibitors. *Proc Natl Acad Sci U S A*, *74*(12), 5463–5467.
Schaub, A., Fütterer, A., & Pfeffer, K. (2001). PUMA-G, an IFN-gamma-inducible gene in macrophages is a novel member of the seven transmembrane spanning receptor superfamily. *European Journal of Immunology*, *31*(12), 3714–3725.
Shah, R., Hinkle, C. C., Haris, L., Shah, R., Mehta, N. N., Putt, M. E., & Reilly, M. P. (2012). Adipose genes down-regulated during experimental endotoxemia are also suppressed in obesity. *The Journal of Clinical Endocrinology and Metabolism*, *97*(11), E2152–9. doi:10.1210/jc.2012-1988
Smith, L. M., Sanders, J. Z., Kaiser, R. J., Hughes, P., Dodd, C., Connell, C. R., et al. (1986). Fluorescence detection in automated DNA sequence analysis. *Nature*, *321*(6071), 674–679. doi:10.1038/321674a0
Soga, T., Kamohara, M., Takasaki, J., Matsumoto, S.-I., Saito, T., Ohishi, T., et al. (2003). Molecular identification of nicotinic acid receptor. *Biochemical and Biophysical Research Communications*, *303*(1), 364–369.
Soronen, J., Laurila, P.-P., Naukkarinen, J., Surakka, I., Ripatti, S., Jauhiainen, M., et al. (2012). Adipose tissue gene expression analysis reveals changes in inflammatory, mitochondrial respiratory and lipid metabolic pathways in obese insulin-resistant subjects. *BMC Medical Genomics*, *5*, 9. doi:10.1186/1755-8794-5-9
Sorrentino, S. A., Besler, C., Rohrer, L., Meyer, M., Heinrich, K., Bahlmann, F. H., et al. (2010). Endothelial-vasoprotective effects of high-density lipoprotein are impaired in patients with type 2 diabetes mellitus but are improved after extended-release niacin therapy. *Circulation*, *121*(1), 110–122. doi:10.1161/CIRCULATIONAHA.108.836346
Spiroglou, S. G., Kostopoulos, C. G., Varakis, J. N., & Papadaki, H. H. (2010). Adipokines in periaortic and epicardial adipose tissue: differential expression and relation to atherosclerosis. *Journal of Atherosclerosis and Thrombosis*, *17*(2), 115–130.
Stephens, M., Smith, N. J., & Donnelly, P. (2001). A new statistical method for haplotype reconstruction from population data. *American Journal of Human Genetics*, *68*(4), 978–989. doi:10.1086/319501
Stewart, S. A., Dykxhoorn, D. M., Palliser, D., Mizuno, H., Yu, E. Y., An, D. S., et al. (2003). Lentivirus-delivered stable gene silencing by RNAi in primary cells. *RNA (New York, N.Y.)*, *9*(4), 493–501.
Taggart, A. K. P., Kero, J., Gan, X., Cai, T.-Q., Cheng, K., Ippolito, M., et al. (2005). (D)-beta-Hydroxybutyrate inhibits adipocyte lipolysis via the nicotinic acid receptor PUMA-G. *J Biol Chem*, *280*(29), 26649–26652. doi:10.1074/jbc.C500213200
Talmud, P. J., Shah, S., Whittall, R., Futema, M., Howard, P., Cooper, J. A., et al. (2013). Use of low-density lipoprotein cholesterol gene score to distinguish patients with polygenic and monogenic familial hypercholesterolaemia: a case-control study. *Lancet*, *381*(9874), 1293–1301. doi:10.1016/S0140-6736(12)62127-8

Tan, G. D., Goossens, G. H., Humphreys, S. M., Vidal, H., & Karpe, F. (2004). Upper and lower body adipose tissue function: a direct comparison of fat mobilization in humans. *Obesity Research*, *12*(1), 114–118. doi:10.1038/oby.2004.15
Tchkonia, T., Giorgadze, N., Pirtskhalava, T., Thomou, T., DePonte, M., Koo, A., et al. (2006). Fat depot-specific characteristics are retained in strains derived from single human preadipocytes. *Diabetes*, *55*(9), 2571–2578. doi:10.2337/db06-0540
Tchkonia, T., Lenburg, M., Thomou, T., Giorgadze, N., Frampton, G., Pirtskhalava, T., et al. (2007). Identification of depot-specific human fat cell progenitors through distinct expression profiles and developmental gene patterns. *American Journal of Physiology Endocrinology and Metabolism*, *292*(1), E298–307. doi:10.1152/ajpendo.00202.2006
Tchoukalova, Y. D., Koutsari, C., Votruba, S. B., Tchkonia, T., Giorgadze, N., Thomou, T., et al. (2010). Sex- and depot-dependent differences in adipogenesis in normal-weight humans. *Obesity (Silver Spring, Md)*, *18*(10), 1875–1880. doi:10.1038/oby.2010.56
Tunaru, S., Kero, J., Schaub, A., Wufka, C., Blaukat, A., Pfeffer, K., & Offermanns, S. (2003). PUMA-G and HM74 are receptors for nicotinic acid and mediate its anti-lipolytic effect. *Nat Med*, *9*(3), 352–355. doi:10.1038/nm824
van Capelleveen, J. C., Bochem, A. E., Motazacker, M. M., Hovingh, G. K., & Kastelein, J. J. P. (2013). Genetics of HDL-C: A Causal Link to Atherosclerosis? *Curr Atheroscler Rep*, *15*(6), 326. doi:10.1007/s11883-013-0326-8
Venter, J. C., Adams, M. D., Myers, E. W., Li, P. W., Mural, R. J., Sutton, G. G., et al. (2001). The sequence of the human genome. *Science (New York, N.Y.)*, *291*(5507), 1304–1351. doi:10.1126/science.1058040
Voight, B. F., Peloso, G. M., Orho-Melander, M., Frikke-Schmidt, R., Barbalic, M., Jensen, M. K., et al. (2012). Plasma HDL cholesterol and risk of myocardial infarction: a mendelian randomisation study. *Lancet*, *380*(9841), 572–580. doi:10.1016/S0140-6736(12)60312-2
Wahrenberg, H., Lönnqvist, F., & Arner, P. (1989). Mechanisms underlying regional differences in lipolysis in human adipose tissue. *J Clin Invest*, *84*(2), 458–467. doi:10.1172/JCI114187
Wajchenberg, B. L. (2000). Subcutaneous and visceral adipose tissue: their relation to the metabolic syndrome. *Endocrine Reviews*, *21*(6), 697–738.
Walters, R. W., Shukla, A. K., Kovacs, J. J., Violin, J. D., DeWire, S. M., Lam, C. M., et al. (2009). beta-Arrestin1 mediates nicotinic acid-induced flushing, but not its antilipolytic effect, in mice. *J Clin Invest*, *119*(5), 1312–1321. doi:10.1172/JCI36806
Wells, J. C. K. (2007). Sexual dimorphism of body composition. *Best Practice & Research. Clinical Endocrinology & Metabolism*, *21*(3), 415–430. doi:10.1016/j.beem.2007.04.007
Wener, M. H., Daum, P. R., & McQuillan, G. M. (2000). The influence of age, sex, and race on the upper reference limit of serum C-reactive protein concentration. *The Journal of Rheumatology*, *27*(10), 2351–2359.
Wild, S., & Byrne, C. D. (2008). Time to rethink high-density lipoprotein? *Heart (British Cardiac Society)*, *94*(6), 692–694. doi:10.1136/hrt.2007.126326
Willett, W. C., Dietz, W. H., & Colditz, G. A. (1999). Guidelines for Healthy Weight. *The New England Journal of Medicine*, *341*(6), 427–434. doi:10.1056/NEJM199908053410607
Wise, A., Foord, S. M., Fraser, N. J., Barnes, A. A., Elshourbagy, N., Eilert, M., et al. (2003). Molecular identification of high and low affinity receptors for nicotinic acid, *278*(11), 9869–9874. doi:10.1074/jbc.M210695200
M210695200 [pii]
Yudkin, J. S., Kumari, M., Humphries, S. E., & Mohamed-Ali, V. (2000). Inflammation, obesity, stress and coronary heart disease: is interleukin-6 the link? *Atherosclerosis*, *148*(2), 209–214.
Zandi-Nejad, K., Takakura, A., Jurewicz, M., Chandraker, A. K., Offermanns, S., Mount, D., & Abdi, R. (2013). The role of HCA2 (GPR109A) in regulating macrophage function. *FASEB Journal : Official Publication of the Federation of American Societies for Experimental Biology*. doi:10.1096/fj.12-223933
Zellner, C., Pullinger, C., Aouizerat, B., Frost, P., Kwok, P., Malloy, M., & Kane, J. (2005). Variations in human HM74 (GPR109B) and HM74A (GPR109A) niacin receptors. *Hum Mutat*, *25*(1), 18–21. doi:10.1002/humu.20121
Zhang, L. H., Kamanna, V. S., Ganji, S. H., Xiong, X. M., & Kashyap, M. L. (2012). Niacin increases HDL biogenesis by enhancing DR4-dependent transcription of ABCA1 and lipidation of apolipoprotein A-I in HepG2 cells. *J Lipid Res*, *53*(5), 941–950. doi:10.1194/jlr.M020917
Zhang, L., Kamanna, V., Zhang, M., & Kashyap, M. (2008). Niacin inhibits surface expression of ATP synthase beta chain in HepG2 cells: implications for raising HDL. *J Lipid Res*, *49*(6), 1195–1201. doi:M700426-JLR200 [pii]
10.1194/jlr.M700426-JLR200